AD
A066483

1.0

1.1

1.25  1.4  1.6

4.5  2.8  2.5
5.0
5.6  3.2  2.2
6.3  3.6
4.0  2.0
1.8

MICROCOPY RESOLUTION TEST CHART
NATIONAL BUREAU OF STANDARDS-1963-A

①

AD-A066483

# FOREIGN TECHNOLOGY DIVISION

STRENGTH OF REFRACTORY METALS

By

G. S. Pisarenko, V. A. Borisenko, et al.

D D C

MAR 26 1979

F

78 12 22 416

FTD- ID(RS)T-1330-78

# UNEDITED MACHINE TRANSLATION

FTD-ID(RS)T-1330-78                    4 October 1978

MICROFICHE NR: $\mathcal{H}D$-78-C-00136 1L

CSC71299923

STRENGTH OF REFRACTORY METALS

By:  G. S. Pisarenko, V. A. Borisenko, et al.

English pages:  745

Source:  Prochnost' Tugoplavkikh Metallov,
         Izd-vo "Metallurgiya," Moscow, 1970,
         pp. 1-365.
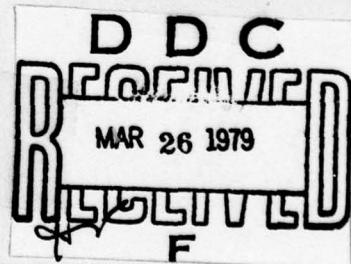
Country of origin:  USSR
This document is a machine translation.
Requester:  FTD/TQTA
Approved for public release; distribution
unlimited.

Table of Contents

1

Chapter 5.


SHORT-TERM STATIC STRENGTH.


Installations for determining short-time strength (20-3000°C).


Short-time static tests make it possible to determine basic mechanical characteristics of high-melting materials, and to also estimate the behavior of these materials under load at the high temperatures, to a certain degree imitating operating conditions of parts and elements of the construction/designs, working under conditions of short-time overloads and superheating.


One of the basic types of short-time static tests is testing for elongation which makes it possible to determine the mechanical characteristics of materials - limits of strength, proportionality and yield, and also elongation per unit length and narrowing.


The methods of short-time static tests of different materials at the room and elevated temperatures (to 1000-2000°C) are sufficiently well known [5, 6, 18, 19]; however, there is very limited information about the tests of materials in temperature range higher than 1500-2000°C.

At present not standard procedures and equipment for the test
work of high-melting materials at very high temperatures. In the
majority of the cases for these purposes, are utilized available
general purpose machines [6, 157, 159], which are equipped with
specially developed heating, measuring and other attachments, by
vacuum chambers, etc. This way has the definite advantages, since it
requires the manufacture only of separate nonstandard parts and it
makes it possible to utilize the existing equipment.

In the institute of the problems of the strength of AS UkSSR in
recent years according to similar principle, is created a series of
installations [60] now successfully operated. Description of one of
such installations (VTU-2V) will be given below. Besides it, for
short-time static tests is developed and created the installation
with the use of the cathode-ray heating of specimen/samples.

The results of experimental studies of strength and plassticity
of refractory metals, presented in this chapter, in essence are
obtained during tests during installation VTU-2V.

Installation VTU-2V is designed for high-melting material
testing in vacuum or inert medium at temperatures of 20-3000°C. It

consists of the following assembly of devices and attachments:
general purpose testing machine, the special vacuum camera/chamber,
the vacuum system, the system of heating specimen/samples, devices
for measurement, the deformation of specimen/sample, tools for
measurement and temperature control and control panel of installation
(Fig. 154).

Page 194.

As basis for constructing the installation VTU-2V served
universal testing machine SzF-1, which makes it possible to conduct
tests for elongation, bend and compression with peak load to 24500 N
(2500 kgf). For an increase of the accuracy/precision of the measured
load in power circuit, is establish/installed the dynamometer of the
type DS-0.2. On the movable crosshead of machine, are mounted the
interchangeable working vacuum camera/chambers.

The vacuum system of installation, which consists of fore pump
VN-2MG, the diffusion pump N1-S2, catch DU-80 and vacuum manifolds
with special tap/cranes, makes it possible to create
evacuation/rarefaction in working chamber to 1.33 $MN/m^2$ ($1\cdot10^{-5}$ mm
Hg) at room temperatures and 1.33 $m/m^2$ ($1\cdot10^{-4}$ mm Hg) at 2000°C. The
inleakage of air into vacuum system does not usually exceed 0.1 $\mu l/s$.

The system of heating specimen/samples makes it possible to reach temperatures of 3000-3100°C, utilizing a ray (radiation) method of heating. For this purpose, is specially designed small electric furnace with the lamellar molybdenum (to 1700°C) and tungsten (200-3000°C) heaters, which present the tubes 12-15 mm in diameter and 70 mm in long (Fig. 155). The length of heater 3-4 times exceeded the working length of specimen/sample ($l_0$ = 15-20 mm). For decreasing radiation losses, was applied the system of shields from tungsten and molybdenum.

Calibration tests showed that in working chamber of furnace it is possible to obtain the sufficiently uniform heating zone. The study of the distribution of the temperature of specimen/sample during tensile tests with the utilization of ray heating showed that at temperatures of 1300-1500°C gradient along the length of the working section of specimen/sample did not exceed 10-20 deg, but at higher temperatures (2000-2150°C) it was 25-30 deg (Fig. 156).

The heater of the construction/design indicated consumes relatively low power ($P \approx 6.5$ kW with ~3000°C).

The horizontally arranged/located current supplies make it possible to utilize heaters of various forms and size/dimensions, and to also establish/install in the camera/chamber interchangeable

attachments for a bend and compression.

Stress on heater enters from step-down transformer OSU-40, which is regulated by bunchers ROT-25/0.5. For measurement and check of temperature, are used the thermocouples of the type PP and VR5/20, and also the optical pyrometer.

Page 195.
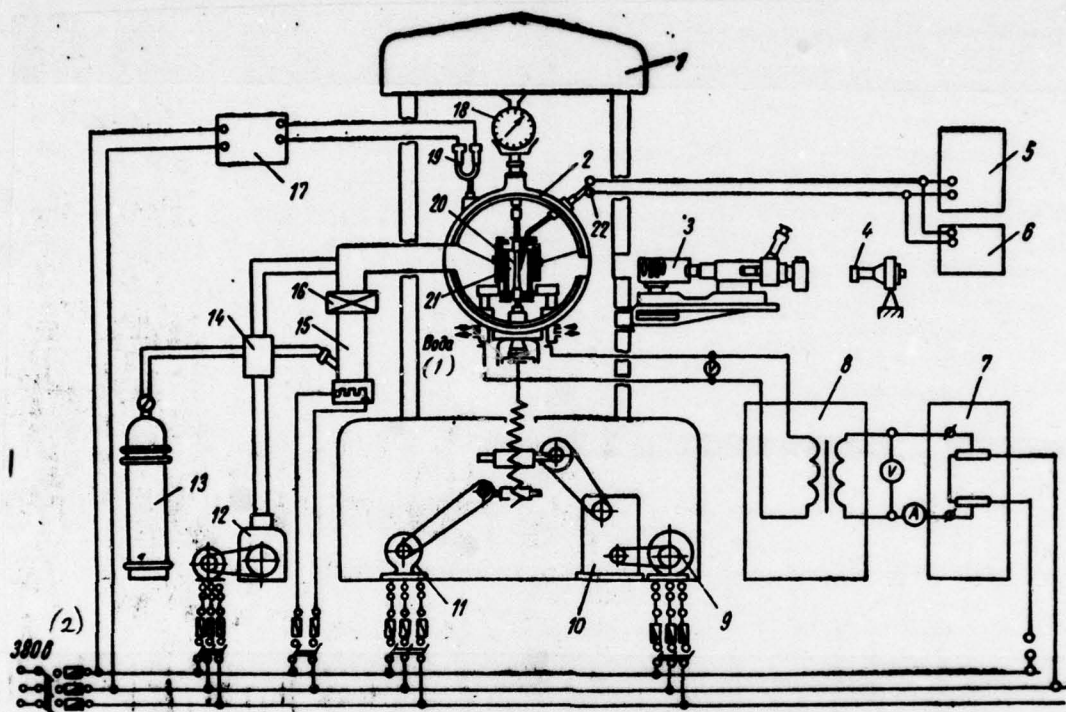


Fig. 154. The schematic diagram of installation VTU-2V: 1 - testing machine; 2 - vacuum camera/chamber; 3 - optical photographic attachment; 4 - pyrometer; 5 - potentiometer PPF-09; 6 - potentiometer KP-59; 7 - bunchers of stress ROT-25/0.5; 8 - transformer OSU-40; 9 - electric motor; 10 - bunchers of the velocities of testing machine; 11 - electric motor quick motion; 12 - fore pump VN-2MG; 13 - bottle; 14 - four-way vacuum tap/crane; 15 - diffusion pump N1-S2; 16 - catch; 17 - vacuum gauge VIT-1A; 18 - dynamometer; 19 - monometric lamps; 20 - specimen/sample; 21 - reheating furnace; 22 - thermocouple conclusion.

Key: (1). Water. (2). V.

Page 196.
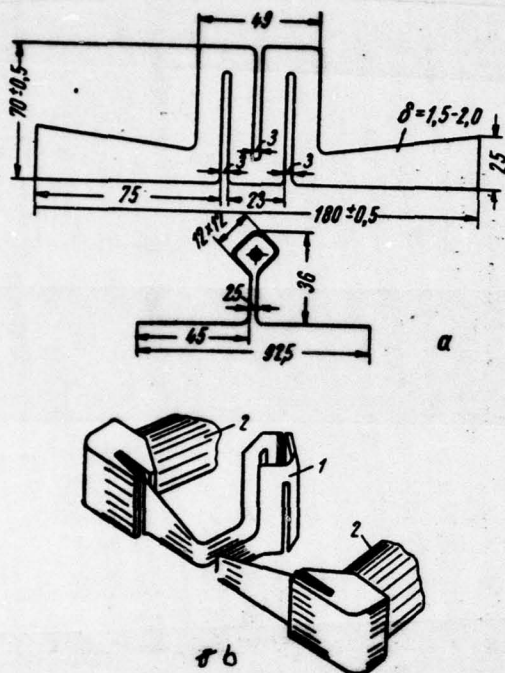


Fig. 155. Heating element of installation VIU-2V: a) the

scan/development of heater; b) the diagram of installation of heater

in current conductors (1 - heating element, 2 - current conductors).
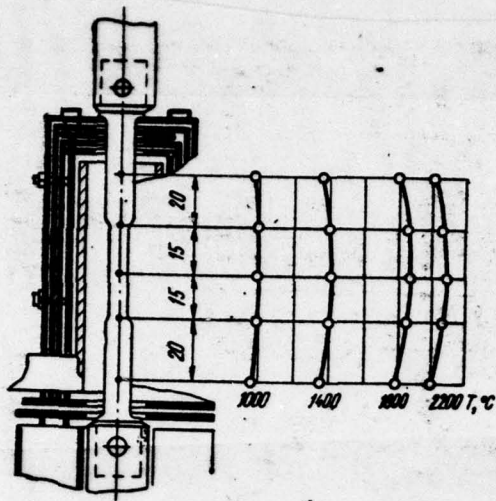
Fig. 156.

Temperature distribution along the length of specimen/sample during tensile tests.

Page 197.

For studying the strength properties of low-plasticity refractory compounds - carbides, borides, nitrides and others - cermet materials in the wide range of temperatures (with the utilization of ray heating of specimen/samples to 2300-2500°C, during heating the direct/straight transmission of the electric current through the specimen/sample to 3000-3500°C) are establish/installed vacuum chambers and interchangeable attachments, which ensure

obtaining different experimental media (inert gas or vacuum) and the
forms of loading (elongation, bend or compression).

For studying the short-time tensile strength of refractory
metals, are utilized proportional circular specimen/samples with
working section 3-4 mm in diameter and 15-20 mm in long, which have
threaded or fillister heads, and also flat/plane laminated
specimen/samples 5.0 mm in wide.
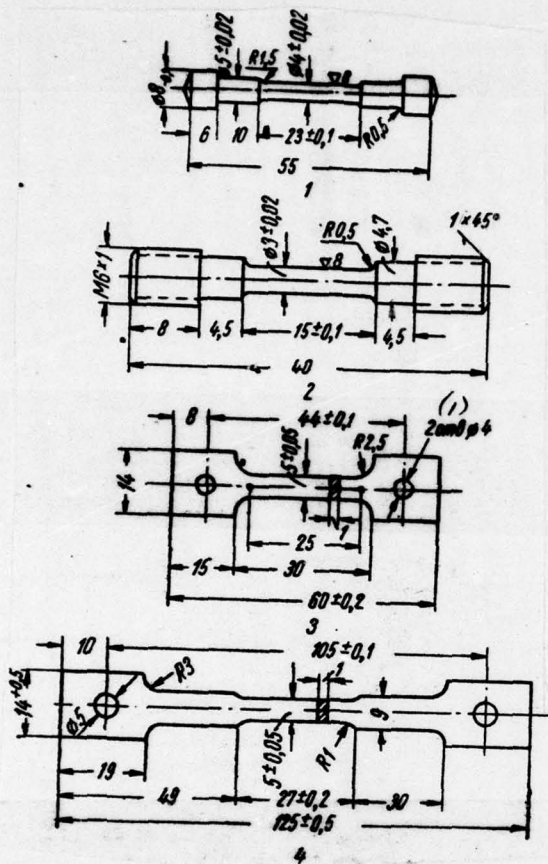
Fig. 157. Specimen/samples for mechanical tests.

Key: (1). opening.

Page 198.

The overall length of the specimen/samples used is 40-50 mm, if the temperature of tests does not exceed 1700°C, and 100-125 mm for the

temperatures more than 2000°C (Fig. 157).

Strain is measured by cathetometer KM-6 and by optical
cap/filling. During tests the elongation of specimen/sample is
determined according to a change in the clearance (0.1-0.2 mm)
between the plates, welded to the thickened parts of the
specimen/sample.

For measurements of the temperatures, which exceed 2000°C, were
carried out the special tests, which made it possible to calibrate
wire VR5/20 on melting points of pure metals and calibrate the
optical pyrometer, and also determine the corrections which must be
introduced with measurements of the temperature brightness of the
surface of specimen/sample (Figs. 158 and 159).

Installation "electron" is intended for determining the
mechanical properties of high-melting materials in vacuum with
heating of specimen/sample by electron beam to 3200°C. The block
diagram of installation is represented on Fig. 160.

By framework is water-cooled camera/chamber 1 diameter 310 mm,
which is fasten/strengthened to vacuum assembly.
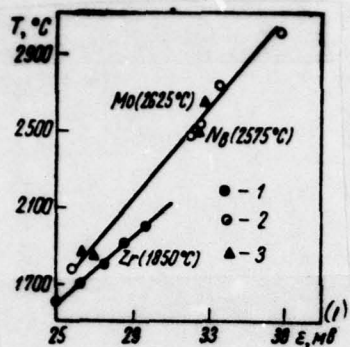
Fig. 158. The dependence thermcelectrcactive fcrce of wire VR5/20 on the temperature: 1 - on the data of TsLA [32]; 2 - on the data of work [22]; 3 - on our data.

Key: (1). mV.
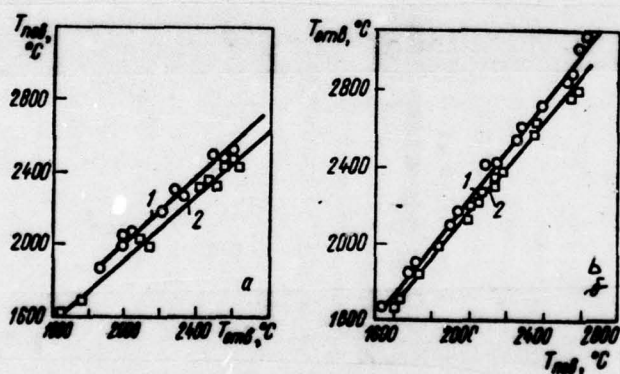


Fig. 159. Calibration curve/graphs of the temperature: a) during tests for elongation (1 - for the circular specimen/samples W; 2 - for laminated specimen/samples W); b) during tests fcr bend (1 - for the circular specimen/samples W; 2 - fcr prismatic specimen/samples made of refractory compcunds).

Page 199.
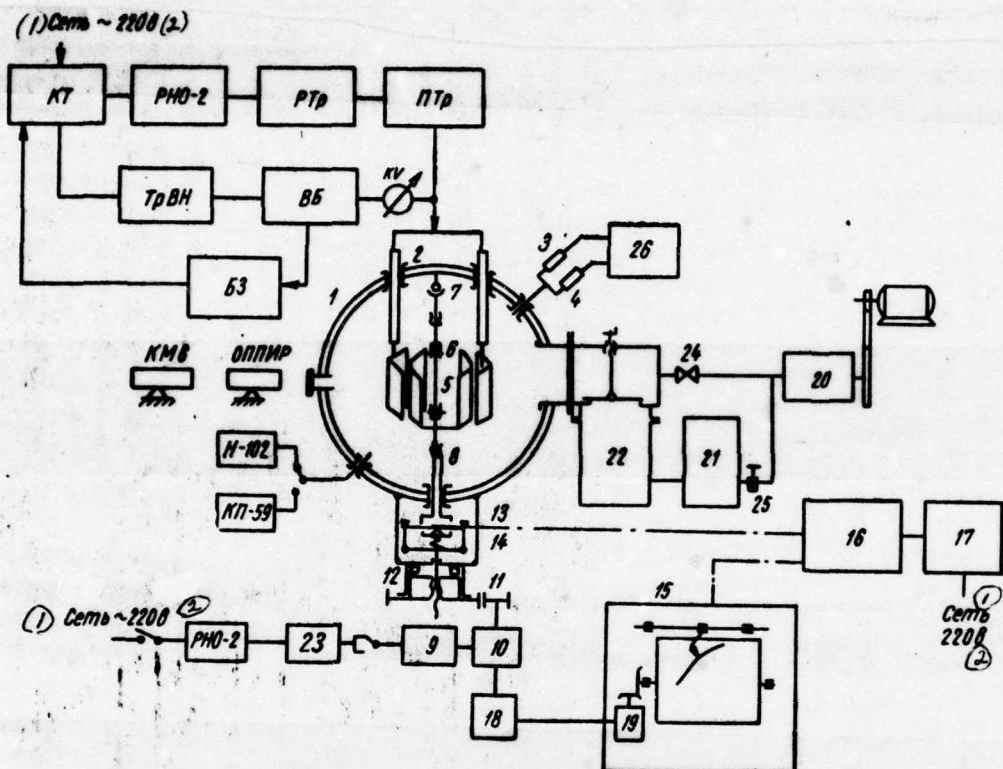


Fig. 160. Block diagram of installation "electron".

Key: (1). Grid/network. (2). V.

Page 200.

In the chamber are placed current conductors of high voltage 2,
manometric lamps 3 and 4, the vacuum-tight input/introductions for
thermocouples, inspection window, etc.

Specimen/sample 5 is reinforced by pins 6 mm in diameter in captures by 6, made from molybdenum or tungsten. Captures are screwed in into the thrust/rod of spherical bearing 7 and into movable water-cooled stock/rod 8. This system provides good centering of specimen/sample and axiality of the load application. The loading of specimen/sample realize/accomplishes with the aid of series direct-current motor 9 through reducer 10, the pair of spur gears 11, the power pair screw/propeller - nut 12 and the elastic cell/element with strain gauge 13. The control of the rate of the displacement/movement of active capture within the limits of 0.2-0.4 mm/min are manufactured with the aid of voltage regulators RNO-2 and 23, and also serrated pair 11.

Load in specimen/sample is measured according to the elastic deformation of beam with free supports with the aid of the strain gauge, connected in the bridge measuring circuit of strain measuring station 8ANCh-7M, with the subsequent recording of output signal on electronic potentiometer 15 (type EPP-02). The feed of strain measuring station 16 realize/accomplishes separate stabilized block 17.

The rigidity of beams, the parameters of strain gauges, strain

measuring station and EPP-09 are agreed in such a way that during
load change within the limits of 200-5000 N (20-500 kgf) is possible
the scan/development of signal to entire scale EPP-09. For the
kinematic closing/shorting of power circuit (active stock/rod -
simple beam - forcing screw) is establish/installed spring 14. The
mechanism of the recording of strain includes selsyn transmitter 18,
connected with the connecting shaft (n≈250 r/min), reducer 10
receiving synchro 19 which is establish/installed swept synchronous
motor SD-09 into the system of the displacement/movement of the graph
paper of potentiometer EPP-09. Servo system is carried out on the
noncontact selsyns of the type ES-404A, of the workers in indicator
conditions/mode. After the disconnection/cutoff of the mechanism of
press/printing, switch of sensors and some assemblies of tape-drive
mechanism EPP-09, is obtained the stable operation of the synchronous
rotation of the rotors of sensor and receiver with the regulating of
the scale of recording the strain of specimen/sample in the range
(10:1)-(210:1). The vacuum system of installation provides
evacuation/rarefaction 1.33-0.133 mN/m² (10⁻⁵-10⁻⁶ mm Hg) during the
electronic heating of specimen/sample without preliminary degassing.
It switches on fore pump by 20 (type VN-1), booster pump 21 (type
BN-3) and a high-vacuum pump (of type MM100C). Vacuum manifold (22,
25) makes it possible to manufacture the direct/straight and bypass
pumping out of the camera/chamber through catch 24, in consequence of
which during the exchange of specimen/sample in the camera/chamber it

is not necessary to disconnect/turn off diffusion pumps.

Pressure in the camera/chamber is measured with the aid of the
sanometric lamps LT-2 and LM-2, connected to vacuum gauge VIT-1A
(26).

Page 201.

The inleakage of air into vacuum system does not usually exceed
0.15-0.2 $\mu l$/s.

For heating of specimer/samples by electron beam were tested the
diagrams of autoheating (specimen/sample - anode) and of heating by
the cathode-ray guns of pier (specimen/sample out of electric field).
Autoheating is economical, but it has the essential deficiencies:
degassing specimen/sample in heating-up period leads to the
ionization of interelectrode interval/gap, the emergence of the glow
discharge and punctures; it is difficult to stabilize the temperature
of specimen/sample during heating higher than 1200-1500°C; is
feasible the superheating of specimen/sample in neck. Therefore, for
investigations utilizes electron beam guns of pier.

The electric circuit of installation provides accelerating
voltage 8 kV and has necessary mechanical and electrical interlocks

on high tension and vacuum.

The calculation of the probable errors in the direct measurements showed that during the correct agreement of the ranges of the measuring systems of installation and measured values of defect of measurement of load comprise not more than 1.5-2o/o, strains - to 5o/o and temperature 2-4o/c.

Temperature effect on the mechanical properties of tungstén, molybdenum and alloys on their basis.

Tungsten. Tungsten and alloys on its basis it is most expedient to apply in the construction/designs, working at the temperatures more than 1800°C [ 163]. In works [ 163-165] shown wide application of tungsten, in particular, in electric vacuum industry for manufacturing the filaments, grids, input/introductions and many other articles.

In aviation and rocket engineering is possible the utilization of tungsten for manufacturing the nozzle insert/bushings of critical section/cut, and also the parts, located near nozzle and workers at the temperatures more than 2000°C [ 162].

However, the utilization of pure tungsten as structural material

in a number of cases is hinder/hampered first cf all due to its low
plasticity with room temperatures (in spite of high heat resistance).

The wide application of tungsten in construction/designs is
limited also by its powerful oxidation in air with temperatures of
more than 600°C; therefore it is completely logical that with the
development of the sufficiently reliable coatings of the field of
application of tungsten alloys in technology considerably they will
be expanded.

One should note that working tungsten also presents specific
technological difficulties. Therefore at present during the creation
of new heat-resistant alloys on the basis of tungsten researchers
direct their efforts both for the perfection/improvement of
technology of production (improvement of methods of melting and the
decontamination of metals) and on improving technological and
mechanical properties because of the alloying of material.

Page 202.

In present section are represented the results of the
investigation of the strength properties and form of fracture of
tungsten, obtained by the methods of powder metallurgy and by
vacuum-arc melting. Furthermore, is shown the effect of alloying of

tungsten by some cell/elements on its heat resistance.

The part of the specimen/samples was made of cast tungsten, it is smelted in vacuum-arc furnace with the consumable electrode. The ingots of tungsten with a diameter of 80 mm were melted at approximately 20 kg/h in speed, then were subjected to hot deformation with 1400-1600°C with the degree of reduction 60-85o/o. As usual, the process of the deformation of tungsten was realize/accomplished in several stages accompanied by reheatings. With unrolling to sheet 1.5-2.0 mm in thickness deformation were conducted with prerecrystallization temperatures.

Remaining specimen/samples were prepared from the cermet tungsten, obtained by the common methods of powder metallurgy. Powdered metal of tungsten they pressed, sintered, and then they subjected to forging and annealing [3, 169].

In initial state the rods of cermet tungsten had a diameter of 8-10 mm, sheet - thickness 1.5-2.0 mm. For relieving the peening after strain molding/bars and sheets they annealed in vacuum with 1200°C for 1 h.

The chemical composition of the materials being investigated was given in Table 3.

From sheets and molding/bars, were cut out the blanks for manufacturing the tensile-strength specimens. Circular specimen/samples were machined on grinding machines and in final mind they kept a diameter of working section 4.0 mm.

On sheet blanks by initially anode-mechanical method broached holes 5 mm in diameter under mounting boards. Then sheet blanks in a quantity of 5-7 pieces were gathered into piles and after installation in special jig were ground on cutline/contour. The manufactured specimen/samples they thoroughly cleaned from projecting edges, and the working section of specimen/sample additionally was polished.

The mechanical properties of tungsten and alloys on its basis were determined during installation VTU-2V in vacuum 1.33 sn/m$^2$ (1·10$^{-4}$ mm Hg).

The results of the investigation of strength and plasticity of the pure tungsten at temperatures to 2700°C, obtained by the methods of powder metallurgy and by vacuum-arc melting, are given to Figs. 161 and 162 [35, s. 20]. On graphs are represented the average values of test results.

Page 203.

Test results attest to the fact that in the range of temperatures of 20-1600°C the strength properties of poured tungsten are considerably higher than cermet one. With an increase in the temperature of testing to 800°C, is observed a sharp reduction in the strength of cermet tungsten.
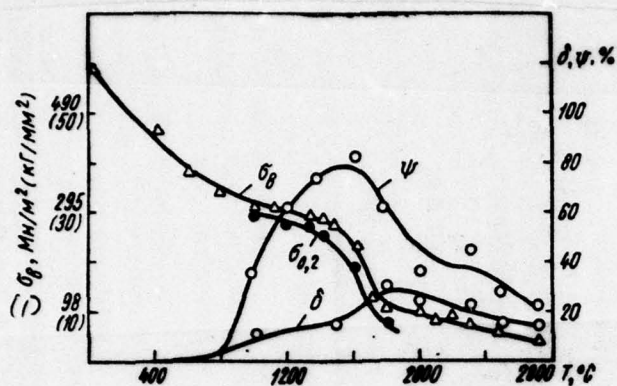
Fig. 161. Dependence of strength and plasticity of cermet tungsten on temperature.

Key: (1).     MN/m² (kg/mm²).
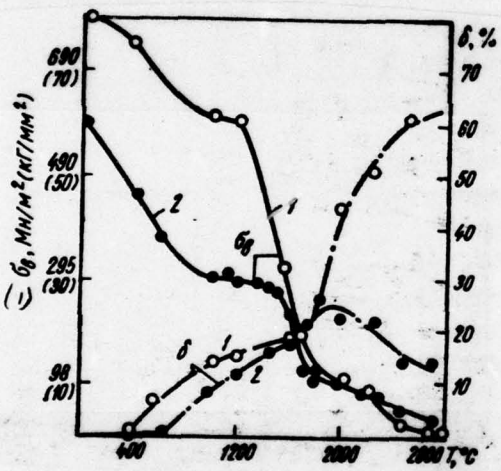


Fig. 162. The temperature dependence of strength and plasticity: 1 - poured tungsten; 2 - cermet tungsten.

Key: (1).     MN/m² (kg/mm²).

Page 204.

So, already at 1200°C limit of the strength of cermet tungsten is 295 mN/m² (30 kg/mm²), and for poured - 590 mN/m² (60 kg/mm²) with identical plasticity. With further increase of temperature, a difference in the values of ultimate strength is decreased and at 2000°C limits of the strength of the poured and cermet tungsten are equal to [~98.1 mN/m² (~10 kg/mm²)]; however, the plastic properties of the poured material are twice as high.

With temperatures higher than 2000°C strength of cermet tungsten somewhat higher than cast, but plasticity - only is temporarily lower, Analogous results obtained by Poil' - see [162]. The plastic properties of the poured tungsten in the range of temperatures of 2000-3000°C steadily grow/rise. The plastic properties of cast tungsten in the temperature range of 2000-3000°C continuously increase. Fig. 163 gives an illustration of the behavior of tungsten at the indicated temperatures.

A reduction in the plastic properties of cermet tungsten at temperatures is more than 2000°C connected, apparently, with the presence of different metallic and nonmetallic impurity/admixtures in

material, generatrices of the phase of implementation of the type of oxides, carbides and nitrides [45], the concentration of impurity/admixtures in intercrystalline zones continuously grow/rising at the temperatures more than 1800°C [167].

On microphotography/microphotographs of the structure of the specimen/samples of cermet tungsten after testing at the temperatures more than 2000-2200°C, are observed considerably wider boundary/interfaces in comparison with the poured tungsten (Fig. 164), which, apparently, confirms the representation of the considerable concentration of impurity/admixtures in intercrystalline zones, as a result of which of boundary/interface they possess lower chemical stability, than basis, and easily are etched [167].

The mechanical properties of alloys on the basis of tungsten are tested in essence on laminated specimens. Therefore, special interest they present the results of the test of the unalloyed tungsten, obtained in flat/plane laminated specimen/samples (1.2-2.0 mm in thickness). They are represented on Fig. 165. the general character of the dependence of strength and plastic properties of material in the form of sheets and rods on temperature proved to be analogous. To temperatures on the order of 800°C, values of limit of strength of poured laminated tungsten are higher than for the specimen/samples, manufactured from molding/bars and rods. It is obvious that this is

connected with the larger degree of the peening of sheet material. Is higher than 1700°C limit of the strength of the specimen/samples of laminated tungsten lower than for rods. It is possible that in this temperature range on strength characteristics have effect the flaw/defects in the form of flaws and laminations which were reveal/detected in the fractures of laminated specimen/samples and on sections during their study after destruction. Furthermore, was noted certain heterogeneity of material over the cross section of the laminated specimen/samples, tested in the temperature range of 1700-2600°C.

Page 205.
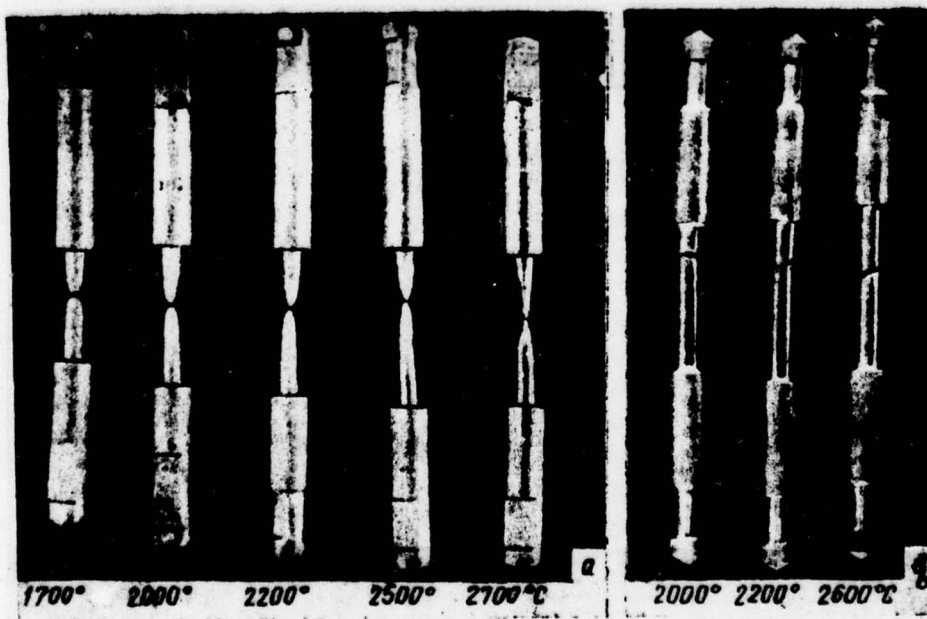


Fig. 163. Specimen/samples of tungsten after mechanical tests at the high temperatures: a) poured tungsten; b) cermet tungsten.

DOC = 78133007    PAGE 48 412

Page 206.



Fig. 164. Microstructure of tungsten after testing with 2500°C (x200).
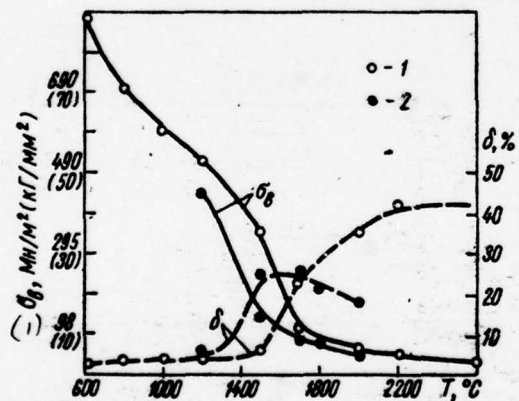


Fig. 165. Temperature effect on the mechanical properties of the laminated tungsten: 1 - poured; 2 - cermet.

Key: (1). MN/m² (kgf/m²).

Page 207.

On Fig. 166, are shown laminated specimen/samples of the poured tungsten, destroyed at temperatures of 2000-2600°C. After tests at temperatures higher than 2200-2300°C, observed considerable roughness and the coarsening of the surface of specimen/samples.

Thus, the strength properties of pure tungsten in the range of temperatures from 20 to 1700°C completely strongly depend on the production method and value of its surface finish and virtually do not depend on these factors at higher temperatures, which will agree with the data of the works of Harmon [168] and Jaffy - see [163].

The alloying of tungsten is very promising from the point in time, an improvement in its castabilities and tendency toward hot working, and also mechanical properties. Furthermore, alloying makes it possible to increase heat resistance and heat resistance and resistance of recrystallization [45, 166].

As a result of studies of the mechanical properties of the tungsten, alloyed by the small additions of molybdenum (to 1o/o), of titanium (to 0.02o/o), of niobium (to 0.05c/c) and of rhenium (to

0.Q5o/c), was reveal/detected an increase of the plasticity in
interval of 1500-2200°C by 15-20o/c in comparison with unalloyed
tungsten at the virtually identical values of ultimate strength. More
essential results can be obtained, by increasing the content in the
alloy of such alloying cell/elements as molybdenum and, especially,
rhenium, capable together with an improvement in the technological
properties and heat resistance to also neutralize the action/effect
of interstitial impurities and to considerably lower temperature of
transition in brittle state [3, 45, 163].

The investigation of the heat resistance of the poured alloys
W-Mo and W-Re was carried out in laminated and circular
specimen/samples in an interval of temperatures of 800-2800°C.

The results of the test of the poured pure tungsten and its
alloys from 3.12 to 67o/c (throughout mass)      Mo in state of strain
are given to Fig. 167. With temperatures higher than 1600°C, the
density properties of pure tungsten and alloys W-3o/c Mo and W-12o/o
Mo are virtually little distinguished; considerably more powerfully
is softened at these temperatures alloy W-67o/c Mo.

Fig. 166. Specimen/samples of sheet tungsten after tests with high temperature.

Page 208.
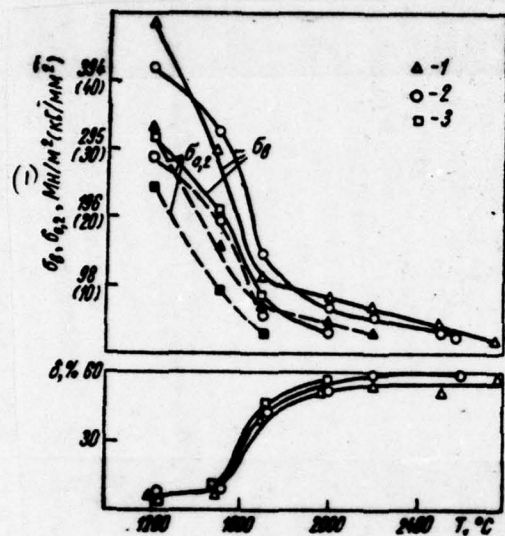


Fig. 167.
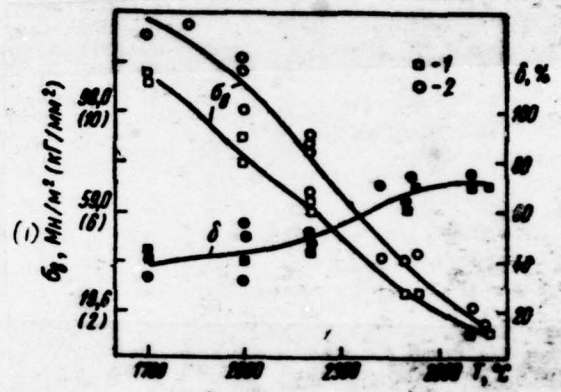


Fig. 1.68.

Fig. 1.67. The dependence of strength and plasticity of the tungsten-molybdenum alloys, which contain: 1 - 3c/o Mo; 2 - 12o/o Mo; 3 - 67o/o Mo.

Key: (1).     M N/m² (kg/mm²).

Fig. 168. The temperature dependence of strength and plasticity of alloy W+3o/o Mo: 1 - laminated specimen/samples; 2 - circular specimen/samples.

Key: (1).   MN/m² (kg/mm²).

Page 209.


During testing of round specimen/samples of alloy W-3o/o Mo, cut
cut from molding/bars, were obtained the higher values of ultimate
strength, than for flat/plate laminated specimen/samples, as is
evident on Fig. 168. (It should be noted that in the fractures of
some laminated specimen/samples after tests observed the longitudinal
microcracks).


Tungsten forms with molybdenum the continuous number of the
solid solutions for which the characteristically linear increase of
the melting point, module/modulus and density at an increase in the
content of tungsten [3, 22]. It turned out that for strength
properties also is fulfilled a similar dependence, as is evident from
test results, presented in Fig. 169.


The strength characteristics of alloys W-Re were determined in
flat/plane laminated specimen/samples in the range of temperatures
from 1200 to 2700°C. Test results are given to Fig. 170.
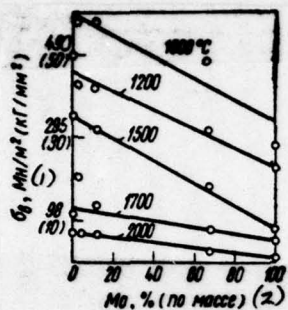
Fig. 169.
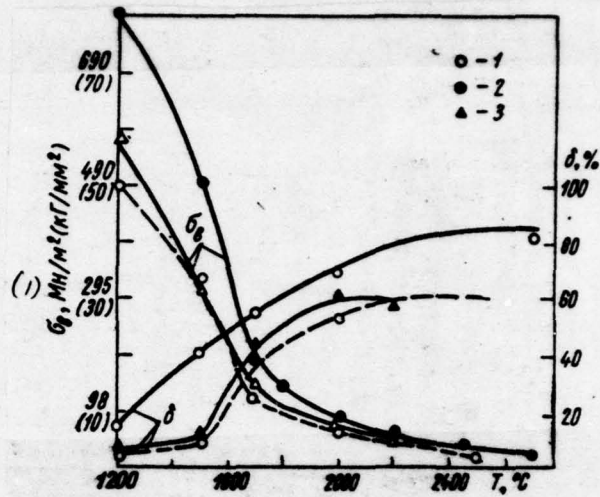


Fig. 170.

Fig. 169. Change of the limit of the strength of tungsten-molybdenum alloys in dependence on composition.

Key: (1). ——, mN/m² (kg/mm²).

Fig. 170. Temperature effect on the mechanical properties of the tungsten-rhenium alloys: 1 - pure tungsten; 2 - W-27o/o Re; 3 - W-1.2o/o Re.

Key: (1). ——, mN/m² (kg/mm²).

Page 210.

Ultimate strength and elongation per unit length of alloy W-27o/o Re
is considerably higher than for unalloyed tungsten. The strength
properties of the alloy indicated, was melted in vacuum-arc furnace,
render/showed were very close to the properties of the alloy of the
same composition, but subjected to cathode-ray remelting.

The high heat resistance of alloys W-Re is explained by
strengthening solid solution. Is expressed also assumption about the
fact that the positive effect of rhenium on the plasticity of
tungsten is connected with a change in the energy of interfaces, as a
result of which it is hinder/hampered by the formation of the
boundaries of the grains of solid films of oxides, which are usually
present in tungsten [165].

In Fig. 171 is given data on the strength properties some of
investigated alloys, and also pure tungsten. The comparison of these
results shows that during the introduction addition, especially
rhenium, it is possible to substantially raise strength and
plasticity of tungsten.
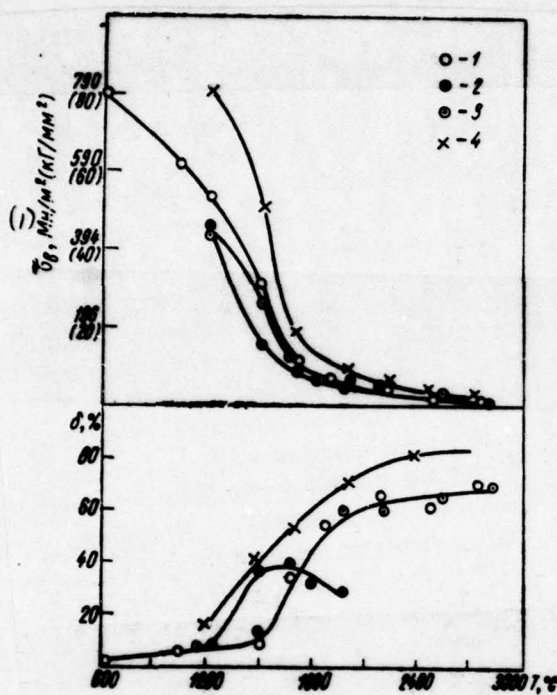
Fig. 171. The comparison of the strength and plastic properties of some alloys of the tungsten: 1 - tungsten poured; 2 - tungsten cermet; 3 - W-3o/o Mo; 4 - W-27o/o Re.

Key: (1). ——, MN/m² (kg/mm²).

Page 211.

So, at 1200°C limit of the strength of alloy W-27o/o Re is equal to 785 MN/m² (80 kg/mm²) in comparison with 520 MN/m² (53 kg/mm²) for the unalloyed tungsten. At temperatures is higher than 2200°C effect

of rhenium and molybdenum not so/such substantially. More considerable strengthening of tungsten can be reached by the introduction to oxide of thorium to quantity 1-2c/o, or the dispersed particles of carbide of tantalum [162].

The study of form of fracture of the specimen/samples of the poured and cermet tungsten detected the existence of several most characteristic temperature ranges of the process of destruction.

In the first range the destruction proceeded via breakaway, without noticeable signs of plastic flow: for the poured tungsten in the range of temperatures of 20-500°C, for cermet tungsten from 20 to 800°C.

In the second range occurred the decomposition of cermet tungsten in the range of temperatures from 1000 to 2000°C, for the poured tungsten - from 800 to 2200°C.

On Fig. 172a shows the typical viscous fracture of the specimen/sample of cermet tungsten after the tests with 1500°C. From the surface of the working section of specimen/sample is visible the developed network of cracks. In the case of the poured tungsten the appearance of macrofissures near the position of fracture could be observed at ~1700°C (Fig. 172b), the size/dimensions of these cracks

considerably were increased at ~2200°C.

The microstructural analysis of the specimen/samples of the poured and cermet tungsten showed that the cracks pass on boundaries of the grains (Fig. 173), i.e., in the second temperature range occurs intercrystalline fracture.

The third characteristic temperature range begins for cermet tungsten from 2000°C, for poured - from 2200°C. The specimen/samples of cermet tungsten in this temperature range failed themselves via breakaway, as is evident from Figs. 163b, 172a. A quantity of intergranular cracks considerably was decreased at the temperatures, close to 2600°C, separate grains were strongly deformed.

The specimen/samples of the poured tungsten after testing at temperatures of ~2500-2700°C did not have surface cracks (see Fig. 172d), Furthermore, during the investigation of specimen/samples near the position of fracture it was possible to note rough bands in the form of folds. Analogous bands observed on the single crystals of tungsten and molybdenum at the same temperatures [67, 12, s. 626].

Communication/connection of form of fracture of the specimen/samples of tungsten with the strength properties will be discussed at the end of the present chapter.

Molybdenum. The investigation of the mechanical properties of molybdenum and its alloys is carried out in the range of temperatures from 20 to 2000°C on the materials, obtained by the methods of powder metallurgy and by vacuum-arc melting.

Page 212.

The molding/bars of cermet molybdenum (by size/dimensions 15x15x500 mm), prepared on technology accepted [3, 73], were subjected to hot working in rotary forging machines at temperatures of 1200-1400°C before obtaining of the rods of the diameters of 8-10 mm.
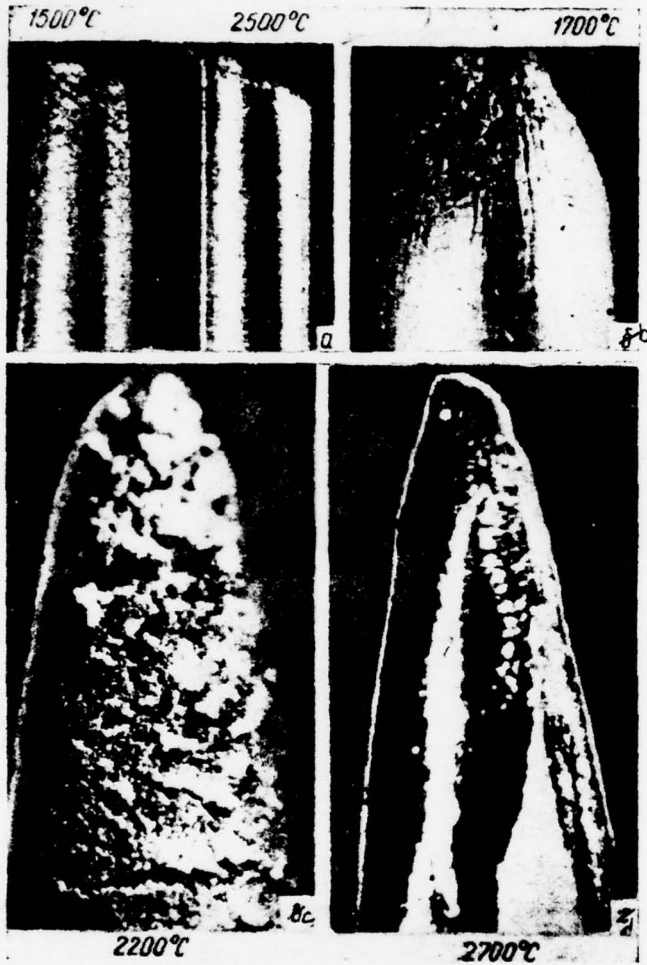
Fig. 172. Nature of the decomposition of tungsten at the high temperatures: a, b) cermet (x4); c, d) poured (x10).

Page 213.

The common/general/total impurity content in material on exceeded
0.1o/o, in this sum entered one-and-one-half oxides, nickel, oxides
of silicon, calcium and magnesium in the following quantities:
0.04o/o $R_2O_3$; 0.02o/o Ni; 0.03o/o $SiO_2$; 0.008o/o (CaO+MgO).

One batch of specimen/samples to heat treatment they did not
subject to, another batch they annealed in vacuum 1.33 sn/m² (1•10 ¹
sm Hg), for 1 h with 1450°C.

Cast molybdenum was obtained in vacuum-arc furnace with the
consumable electrode (rate of melting ~2 kg/min); it had the
following chemical composition: ~0.02o/o C, <0.001o/o Cr, Ni, Al, Ti;
<0.001o/o $H_2$, $N_2$ and ~(1-2)•$10^{-3}$o/o $O_2$.

The study of the strength properties was conducted in the
deformed and annealed specimen/samples (in vacuum with 1400°C for 1
h) of the poured molybdenum.

Was investigated also the effect of alloying on the mechanical
properties of molybdenum. Into the charge of the poured molybdenum,
they added by ~1o/o (throughout mass)    Nd.

Powder molybdenum they alloyed by the finely dispersed particles
$ZrO_2$ and ZrN in quantity 5-7o/o (throughout mass). Alloys Mo-$ZrO_2$ and

Mc-ZrN were obtained on technology, developed in the institute of the problems of the science of materials of AS UkSSR. The hot pressing was done at 1750°C. The obtained blanks tooled with the subsequent extrusion during the installation of the institute of the physics of metals of the AS USSR [170].
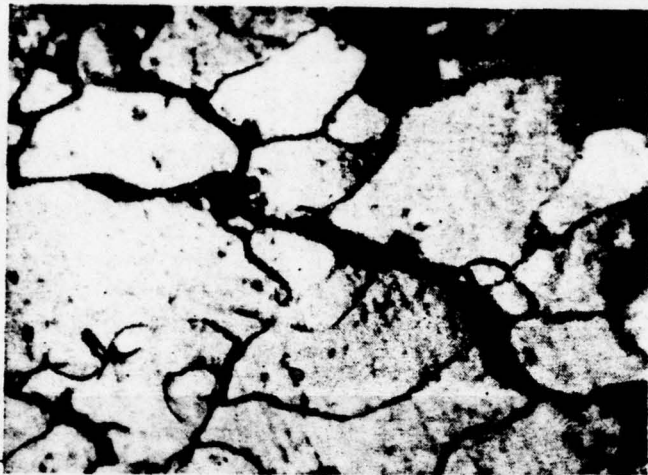
Fig. 173. Form of fracture of cermet tungsten with 2200°C (x500).

Page 214.

Short-time tests with elongation conducted both in the vacuum and in inert medium (helium) taking into account the systematic special feature/peculiarities, presented in Chapter I.

The results of the investigation of the strength properties of cermet molybdenum are given in Table 24 and on the poured molybdenum in Tables 25 and 26.

Table 24. Temperature effect on the mechanical properties of cermet molybdenum.

| (1) Температура испытания, °C | (2) σв, Мн/м² (кГ/мм²) | (2) σ0,2, Мн/м² (кГ/мм²) | δ, % |
|---|---|---|---|
| 20 | 510 (52,0) | 294 (30,0) | 35,0 |
| 300 | 314 (32,0) | — | 47,0 |
| 500 | 265 (27,0) | 78,5 (8,0) | 48,0 |
| 1000 | 167 (17,0) | 59 (6,0) | 47,0 |
| 1250 | 133 (13,5) | 55 (5,6) | 45,0 |
| 1300 | 110 (11,2) | 51 (5,2) | 43,0 |

Key: (1). Temperature of the testing, °C. (2). MN/m² (kg/mm²).

Table 25. Temperature effect on the mechanical properties of the deformed molybdenum of vacuum-arc melting.

| (1) Температура испытания, °C | (2) σв, Мн/м² (кГ/мм²) | (2) σ0,2, Мн/м² (кГ/мм²) | δ, % | ψ, % |
|---|---|---|---|---|
| 20 | 640 (65,0) | 515 (52,5) | 31,0 | 58,0 |
| 300 | 470 (48,0) | — | 32,0 | — |
| 1000 | 255 (26,0) | 226 (23,0) | 20,0 | 74,0 |
| 1250 | 114 (11,6) | 78,5 (8,8) | 42,0 | 92,0 |
| 1300 | 109 (11,0) | 62 (6,3) | 33,0 | 75,0 |
| 1500 | 44 (4,5) | — | 48,0 | — |

Key: (1). Temperature of testing, °C. (2). MN/m² (kg/mm²).

Table 26. Temperature effect on the mechanical properties of the annealed molybdenum of vacuum-arc melting.

| (1) Температура испытания, °C | (2) σв, Мн/м² (кГ/мм²) | (2) σ0,2, Мн/м² (кГ/мм²) | δ, % | ψ, % |
|---|---|---|---|---|
| 20 | 540 (55,0) | 325 (33,0) | 15,0 | 16,0 |
| 300 | 295 (30,0) | — | 52,0 | 86,0 |
| 1000 | 128 (13,0) | 59 (6,0) | 47,0 | 95,0 |
| 1200 | 98,1 (10,0) | 29,5 (3,0) | 50,0 | 98,0 |

Key: (1). Testing temperature, °C. (2). MN/m² (kg/mm²).

Page 215.


On Fig. 174, is shown the temperature dependence of strength and the plasticity of cermet molybdenum. During the first stage of the increase of testing, temperature occurs sharp reduction of strength [at 300°C limit of the strength of the work-hardened molybdenum it is approximately 392 MN/m² (40 kg/mm²)], with further increase of temperature to 1200°C tc curve is observed more slanting section.


The phenomenon of the considerable softening of cermet molybdenum at elevated temperatures they observed also during the investigation of the hot hardness (see Fig. 132).


At temperatures of testing more than 1100°C, occurs the intense softening of the cermet molybdenum (see Fig. 174), which in this case, apparently, is caused by the recrystallization, which takes

place in material at the temperatures indicated. In the temperature range of collecting recrystallization (1500-1800°C) the strength properties are measured less substantially.

Thus, on curved temperature dependence of strength of cermet molybdenum it is possible to separate, just as for tungsten, three breaks - one low-temperature at 300°C and two high-temperature - with 1080 and 1500°C.

Analogous course has the temperature dependence of strength and plasticity of the poured molybdenum of vacuum-arc melting (Fig. 175).

As can be seen from the presented results, the properties of molybdenum after peening and after annealing are distinguished completely insignificantly.
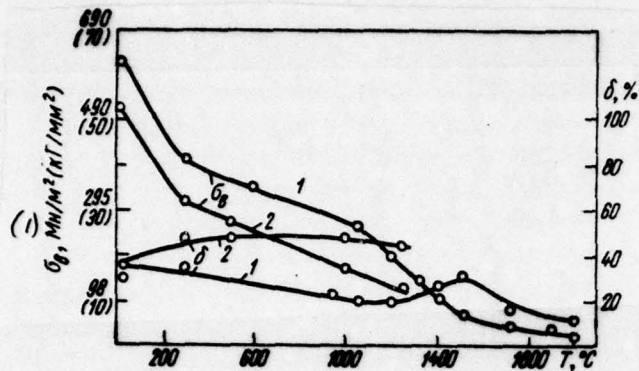
Fig. 174. Dependence of strength and the plasticity of cermet molybdenum on the temperature: 1 - deformed; 2 - annealed.

Key: (1). —, MN/m² (kg/mm²).

Page 216.

Certain increase of the limit of the strength of cermet molybdenum at temperatures is more than 1080°C, obviously, connected with higher impurity content which shift/shear the beginning of the recrystallization of the sintered material to the higher temperatures and to a certain extent brake its development. As it was shown in [4], in the case of the nonuniform distribution of impurity/admixtures in the sintered molybdenum wires, was observed the delay of recrystallization.
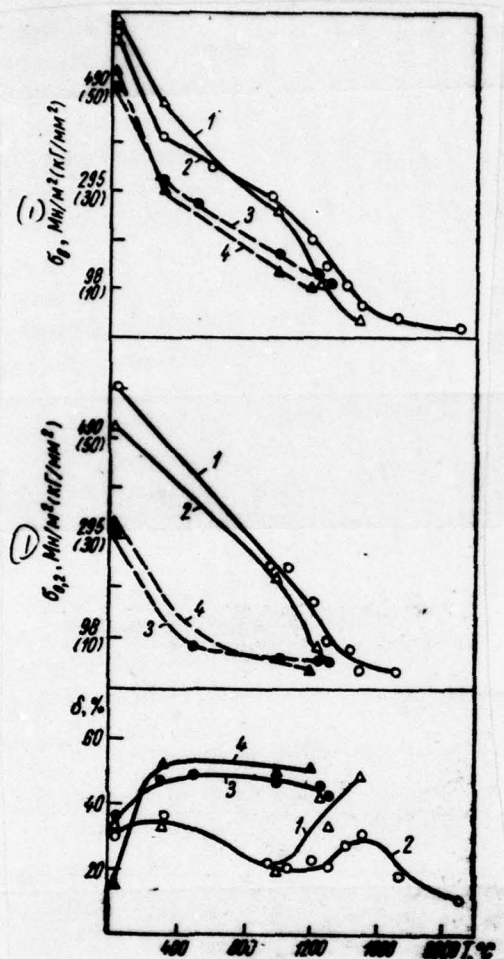
Fig. 175. The comparison of the temperature dependences of the mechanical properties of molybdenum in different state: 1 - poured; 2 - sintered; 3 - sintered and annealed; 4 - poured and annealed.

Key: I1). —, MN/m² (kg/mm²).

Page 217.

Furthermore, braking grain-growth can be attributed because of the effect of the dispersed particles of oxides on grain boundaries.

Work [12, p. 626] shows that in the specific temperature intervals the segregation of impurity/admixtures can lead to the decrease of cohesion/coupling between grains and, as a result, to a reduction in the strength properties, which, apparently, and was observed at temperatures of 20-300°C (see Fig. 174).

Fig. 176.



Fig. 177.

Fig. 176. Specimen/samples of cermet molybdenum after testing with 20°C.

Fig. 177. Form of fracture of the specimen/samples of the molybdenum: a) cermet, 20°C; b) the same, 1750°C; c) poured by 20°C.

Page 218.

The character of failure of the specimen/samples of molybdenum at room and high temperatures is shown on Figs. 176 and 177.

At room temperatures it was observed both the brittle and ductile fracture of the specimen/samples of cermet molybdenum with

necking, moreover in the latter case of $6 \div 30o/c$ and $\psi \approx 46\%$.     This difference in the plastic properties of the cermet molybdenum (research were conducted for two batches of specimen/samples, very close in composition) is connected with the fact that the room temperatures correspond to the range of transition from plastic state into brittle, which in the case of molybdenum stretches from -100 to +100°C [73].

Poured the molybdenum of vacuum-arc melting in all investigated temperature range had viscous fracture.
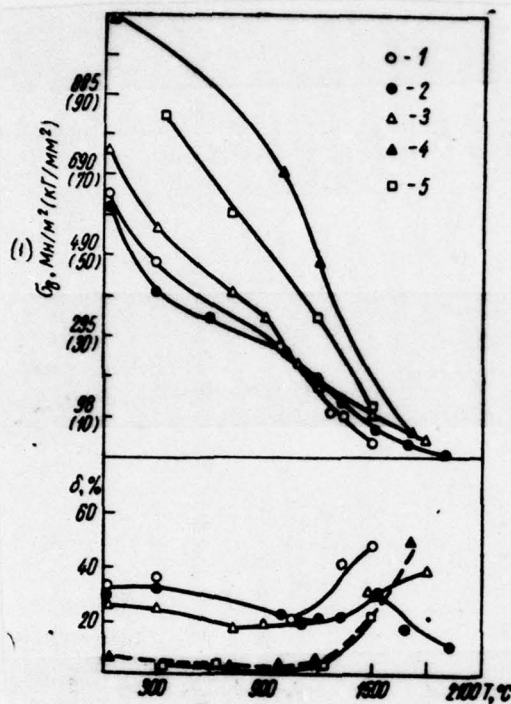
Fig. 178. The comparison of the mechanical properties of molybdenum and its alloys: 1 - molybdenum poured; 2 - cermet molybdenum; 3 - Mo-1o/c Nd; 4 - Mo-ZrN; 5 - alloy VM-1.

Key: (1). ___, MN/m² (kg/mm²).

Page 219.

On the surface of the specimen/samples of cermet molybdenum after tests at the temperatures higher than 1500-1600°, it was possible to note the large strains (see Fig. 177), which present

micro- and macrofissures on grain boundaries.

Thus the molybdenum of industrial purity/finish at temperatures higher than 1000°C loses strength, obtained during preliminary strain (rolling or forging). Consequently, an increase in the high-temperature strength of molybdenum depends on the increase of the temperature of recrystallization, which can be reached by alloying. In particular, is very promising the utilization of rare-earth metals as small ones addition to the refractory metals which, being deoxidizers and degasifers, also strengthen solid solution and increase the temperature of the beginning of recrystallization [172].

The investigation of the strength properties of alloy Mo-1o/o Nd showed that during introduction 1o/o Nd the limit the strength of material is increased by 23o/o. So, poured molybdenum has $\sigma_B=255$ MN/m² (26.0 kgf/mm²), and alloy Mo-1o/o Nd has ultimate strength, equal to 305-313 MN/m² (31-32 kg/mm²). Furthermore, as can be seen from Fig. 178, the threshold of softening somewhat is shift/sheared into the range of higher temperatures.

The more essential effect of strengthening molybdenum can be achieve/reached during the introduction of the finely dispersed particles of oxide of zirconium and nitride of zirconium (in quantity

DOC = 78133007    PAGE 75 438

5-7c/q), as is evident from the preliminary results, presented in Table 27 and in Fig. 178.

Temperature effect on the mechanical properties of niobium, tantalum and alloys on their basis.

Niobium, tantalum and especially alloys on their basis are promising structural materials for a work at elevated temperatures [21, 22, 24, 27, 78].

In this paragraph are represented the results of the investigation of strength and plasticity of the polycrystalline niobium of commercial frequency, obtained by the method of powder metallurgy, by vacuum-arc and electron-beam melting.

The chemical composition of the investigated materials was given in Table 3.

The specimen/samples of compact cermet niobium were prepared from initial molding/bars by length ~500 mm by section/cut 17x20 mm. From molding/bars were made circular specimen/samples 4.0 mm in diameter, laminated specimen/samples in final mind kept size/dimensions of section/cut 5x1.0 mm and length 60 mm. The part of the specimen/samples subjected to annealing with 1200°C for 1 h in vacuum 1.33 MN/m² (1·10⁻⁵ mm Hg).

Page 220.

The ingots of niobium and tantalum, smelted in vacuum-arc furnace, subject to consecutively to forging and unrolling to sheet 1.0 mm in thickness. One batch of specimen/samples they anneal at 1200°C for 1 h in vacuum 1.33 MN/m² (1•10⁻⁵ mm Hg).

Furthermore, the part of the molding/bars of cermet niobium they will remelt in cathode-ray setting up in the institute of the electric welding im. Ye. O. Paton. The obtained ingot 50 mm in diameter are subjected to the cold rolling. The value of reduction with first pass composes 70-80o/o. From sheet 7.0 mm in thickness in parallel to direction of rolling were cut the specimen/samples 3.0 mm in diameter and of working part 15 mm in lcng. The remaining part of the sheet 7.0 mm in thickness will roll out into sheet 1.0 mm in thickness. Flat/plane laminated specimen/samples have section/cut 5x1.0 mm and common/general/total length 60 mm.

As is known, niobium and tantalum are very sensitive to the conditions of test work (deformation rate, medium, etc.). For correct

estimation and the comparison of the obtained results, it is
necessary to have a representation of the basic systematic special
feature/peculiarities of tests.

Niobium and tantalum experience/test in vacuum not worse than
1.33 sn/m² (1•10⁻⁴ mm Hg) at operating temperatures (tantalum is
experience/tested at a pressure 2.66 MN/m² (2•10⁻⁵ mm Hg)⁄ inleakage
into vacuum system does not exceed 0.1 μl/s.

The part of the specimen/samples of cermet niobium test in
argon, in this case the total time of testing it is 5-10 min.

Table 27. High-temperature mechanical characteristics of molybdenum also of its alloys.

| Материал (1) | Предел прочности, Мн/м² (кг/мм²), при температуре, °C (2) | | | | Относительное удлинение, %, при температуре, °C (3) | | | |
|---|---|---|---|---|---|---|---|---|
| | 20 | 1000 | 1200 | 1700 | 20 | 1000 | 1200 | 1700 |
| Молибден металлокерамический, экструдированный (4) | — | 334—374 (34—38) | — | 54 (5,5) | — | 2—3 | — | 20 |
| Сплав Mo—ZrO₂ (5) | 942 (96) | 334—413 (35—42) | 128—158 (13—16) | 56 (5,7) | 13 | 1—2 | 5 | 13 |
| Сплав Mo—ZrN (6) | 1150 (113) | 670—710 (68—72) | 472 (48) | 55 (5,6) | 6 | 3—7 | 5 | 50 |

Key: (1). Material. (2). Limit of strength, MN/m² (kg/mm²), at temperature, °C. (3). Elongation per unit length, o/o, at temperature, °C. (4). Molybdenum (cermet, extruded). (5). Alloy.

Page 221.

Heating in vacuum manufacture under the following conditions:

1) slow temperature rise to 300°C with heating and degassing of system during 10-15 min during the maintenance of vacuum not worse than 2.66 MN/m² ($2 \cdot 10^{-5}$ mm Hg);

2) temperature rise to the assigned/prescribed values during 5

min; in this case, vacuum in system maintain within the limits of 3.99-5.32 MN/m² (3-4•10⁻⁵ mm Hg):

3) holding before loading not more than 3 min;

4) testing during 10-15 min, which corresponds to the velocity of loading $v_3 = 0.4-0.6$ mm/min either rate of relative deformation $v_\epsilon = 5 \cdot 10^{-4}$ s⁻¹.

The measurement of strain and the determination of yield limit was manufactured with the aid of microcathetometer or by the periodic photographing of the clearance between the lug/lobes, welded to the knob/caps of tensile-strength specimens.

Niobium. The strength and plastic properties of niobium are determined in the range of temperatures from 20 to 1900°C.

The temperature dependences of the mechanical properties of the niobium, obtained by the methods of powder metallurgy, by vacuum-arc melting and cathode-ray remelting, are represented in Fig. 179-181.
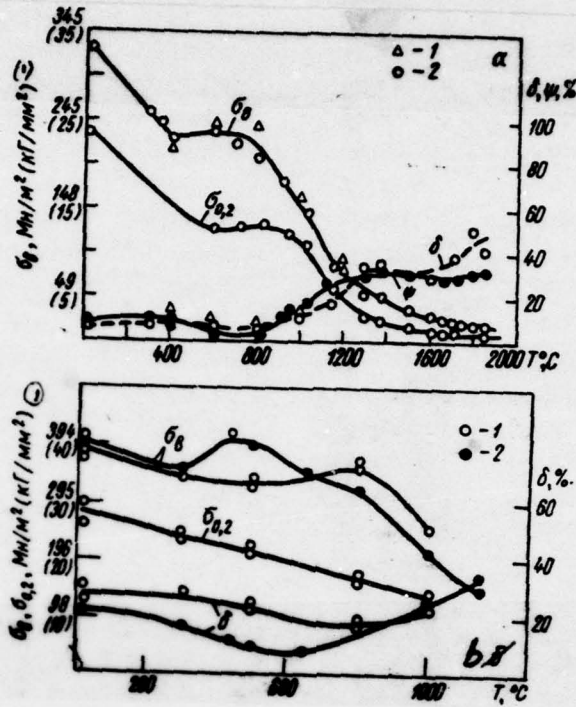
Fig. 179. The dependence of the mechanical properties of cermet
niobium on the temperature: a) deformed (rod); b) the sheet, annealed
at 1200°C in vacuum; 1 - vacuum; 2 - argon.

Key: (1). MN/m² (kg/mm²).

Page 222.

Figures 179a shows that the limit of the strength of rod cermet
niobium with the increase of temperature is decreased to 226 MN/m²
(23.0 kg/mm²) at 400°C. Subsequently is observed the small increase

$\sigma_B$ to 236 MN/m² (24 kg/mm²) at 600-800°C, which can be caused by aging process under conditions of heating under the action/effect of stress. Furthermore, a change in the strength and plastic properties of niobium can be caused by the contamination of the surface layers of material, if during test work by protective medium is technical argon or helium and time of tests relatively greatly (15-20 min). In Fig. 179 for a comparison, are given the results, obtained during the tests in inert medium and in vacuum, from which it follows that an increase in ultimate strength and a reduction in the plasticity of laminated cermet niobium (Fig. 179b) at ~500°C is caused by the effect of the impurity/admixtures, which are contained in argon.

The tests of the poured niobium of vacuum-arc plate/bar and after cathode-ray remelting are conducted in vacuum. Nevertheless on the curved temperature dependence of the strength of the niobium of vacuum-arc melting (Fig. 180) at ~500°C is observed considerable peak.

It is known that the maximums on the curves of the temperature dependence of the internal friction of niobium with 200 and 400°C [97] and straight-line relationship of the modulus of elasticity with small lift curved in the temperature range of 500-800°C [21] are caused by presence in the material of carbon, nitrogen and oxygen. Thus, is a specific interrelation between the phenomena, observed during the study of strength and internal friction, and also the elasticity characteristics of niobium.
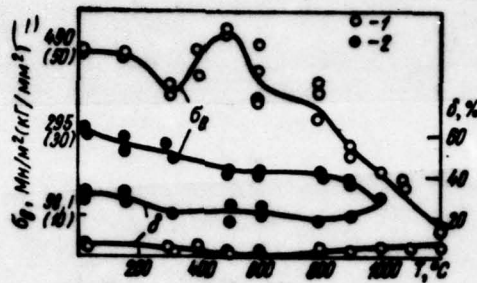
Fig. 180. The temperature dependence of the limit of strength and plasticity of the poured niobium of the vacuum-arc melting: 1 - deformed; 2 - annealed.

Key: (1). MN/m² (kg/mm²).

Page 223.

Furthermore, works [20, 163] show, that the interstitial impurities in niobium and tantalum with 500-800°C brake movement of dislocation and thereby they lead to the increase of ultimate strength.

The expressed above considerations confirm the results of the investigation of the strength and plastic properties of the niobium of the high surface finish value, obtained after mono- and twofold remelting during cathode-ray setting up. These results are

represented in the form of graph in Fig. 181, from which it follows that ultimate strength with the increase of temperature is decreased monotonically.

Form of fracture of the specimen/samples of niobium at high temperatures illustrates Fig. 182. After tests is observed considerable cracking over an entire surface of the working section of the specimen/sample of cermet niobium, at the same time in the specimen/samples of the poured niobium of cracks, it was not. Crack formation they observe in the process of the deformation of sintered nickel [160], and also of molybdenum and tungsten, as interlocked in the preceding/previous paragraphs.

For the specimen/samples of the deformed niobium of cathode-ray remelting in the range of temperatures of 20-800°C, was characteristic small plastic deformation in the range of neck.

As a result of the conducted investigations, establish/installed that the strength properties of pure niobium in the temperature range of 900-1000°C are relatively low and therefore further increase of its heat resistance and heat resistance can be reached by alloying. In connection with this were investigated the strength properties of niobium fusions with different content of molybdenum, tungsten, zirconium and vanadium.
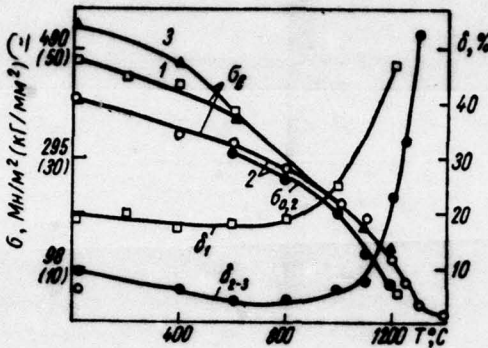
Fig. 181. Temperature effect on the mechanical properties of the niobium of electron-beam melting: 1 - after the single remelting of rods; 2 - twofold remelting of rods; 3 - the same, specimen/samples laminated.

Key: (1). MN/m² (kg/mm²).

Page 224.

Alloys were obtained via the remelting of the welding/bars of niobium in electron-beam furnace, after which to annealed in vacuum for 1 h with 1400°C.

The comparison of the obtained results makes it possible to make the conclusion that the alloying of niobium with the cell/elements indicated increases the limit of strength with 1200°C by 50-60o/o (Table 28). It is necessary to note that at these temperatures noticed the essential difference between the strength of three- and four-component alloys.
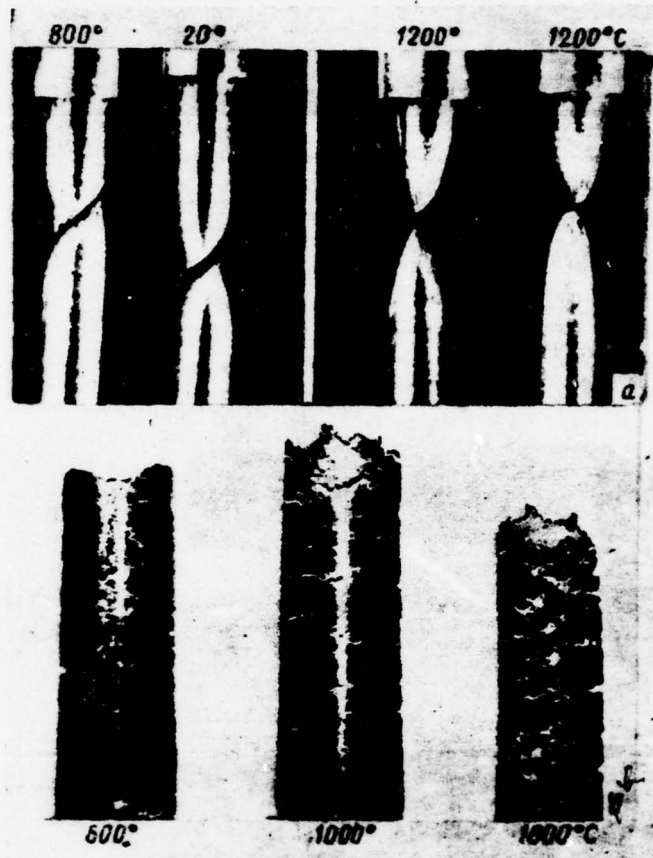
Fig. 182. Specimen/samples cf niobium after the mechanical tests: a) poured, testing in vacuum (x4); b) cermet, testing in argon (x6).

Page 225.

The temperature dependences of the mechanical properties of the investigated materials are given tc Fig. 183.

Table 28. Mechanical properties of niobium and niobium alloys with 1200°C.

| Материал (1) | σ<sub>в</sub> MN/м² (кГ/м.м²) (2) | δ, % |
|---|---|---|
| Металлокерамический ниобий (3) | 78,5—88,5 (8,0—9,0) | 30,0 |
| Ниобий электроннолучевого переплава (4) | 59 (6,0) | 47,5 |
| Nb —Mo—W—Zr | 13,8 (14,0) | 20,0 |
| Nb—Mo—W | 128 (13,0) | 22,0 |
| НРМЦ—3 | 149 (15,0) | 18,0 |

FOOTNOTE 1. Alloys were obtained on technology, developed by I. S. Malashenko in the institute of the electric welding of AS UkSSR.

Key: (1). Material. (2). MN/m² (kg/mm²). (3). Cermet niobium. (4). Niobium of cathode-ray remelting.
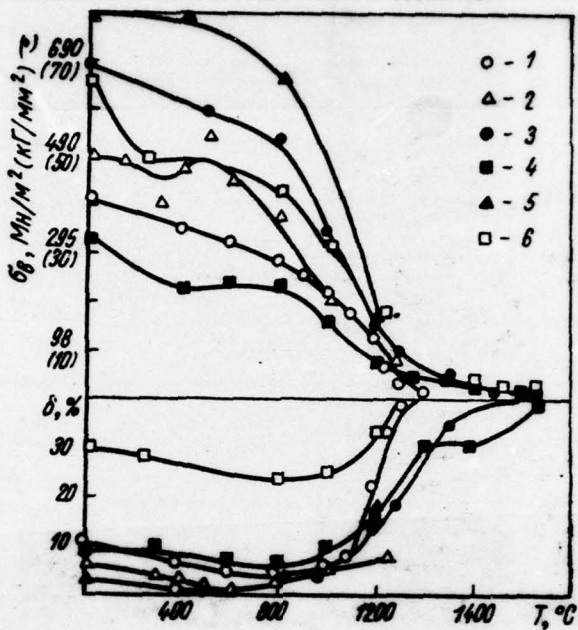
Fig. 183. Comparison of mechanical properties of niobium, obtained by different methods: 1 - electron-beam melting, sheet; 2 - vacuum-arc melting, sheet; 3 - powder metallurgy, sheet; 4 - the same, rod; 5 - alloy VN-2, sheet; 6 - the same, rod.

Key: (1). MN/m² (kg/mm²).

Page 226.

Tantalum and its alloy. Temperature effect on the mechanical properties of pure tantalum illustrates Fig. 184. As can be seen from

data given to the figure, with the increase of testing, temperature the limit of the strength of deformed tantalum (cathode-ray remelting) monotonically descends to 44 MN/m² (4.5 kg/mm²), and elongation per unit length - to 3-40/o, at 650-800°C; during further temperature rise, the elongation per unit length is increased to 40-50o/o. On the curved temperature dependence of the strength of cold-worked tantalum, it is possible to note the small area/site, which testifies to strengthening in the range of temperatures of 650-800°C. Somewhat larger strengthening they observed during the investigation of recrystallized tantalum (vacuum-arc melting) (see Fig. 184).

Strengthening tantalum (just as niobium) in the process of deformation they usually relate with the effect of interstitial impurities. So, works [27, 173] show, that oxygen causes strengthening tantalum with ~350°C, and at higher temperatures the most effective strengthened/hardened action/effect exerts nitrogen, the value of peaks in strength curves depending on oxygen concentration and nitrogen in tested material.

On the aging processes of materials under stress, as is known, it is possible to judge by the discontinuity of deformation in the process of the loading of material. During the test work of recrystallized tantalum in the temperature range of 600-650°C and

alloy Ta-3o/o W at 800°C, observed characteristic teeth on diagram load - deformation (Fig. 185), which testify to the unstable character of plastic deformation.

The obtained results of the investigation of the strength of unalloyed tantalum will agree with literature data [27, 162, 173].
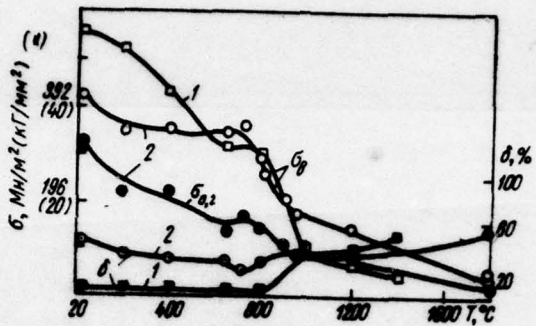
Fig. 184. Temperature effect on the mechanical properties of pure tantalum: 1 - electron-beam melting, cold-worked (sheet - 1.0 mm); 2-vacuum-arc melting, the annealed sheet (1300°C, 1 h).

Key: (1). MN/m² (kg/mm²).

Page 227.

For example, it is shown, what recrystallized tantalum at room temperature has the limit of strength 440-490 MN/m² (45-50 kg/mm²) and elongation per unit length within limits of 26o/o, at temperature of 750°C - with respect to 345 MN/m² (35 kg/mm²) and 40o/o; with the increase of temperature to 1000°C, ultimate strength is decreased to 177-197 MN/m² (18-20 kg/mm²), and elongation per unit length in this case composes 30-5,0o/o. The conducted investigations show that the strength properties of pure tantalum at high temperatures are relatively low. However, tantalum has sufficiently good plasticity in

the wide temperature range and therefore it can serve as basis for
many alloys. By prospecting investigations [27] establish/installed
that tungsten as the alloying cell/element was capable to
considerably increase the high-temperature strength cf tantalum
fusions as a result of the formation of solid solutions and increase
of the temperature of recrystallization. In this case, tantalum
fusions with tungsten possess good technological properties.

The mechanical properties of alloys Ta-W are investigated in the
range of temperatures from 20 to 1800°C. On the basis of experimental
data, are constructed curved changes of the limit of strength and
plasticity in dependence on the composition of alloy Ta-W at the
investigated temperatures. It is establish/installed that the
alloying of tantalum with tungsten causes a considerable increase in
the strength both at room and at high temperatures (Fig. 186).
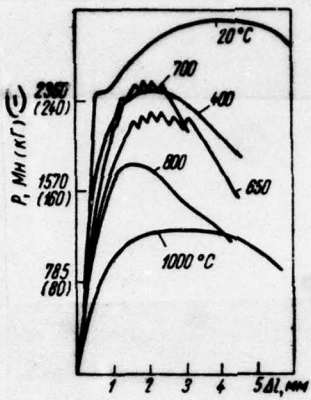
Fig. 185. Stress-strain diagrams of tantalum. Key: (1). MN(kgf).
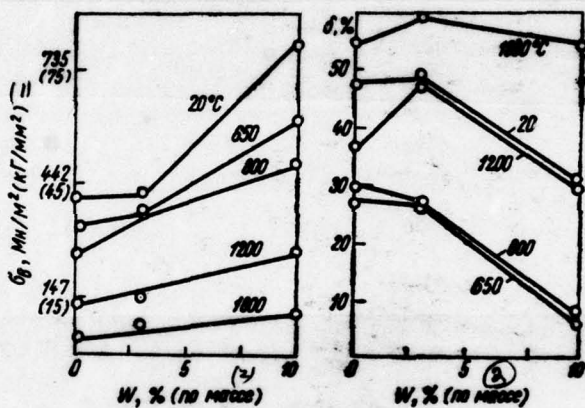


Fig. 186. Dependence of strength and plasticity of alloy Ta-W on content of tungsten.

Key: (1). MN/m² (kg/mm²). (2). (throughout mass).

Page 228.

The plastic properties of alloys with an increase in the content of tungsten deteriorate. Highest strength properties with satisfactory plasticity possesses alloy Ta-10o/c W.

The investigations of mechanical properties at high temperatures were carried out for alloy Ta - 10c/o W in laminated specimen/samples. The obtained results are represented in Fig. 187, where for a comparison are given also data for pure tantalum. Alloy Ta-10o/o W (in as-received condition) as a result of peening has the high strength properties which are retained approximately to 1200°C.

The plastic properties of the annealed material in the range of temperatures from 20 to 800°C are considerably higher than for that work-hardened (laminated). In the case of the annealed material at temperatures of 650-800°C, as in the case of pure tantalum, is observed the dip of plasticity, which, apparently, is connected with the effect of interstitial impurities.

The decomposition of specimen/samples in all investigated temperature range bears viscous character, with exception of temperatures of 650-800°C, when some specimen/samples of the annealed alloy have brittle failure.

Common/general/total laws governing deformation and decomposition of

refractory metals with static loading.

In the preceding/previous paragraphs of this chapter, were represented the results of the investigation of the temperature dependences of strength and plasticity of refractory metals and alloys on the basis of tungsten, molybdenum, niobium and tantalum. Is accumulated the sufficiently large experimental material (is investigated more than 40 alloys on the basis of refractory metals); therefore it is expedient to generalize some.
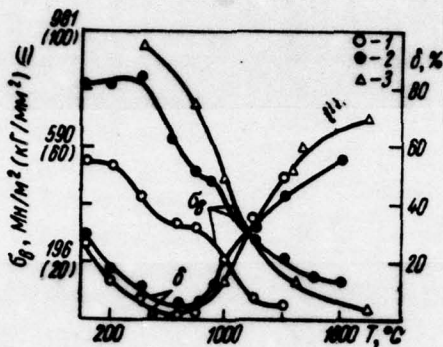
Fig. 187. The comparison of the dependences of the strength and plastic properties of tantalum and its alloys on the temperature: 1 - tantalum of electron-beam melting, sheet; 2 - Ta - 10o/o W, rod; 3 - that - 10o/o W, sheet.

Key: (1). MN/m² (kg/mm²).

Page 229.

For this purpose it is possible to draw a comparison of the mechanical properties of the investigated metals and alloys at high temperatures, to show the possibility of the analytical description of the temperature dependence of these properties, and to also establish/install communication/connection of the laws, obtained for the strength properties, with the results of measuring of hardness,

module/moduli of elasticity and internal friction of high-melting
materials in the wide temperature range.

The temperature dependences of the mechanical properties some of
the investigated metals and the alloys are given in comparison to
Fig. 188 for the specimen/samples, obtained from sheets and rods.
Data this figure make it possible to manufacture the evaluation of
the possibility of use of these materials in the
construction/designs, working under varied conditions. It should be
noted that the bearing capacity of parts and structural cell/elements
at high temperatures it is possible to estimate only on the basis of
the data on stress-rupture strength and creep; however the
information about mechanical ones to properties, obtained during
short-time tests, sufficient for the selection of the materials which
are intended for the articles, working during short time intervals.

As it follows from Fig. 188, at 1200°C pure niobium and its
alloys have very close values of the mechanical properties: $\sigma_b$
=138-158 MN/m$^2$ (14-16 kg/mm$^2$) and $\delta$=18-22o/c; molybdenum pure/clean
and alloyed has ultimate strength more than 197 MN/m$^2$ (20 kg/mm$^2$),
but molybdenum fusion with nitride of zirconium - 472 mN/m$^2$ (48
kg/mm$^2$). The alloys of tantalum with tungsten and tungsten alloys at
this temperature also retain the high values of mechanical
properties. At temperatures of ~1500°C, alloys on the basis of

molybdenum have limit of strength ~118-197 MN/m² (12-20 kg/mm²),
tantalum fusion with tungsten - 197 MN/m² (20 kg/mm²), but pure
tungsten and its alloys - is more than 295 MN/m² (30 kg/mm²). It is
completely logical that at temperatures it is more than 1800°C most
expedient to utilize tungsten and its alloys.

When selecting of the materials, intended for a work at high
temperatures, is necessary to consider many different factors, such
what speed and the method of the load application, the source
distribution of heat, dependence of strength and modulus of
elasticity of material on temperature, the duration of work, and also
relation to the strength of material to its density [161]. In
connection with this is carried out the comparison some of the
investigated refractory metals and the alloys in the value of ratio $\sigma_B$
/$\gamma$ (Fig. 189). From curve/graph Fig. 189 shows that the niobium and
molybdenum alloys to 1200°C, and alloy Mo+ZrN to 1500°C in comparison
with tantalum and tungsten alloys have great advantages during the
utilization of the construction/designs whose total weight is
limited.

Page 230.
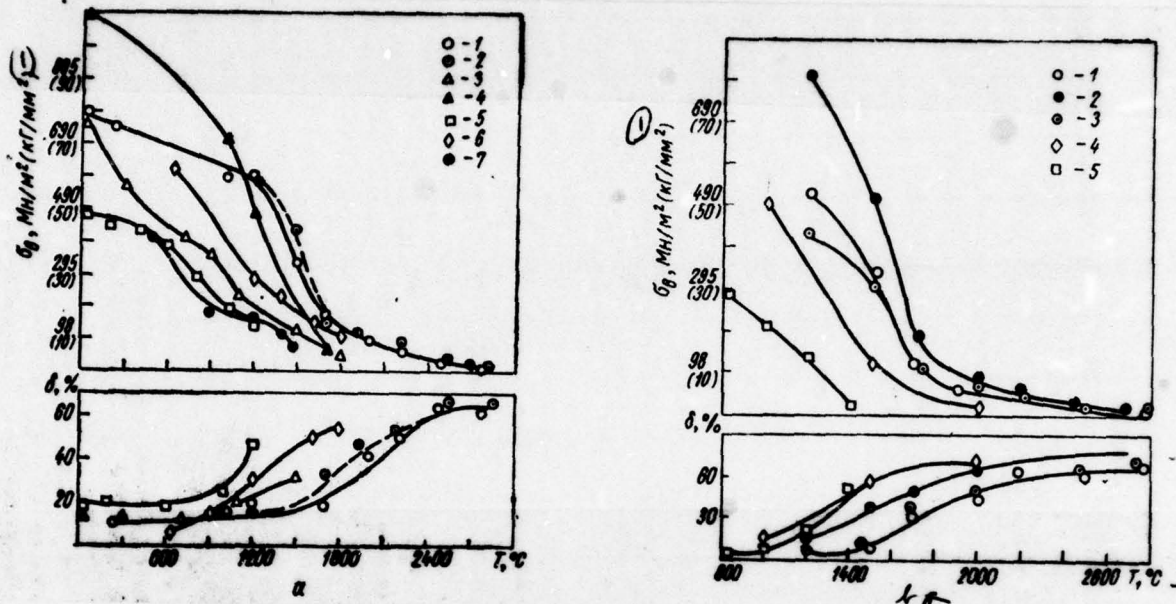


Fig. 188. Comparison of strength and plastic properties of investigated refractory metals: a) specimen/samples make made of molding/bars (1 - tungsten poured pure/clean; 2 - W-3o/o Mo; 3 - molybdenum poured alloyed; 4 - Mo-ZrN; 5 - niobium poured; 6 - alloy Ta-10o/o W poured; 7 - Cr-4c/o V - 0.5o/o Nb); b) laminated specimen/samples (1 - tungsten poured deformed; 2 - W - 27o/o alloy Be poured; 3 - alloy W - 3c/i Mo poured; 4 - alloy Ta - 10o/o W poured; 5 - niobium poured).

Key: (1). MN/m² (kg/mm²).

Page 231.

Research and comparison of the mechanical properties of
different metals is expedient to conduct at congruent (homologous)
temperatures [19, 186, 192] and in this case to the temperature
dependence of mechanical properties to present in the coordinates of
common ones: $\sigma_{\text{в}} = f\left(\dfrac{T}{T_{\text{пл}}}\right)$, or semilogarithmic ones $\ln\sigma = f\left(\dfrac{T}{T_{\text{пл}}}\right)$. In the
latter case more distinctly are developed the characteristic features
of the behavior of different metals with a change in temperature. So,
from the results, presented Fig. 190 it is apparent that shows in
temperature range to $0.4T_{\text{пл}}$ the strength properties depend to a
considerable extent on the degree of preliminary peening, the
purity/finish of the metal and many other factors, while in the range
of temperatures, which exceed $0.5T_{\text{п.л.}}$   the strength properties they do
not virtually depend on the state of the material (experimental
points are packed to one curve).

Many researchers' works establish/installed that the temperature
dependences of the characteristics of the resistivity of metallic
materials to deformation can be expressed with the aid of following
equation [174-178]:

$$M_2 = M_1 e^{-\alpha(t_2 - t_1)}, \quad (5.1)$$

where $M_1$ - mechanical characteristic at temperature $t_1$:

$N_2$ - the same, at temperature $t_2$;

$\phi$ - temperature coefficient.

By S. I. Gubkin he established that the temperature coefficient depends on following factors:

1) the character of the stressed state;

2) the degree of deformation;

3) the rate of deformation (the greater the deformation rate, the lesser the temperature coefficient);

4) the coefficient of external friction;

5) the physicochemical state of substance [176, 178].

Ye. M. Savitskiy will assume that many phenomena and the processes, connected with the transition of material from unsteady state into more stable, and also with formation and increase in the nuclei of new phase (recrystallization, crystallization, relaxation, diffusion, etc.), sufficiently accurately describes exponential temperature dependence [178].
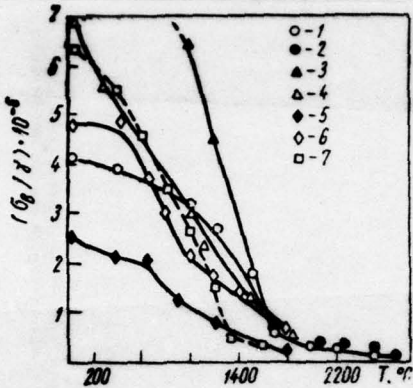
Fig. 189. The dependence of the specific strength of refractory metals and alloys on the temperature: 1 - tungsten poured pure/clean; 2 - W - 3o/o alloy Mo poured; 3 - Mo-ZrN; 4 - molybdenum alloyed: 5 - tantalum poured pure/clean; 6 - Ta-10o/o W; 7 - niobium poured pure/clean.

Page 232.

Westbrook [179] will examine in detail the numerous data on the dependence of hardness on temperature, and also the existing equations of the temperature dependence of hardness, and it will arrive at the conclusion that Ito [180] and independent of it to V. F. Shishokin [174] they will propose the most satisfactory expression of this dependence

$$H = Ae^{-\alpha T}, \qquad (5.2)$$

where T - temperature, °K;

A - value of hardness, extrapolated to 0°K;

$\alpha$ - temperature coefficient.

The expression of Ito-Shishokin predicts the finite value of hardness with absolute zero and the tendency of hardness toward zero with the infinite increase of temperature.

During the logarithmic operation of expression (5.2) we obtain the dependence

$$\ln H = \ln A - \alpha T, \qquad (5.3)$$

being the equation of straight line. In actuality dependence is proved to be more complex and graph ln H-T takes the form of broken line. Furthermore, the temperature dependence of the hardness of the metals, subjected to aging, is not subordinated to equation (5.2).

Breaks on graphs ln H-T are of two types: with sharp vertical rupture or with sudden slope deviation without rupture.
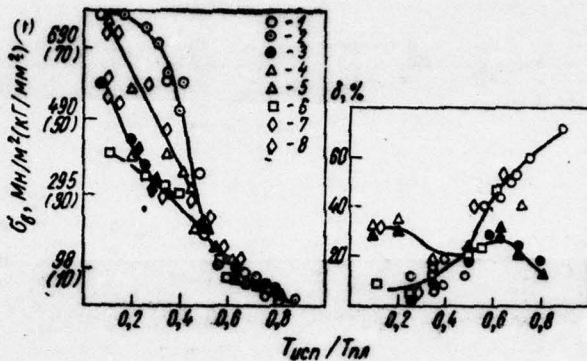
Fig. 190. The dependence of the strength and plastic properties of refractory metals on the temperature: 1 - tungsten poured; 2 - tungsten alloy; 3 - tungsten sintered; 4 - molybdenum poured; 5 - molybdenum sintered; 6 - niobium poured; 7 - tantalum alloy; 8 - tantalum poured.

Key: (1). MN/m² (kg/mm²).

Page 233.

First type break with rupture is observed for those metals which have allotropic change at this temperature, for example for cobalt, titanium, zirconium (Fig. 191)[1].

FOOTNOTE [1]. Graphs in Fig. 191-194 are constructed according to M. G. Lozinskiy's data [107]. ENDFOOTNOTE.

For cobalt at the temperature, equal to $0.42T_{nn}$, or to the homologous temperature, equal to 0.42, occurs the abrupt change in the value of hardness, connected with transformation $\alpha \to \beta$. The analogous transformation of titanium occurs at homologous temperature 0.58, and for zirconium - with 0.53.

Second type break with slope deviation occurs at temperatures about $(0.5-0.55)T_{nn}$. This high-temperature break observe many researchers.

Westbrook [179] examines these hardnesses, available in the literature, and will establish/install the universality of high-temperature break.

Figures 192 and 193 depict the temperature dependences of the hardness of pure metals with pronounced high-temperature break. The temperature dependences of the hardness of polycrystalline and single-crystal copper (Fig. 194) show that in the case of single crystals the high-temperature break is misaligned to the side of higher temperatures (s. 0.55 to 0.69).

By Petti [181] are brought the proofs of the fact that for some metals there is second type one additional break near room temperature. Low-temperature discontinuity of curves H-T for tungsten and molybdenum is observed at temperatures below $0.2T_{nn}$    (Fig. 195).
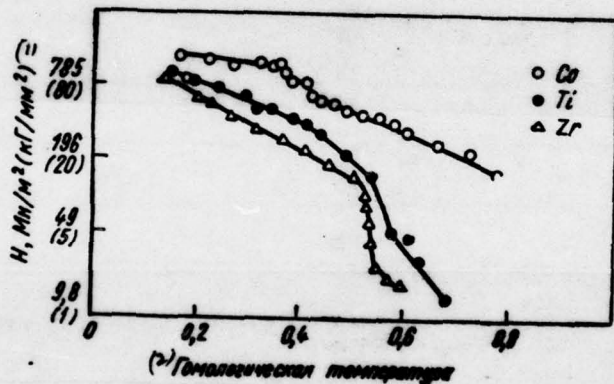


Fig. 191. The temperature dependences of the hardness of cobalt, titanium and zirconium.

Key: (1). MN/m² (kg/mm²). (2). Homologous temperature.

Page 234.
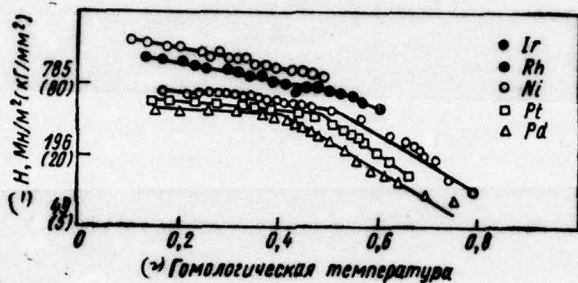


Fig. 192. Temperature dependences of hardness of iridium, rhodium, nickel, platinum, palladium.

Key: (1). MN/m² (kg/mm²). (2). Homologous temperature.
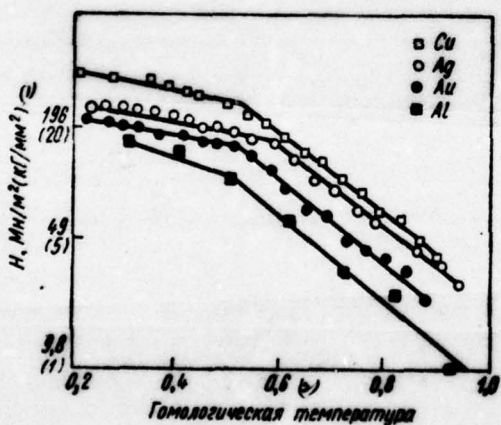


Fig. 193.          Fig. 194.

Fig. 193. Temperature dependences of the hardness of copper, silver, gold, aluminum.
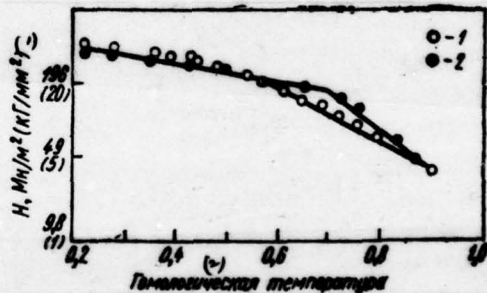
Key: (1). MN/m² (kg/mm²). (2). Homologous temperature.

Fig. 194. Temperature dependences of hardness poly- (1) and single-crystal (2) copper.

Key: (1). MN/m² (kg/mm²). (2). Homologous temperature.

Page 235.

Was determined the hardness of silver, gold, nickel, platinum and iron at temperatures to -183°C (Fig. 196). It turned out that for these materials the break occurs at temperatures below $0.1 T_{nn}$.

Petti notes that the curves of the temperature dependences of the strength characteristics of chromium, molybdenum, tungsten, tantalum and vanadium also have low-temperature break.

Both low-temperature and high-temperature breaks usually relate with a change in the mechanism of deformation.

Figures 197, 198 give the temperature dependences of the hardness of of those deformed of tungsten and molybdenum and annealed of tungsten, molybdenum and tantalum, constructed in semilogarithmic coordinates.
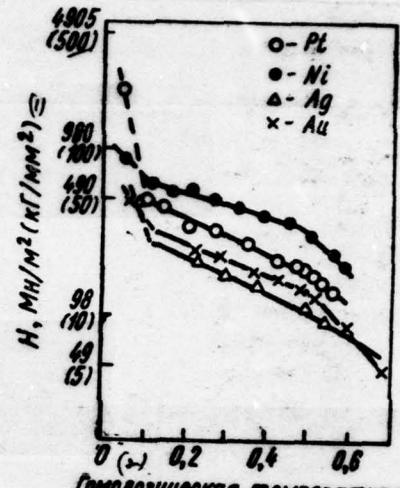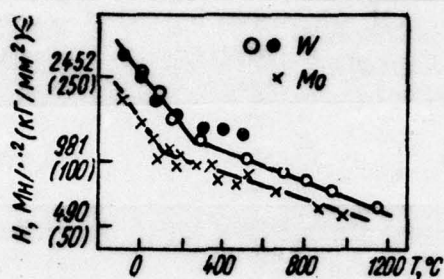
Fig. 196.

Fig. 195. The temperature dependences of the hardness of tungsten and molybdenum [181].

Key: (1). MN/m$^2$ (kg/mm$^2$).

Fig. 196. Temperature dependences of hardness of platinum, nickel, silver and gold [181].

Key: (1). MN/m$^2$ (kg/mm$^2$). (2). Homologous temperature.

Page 236.
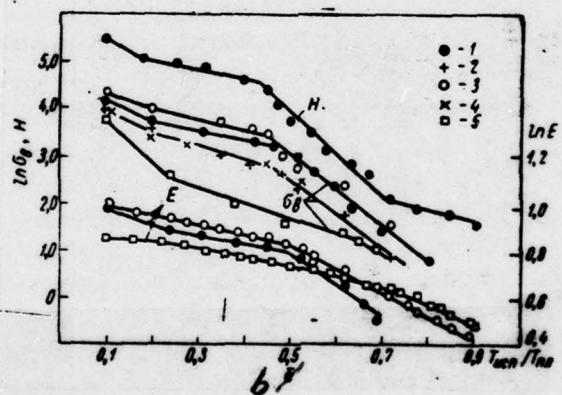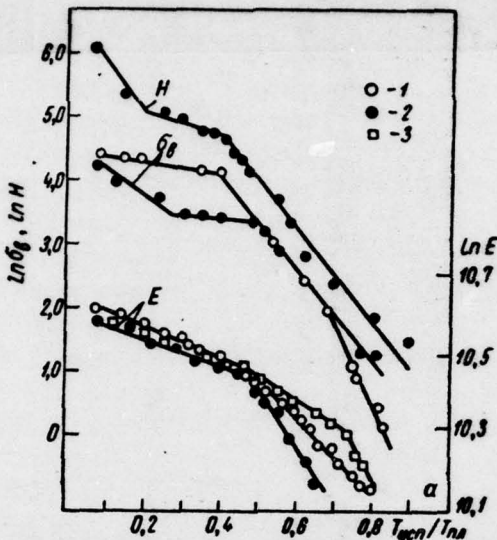


Fig. 197. Dependence of limit cf strength, hardness and modulus of elasticity of tungsten and molybdenum from temperature: a) tungsten (1 - poured, 2 - sintered, 3 - single crystal); b) molybdenum (1 - poured deformed, 2 - poured annealed, 3 - sintered, 4 - the same, annealed, 5 - single crystal).

annealed, 5 - single crystal).

Page 237.

They have two breaks: low-temperature and high-temperature. The position of breaks depends on the degree of the deformation: the more it, fact more powerfully is misaligned second type break to the side low-temperature ones.

The measured values of hardness sufficiently well fit a straight line of all three sections of dependence (5.2) with two constants for each section A and $\alpha$.

It is easy to show (analytically or graphically) that from the constants $A_1$, $A_2$, $A_3$, which are the values of hardness, obtained by extrapolation to $0°K$ each section, it is possible to change to more substantiated by the constant $H_0$, $\Pi_1$ and $\Pi_2$ and expressions (5.2) for sections to record in the form:

$$H = H_0 e^{-\alpha_1 T} \quad \text{при} \quad 0 < T \leqslant \Pi_1. \qquad (5.4)$$
$$H = k_2 H_0 e^{-\alpha_2 T} \quad \text{при} \quad \Pi_1 \leqslant T < \Pi_2; \qquad (5.5)$$
$$H = k_3 H_0 e^{-\alpha_3 T} \quad \text{при} \quad \Pi_2 \leqslant T < T_{пл}. \qquad (5.6)$$

Key: (1). with.

where $H_0$ - value of hardness with $0°K$ (is obtained by the

extrapolation of the low-temperature section of dependence);

$\alpha_1$, $\alpha_2$ and $\alpha_3$ - temperature coefficients of hardness;

$\Pi_1$ and $\Pi_2$ - value of temperature, $^{\circ}K$, that correspond to low- and high-temperature breaks.

In this case,

$$k_2 = e^{-(\alpha_1 - \alpha_2)\Pi_1} \tag{5.7}$$

and

$$k_3 = e^{-(\alpha_1 - \alpha_2)\Pi_1 - (\alpha_2 - \alpha_3)\Pi_2}. \tag{5.8}$$

In general form of formula (5.4) - (5.6) they will be recorded:

$$H = k_n H_0 e^{-\alpha_n T}, \tag{5.9}$$

moreover $k_1 = 1$, and $k_2$ and $k_3$ they are determined from formulas (5.7) and (5.8).
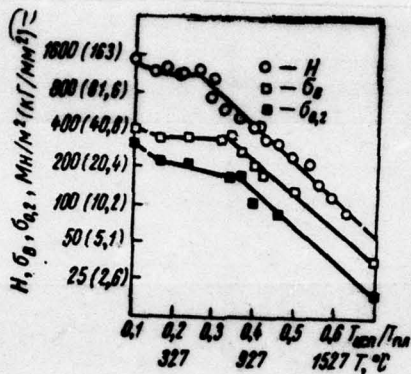
Fig. 198. The temperature dependences of some mechanical properties of tantalum.

Key: (1). MN/m² (kg/mm²).

Page 238.

The values of constants $H_0$, $k_n$ and $\alpha_n$ for the temperature dependences of hardness (5.9) of tungsten and molybdenum are calculated according to the method of least squares and are given in Table 29.

The temperature dependences of the strength of a number of the investigated metals and alloys in semilogarithmic coordinates are also represented in Fig. 197 and 198, their values are packed sufficiently well to the graphs, which consist of straight portions

and the having bends at the specific homologous temperatures.

Consequently, dependences are subordinated to exponential law (5.1), them it is possible to describe by the expression Frantsevich-Vratskiy:

$$\sigma_e = Be^{-\beta T}, \qquad (5.10)$$

where T - temperature, °K;

B - value of ultimate strength, extrapolated to 0°K;

$\beta$ - temperature coefficient of ultimate strength.

The graph/diagram of dependence (5.10) for tungsten, molybdenum and tantalum has three sections with two by the constants B and $\beta$ for each.

Table 29. Values of coefficients in the equation of the temperature dependence of the hardness of molybdenum and tungsten.

| (1) Материал | (2) Состояние | (3) $H_0$, $MN/m^2$ ($\kappa\Gamma/mm^2$) | $\beta_1 \cdot H_0$, $MN/m^2$ ($\kappa\Gamma/mm^2$) | $\beta_1 \cdot H_0$, $MN/m^2$ ($\kappa\Gamma/mm^2$) | $a_1 \cdot 10^{-3}$ | $a_2 \cdot 10^{-3}$ | $a_3 \cdot 10^{-3}$ |
|---|---|---|---|---|---|---|---|
| (4) Вольфрам марки ВРК | (5) Деформированный | 12 600 (1 260) | 2700 (270) | 16 100 (1 610) | 3,54 | 0,674 | 1,89 |
| | (6) Отожженный | 12 500 (1 250) | 1930 (193) | — | 4,35 | 0,791 | — |
| (7) Молибден марки МРН | Деформированный | 4 200 (420) | 1700 (170) | 9 700 (970) | 1,83 | 0,674 | 2,16 |
| | Отожженный | 2 900 (290) | 770 (77) | — | 2,32 | 0,221 | — |

Key: (1). Material. (2). State. (3). MN/m² (kg/mm²). (4). Tungsten of mark/brand of VRK. (5). Deformed. (6). Annealed. (7). Molybdenum of mark/brand of MRN.


Page 239.


As in the case of the temperature dependence of hardness, expression for individual sections it is possible to record in the form:

$$\sigma = \sigma_0 e^{-\beta_1 T} \quad \text{при} \quad 0 < T \leqslant \Pi_1^\circ;$$
$$\sigma = m_2 \sigma_0 e^{-\beta_2 T} \quad \text{при} \quad \Pi_1^\circ \leqslant T \leqslant \Pi_2^\circ; \quad (5.11)$$
$$\sigma = m_3 \sigma_0 e^{-\beta_3 T} \quad \text{при} \quad \Pi_2^\circ \leqslant T < T_{пл},$$

Key: (1). with.


or in general form

$$\sigma = m_n \sigma_0 e^{-\beta_n T}, \qquad (5.12)$$

where $\sigma_0$ - value of the limit of strength with $0°K$ (it is obtained by the extrapolation of the low-temperature section of dependence);

$\beta_1$, $\beta_2$ and $\beta_3$ - temperature coefficients of ultimate strength;

$\Pi_1^\sigma$ and $\Pi_2^\sigma$ - value of temperature, $°K$, for low- and high-temperature breaks;

$m_1$, $m_2$ and $m_3$ - constants for individual sections, they are equal to:

$$m_1 = 1;$$
$$m_2 = e^{-(\beta_1 - \beta_2) \Pi_1^\sigma};$$
$$m_3 = e^{-(\beta_1 - \beta_2) \Pi_1^\sigma - (\beta_2 - \beta_3) \Pi_2^\sigma}.$$

$(5.13)$

The values of constants $\sigma_0$, $m_n$ and $\beta_n$ for the temperature dependences of the limit of the strength of tungsten and molybdenum are calculated according to the method of least squares and are given in Table 30.

Relative to the physical nature of the breaks on the graph/diagrams of temperature dependences $\sigma_n$, $\sigma_T$, $H$ and $E$ in the literature there are different opinions. In particular, breaks relate

with the relaxation processes, which take place on boundaries of grains [154, 187], with a change in the mechanism of plastic deformation [190, 192], with the reaction of dislocations [193].

For the molybdenum and the tungsten, obtained by the methods of powder metallurgy, break they observed at the temperatures, comprising $0.2-0.3T_{пл}$ (see Fig. 197). Analogous low-temperature breaks for pure metals are reveal/detected by researchers' series [154, 187], moreover for molybdenum and tungsten at the same temperatures [181].
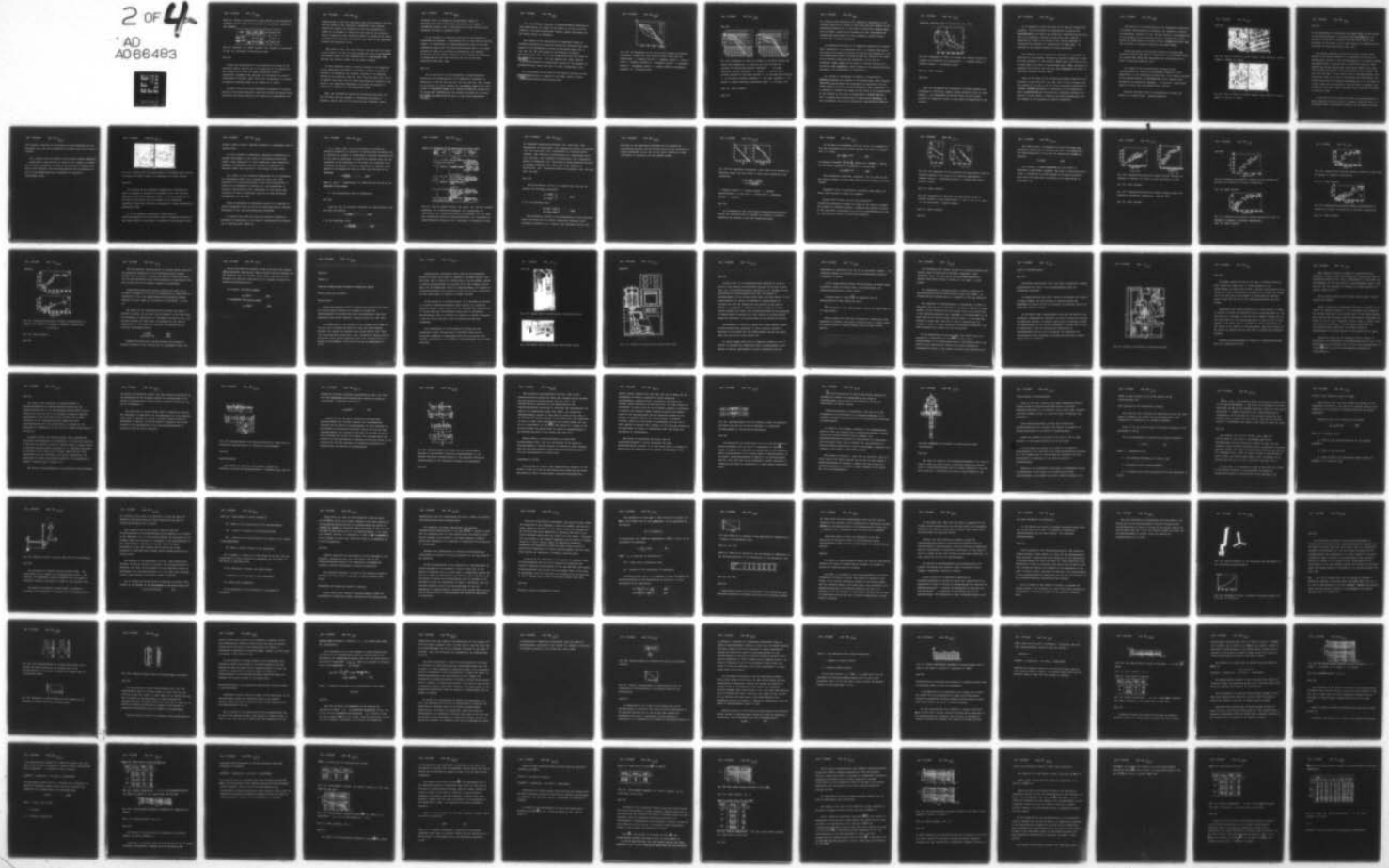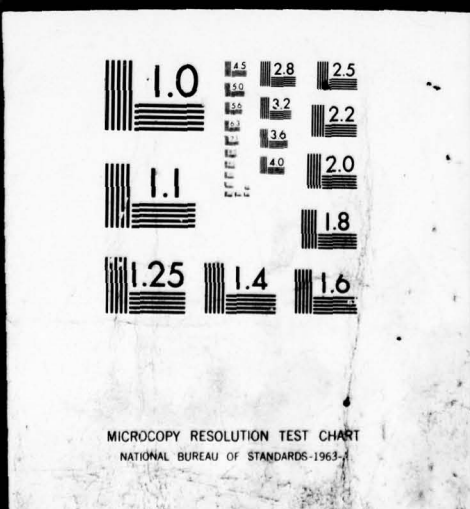
Table 30. Values of coefficients in the equation of the temperature dependence of the limit of the strength of the deformed molybdenum and tungsten.

| Материал (1) | $\sigma_0$, МН/м² (кг/мм²) (2) | $m_1\sigma_0$, МН/м² (кг/мм²) | $m_2\sigma_0$, МН/м² (кг/мм²) | $\beta_1 \cdot 10^{-3}$ | $\beta_2 \cdot 10^{-3}$ | $\beta_3 \cdot 10^{-3}$ |
|---|---|---|---|---|---|---|
| Вольфрам марки ВРН (3) | — | 590 (59) | 4 760 (476) | — | 0,452 | 1,63 |
| Молибден марки МРН (4) | 1000 (100) | 520 (52) | 16 000 (1 600) | 1,50 | 0,444 | 2,90 |

Key: (1). Material. (2). MN/m² (kg/mm²). (3). Tungsten of mark/brand of VRN. (4). Molybdenum of mark/brand of MRN.

Page 240.

During the investigation of the dissipation of energy in the refractory metals, carried out in the institute of the problems of the strength of AS UkSSR, for cermet molybdenum noticed a considerable increase of the decrement of fluctuations in range of temperatures $0.2-0.25T_{nn}$, while during the investigation of tungsten of essential anomalies, they do not observe up to 1000°C.

In work [171] on the curved temperature dependence of internal friction in the same temperature range they observe the maximum whose appearance the authors explain by the reaction of dislocations with

admixed atoms. At the same time these works [189] attest to the fact
that the curves of the temperature dependence of the internal
friction of tungsten and molybdenum do not have maximums up to
1000°C. It is possible to assume that the peaks in the scattering
curves of energy for some refractory metals are caused by the effect
of interstitial impurities and depend on the level of the applicable
stresses and deformation rate.

Data given to Fig. 199, also attest to the fact that the breaks
in the curves ln $\sigma$-T for the poured molybdenum (both in the deformed
and annealed state) are very insignificant at temperatures $\sim 0.2T_{nn}$
and they are virtually absent for the poured tungsten.

In this connection there is special interest in the comparison
of the temperature dependences of strength, hardness and moduli of
elasticity of molybdenum and tungsten, obtained by the different
methods of the production (see Fig. 198). From data given Fig. 199 it
is apparent that shows only for cermet molybdenum and tungsten in the
curves of the temperature dependence of hardness and modulus of
elasticity is observed the low-temperature break.

Thus, our experimental results and literature data [154, 181,
187, 188] show that the presence of low-temperature break of
refractory metals, just as of low-melting ones (aluminum, nickel,

titanium, etc.), it depends on purity/finish (degree of decontamination from interstitial impurities), the degree of preliminary peening, rate of deformation and other factors, which determine the state of material [188].

It is necessary to especially note that if the behavior of molybdenum and tungsten - cell/elements VI A of the group of periodic system - is subordinated to common/general/total laws in the wide temperature range, then for niobium and tantalum from v A of group, inclined to aging in the process of deformation, are observed deviations from the general character of the temperature dependence of properties not only with low ones, but also at the high temperatures (see Fig. 200).

Page 241.

Let us now move on to the examination of high-temperature sections on the graph/diagrams of the temperature dependence of properties. As can be seen from Fig. 199 (see also Fig. 200), breaks in the curves ln $\sigma$-T are observed for molybdenum, tungsten and their alloys in temperature range, which comprise $0.4-0.5 T_{nn}$ for niobium and its alloys when $0.35-0.45 T_{nn}$ but for tantalum and alloys on its basis the breaks are moved into the range of even lower temperatures - $0.3-0.35 T_{nn}$.

for the materials, subjected to recrystallization annealing at high temperatures, the breaks in the curves ln $\sigma$-T and ln E-T are observed at the same temperatures; they are absent from curves for the single crystal of molybdenum.

The results of the investigation of temperature effect on mechanical properties of refractory metals and literature data with respect to the dissipation of energy in refractory metals [97, s. 123, 188, 154, 193] and changes in the mechanism of plastic deformation [188, 190: 192] at high temperatures show that bends in the curves ln ($\sigma$, E, H) - T at the temperatures, which comprise $0.35—0.5\,T_{\text{пл}}$,

$\wedge$ it is not possible to unambiguously explain by the phenomena of recrystallization, which take place at these temperatures [154].

So, the entrance of the study of the internal friction of wire specimen/samples made of tungsten of brand ВА-3 [189] at 1500°C $(\sim 0.5\,T_{\text{пл}})$

$\wedge$ was reveal/detected grain-boundary peak.
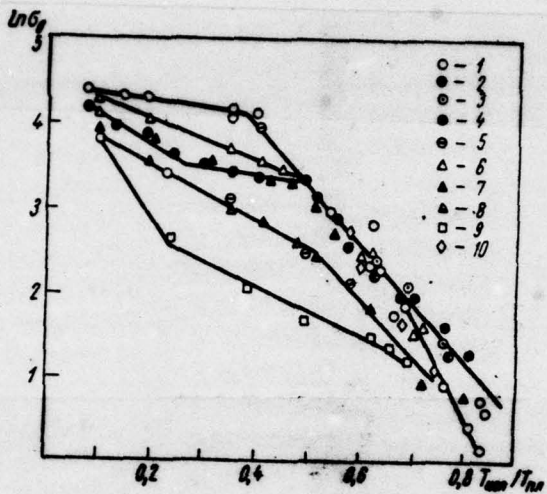
Fig. 199. The dependence of the limit of the strength of tungsten, molybdenum, chromium and some alloys on their basis from the temperature: 1 - tungsten poured; 2 - tungsten cermet; 3 - W-Mo; 4 - W-Re; 5 - tungsten annealed; 6 - molybdenum poured; 7 - molybdenum cermet; 8 - molybdenum poured; 9 - single crystal of molybdenum annealed; 10 - chromium poured.

Page 242.
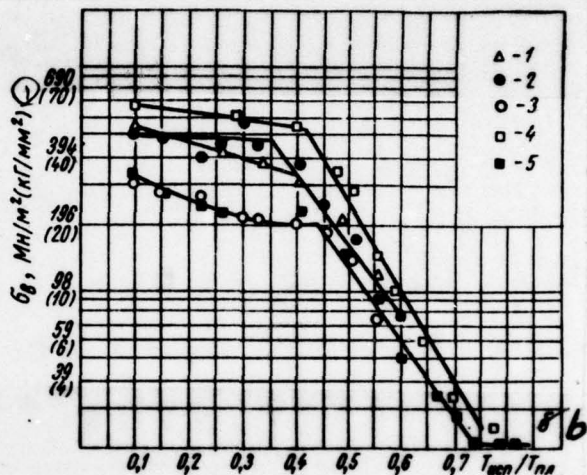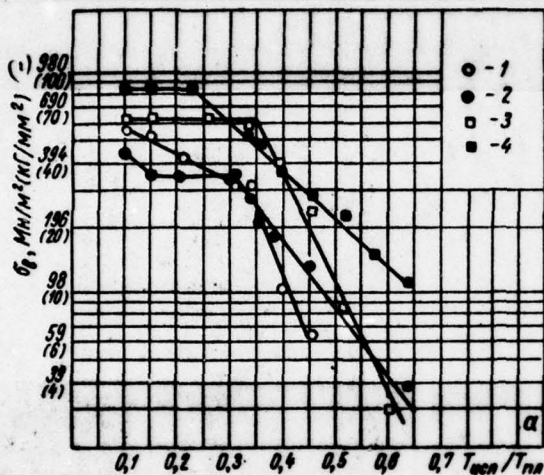


Fig. 200. Dependence of limit of strength of refractory metals and alloys from temperature: a) tantalum and alloy Ta-10o/o W; 1 - tantalum of electron-beam melting (deformed); 2 - the same, vacuum-arc melting (annealed); 3 - cermet; 4 - Ta-10o/o W; b) niobium, obtained by different methods: 1 - by electron-beam melting; 2 - by vacuum-arc melting, deformed; 3 - the same, annealed; 4 - by method of powder metallurgy (deformed); sheet; 5 - the same, rod.

Key: (1). MN/m² (kg/mm²).

Page 243.

As a result of the analysis of the temperature dependences of the internal friction of a series of pure polycrystalline metall, it is establish/installed [97, s. 165] that in temperature range $0.4-0.5T_{nn}$ also are peaks, caused by the existence of grain boundaries; was assumed that these peaks it is not possible to explain only by viscous shift of grain boundaries.

In connection with this it is completely interesting to examine data, obtained by L. N. Aleksandrov and V. S. Mordyuk [193] during the study of the internal friction of tungsten and molybdenum at the high temperatures which in comparison with our results of the tests of the strength properties are represented in Fig. 201. In temperature range $\sim 0.46T_{nn}$ in the curve of internal friction are a relaxation peak, apparently, caused thermal by the promote/activated processes of the displacement of dislocations.

As a result of the thermal activation of dislocations in deformed molybdenum and tungsten at the temperatures, which comprise $0.35-0.45\ T_{nn}$, are developed the processes of polygonization and are formed stable dislocation boundary/interfaces, that, apparently, it is possible to consider the reason for the delay of an incidence/drop in the strength in the range of temperatures indicated (see Fig. 197). It should also be noted that at temperatures $0.35-0.45\ T_{nn}$ is very considerable the role of interstitial impurities and different

additicn, affecting positicn breaks [46, 18E, 193].
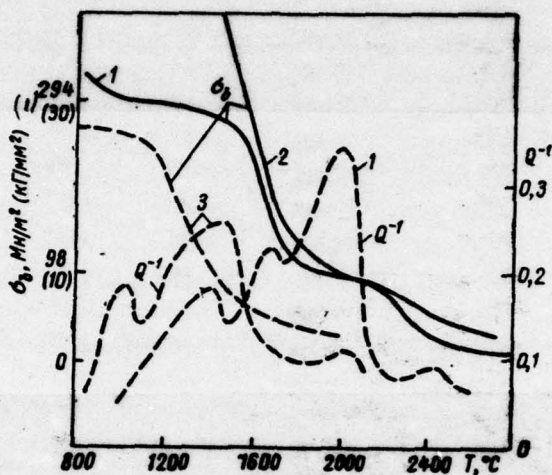


Fig. 201. Dependence of limit cf strength and internal friction of tungsten and molybdenum frcm temperature: 1 - tungsten cermet; 2 - tungsten poured; 3 - molybdenum cermet.

Key: (1). MN/m² (kg/mm²).

Page 244.

With the increase cf the temperature cf testing tungsten and molybdenum to 0.48-0.5 $T_{nn}$ occurs intense scftering [193], on graph property - the temperature is cbserved break and with further increase of temperature occurs a rather sharp ircidence/drop in the strength.

It is necessary to also note that in the range of temperatures $0.4-0.5\ T_{nn}$ on the processes of polygonization is applied the recrystallization and appear new grains with undistorted lattice [46, 193]. It is possible; therefore in some works [162, 188] the appearance of a peak in the curves of the internal friction of polycrystalline materials at temperatures more than $0.5\ T_{nn}$ is explained by the viscous behavior of grain boundaries.

The comparison of the temperature dependence of the modulus of elasticity of the tungsten, measured by resonance (frequency ~5 kHz) and pulse (frequency ~5 MHz) methods, showed that in the latter case to curve there is no bend at temperatures $\sim 0.5\ T_{nn}$. This, obviously, is connected with the fact that the more high frequencies the effect of relaxation processes affects lesser.

Thus, on the basis of the obtained experimental results and the available literary data [97, 154, 188, 193], it can be assumed that the presence of the bend on of the curved temperature dependences of strength, hardness and moduli of elasticity, at the temperatures, which comprise $0.4-0.5\ T_{nn}$, is connected with relaxation processes, the mobility of point defects - vacancies and their accumulations, and also changes in the mechanism of plastic deformation.

The results of the investigation of the temperature dependences of strength, module/modulus of elasticity and hardness of tungsten and molybdenum, presented in Fig. 197-200, testify to the possibility of the existence of one additional break at temperatures $\sim 0.7\, T_{nn}$. During the investigation of tungsten wires, Smithells [67] will also note the break in analogous temperature interval $(\sim 0.8\, T_{nn})$.

During the study of the internal friction of tungsten and molybdenum [193] in the range of temperatures of 2200-2500°C $(\sim 0.7\, T_{nn}$ for tungsten and $\sim 0.8\, T_{nn}$ for molybdenum) was reveal/detected the small in value peak (see Fig. 201).

As a result of the microstructural analysis of the specimen/samples of tungsten and molybdenum, deformed at high temperatures, it was establish/installed that on the working sections of the specimen/samples of the poured and cermet tungsten after deformation at temperatures $0.5-0.7\, T_{nn}$   is observed a considerable quantity of micro and macrofissures (Fig. 202-203).

Analogous character bears the decomposition of cermet and several to a lesser degree - poured molybdenum.
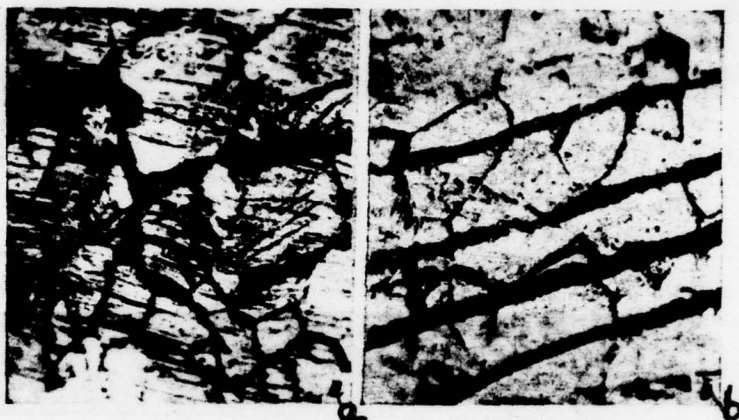
Page 245.



Fig. 202. Type of surface of poured tungsten after testing in vacuum (x200): a) 2200°C; b) 2500°C.



Fig. 203. Type of surface of cermet tungsten after testing in vacuum (x500): a) 2200°C; b) 2500°C.

Page 246.

At the temperatures of deformation more than $0.7 T_{nn}$ on the surface of the specimen/samples of polycrystalline molybdenum near the position of fracture are observed the rough bands (fold), very recalling the slip bands of the single crystals of molybdenum which are formed at these temperatures (Fig. 204).

The similar phenomenon noticed also during specimen/sample testing of the poured tungsten. It is necessary to note that the intergranular fracture of the specimen/samples of the poured tungsten was observed only to temperatures of 2200-2300°C (see Fig. 202a) $(0.5-0.7 T_{nn})$. At the temperatures, which exceed 2500°C (i.e. above $0.75 T_{nn}$), form of fracture of specimen/samples will be changed (see Fig. 172d and 202b). In the range of neck in specimen/samples, were visible the folds in the form of projections and indentations, the intersecting grains and directed perpendicularly or at the angle of 45 deg. toward axis of dilatation. Near the place of rupture, were noticed the very rough bands, obviously, which served as the nuclei of main-line crack.

At the same time the decomposition of the specimen/samples of cermet tungsten and poured alloys of tungsten (W-Mo and W-Re) up to 2500-2600°C bears intergranular character, as is evident from Fig.

203, moreover a quantity of microcracks on grain boundaries will be noticeably less, but grain deformation is greater than for the poured tungsten.

To a change in form of fracture of the poured tungsten when $0.7\,T_{mn}$ corresponds to discontinuity of curve $\ln \sigma - T$. However, at present still no data by operating by which it was possible to unambiguously solve, which phenomena were heavy-duty/critical for the existence of break on the curved temperature dependence of strength at temperatures $\sim 0.7\,T_{n.n.}$.

DOC = 78133008          PAGE 60 493
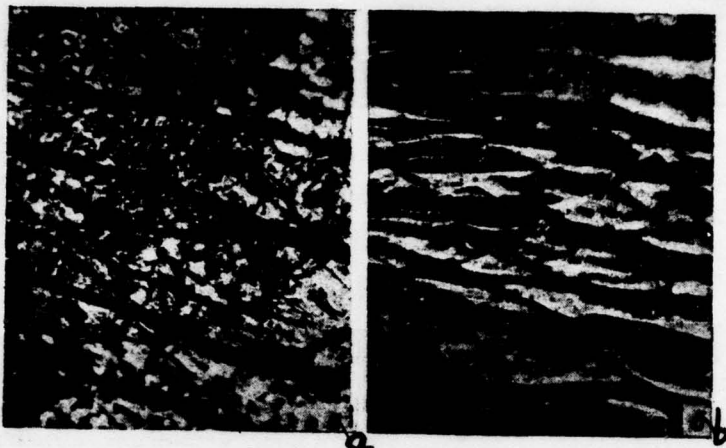


Fig. 204. Surface of the specimen/samples cf molybdenum after testing in vacuum with 1800°C (x200): a) polycrystal; b) single crystal.

Page 247.

On the basis of the temperature dependences of hardness and limit of strength of tungsten and molybdenum [132, 133, 179-182], obtained for the wide temperature range, it can be assumed that in the case of pure metals with an increase in the homologous temperature occurs the consecutive replacement cf three mechanisms of deformation [190].

I. At low homologous temperatures deformation is realize/accomplished via shift/shear, evenly distributed according to very large number of slip planes. In deformation participates entire

volume of grain in metal; therefore resistance to deformation must be greatly [190].

II. With increase cf temperature, character of deformation is changed. Shift/shear is less evenly is distributed between slip planes. Occurs deformaticn cn grain boundaries, since termination impedance to deformatiop with the increase cf temperature is decreased faster than resistance of the volume cf grain [190].

III. Strain at high homolcgous temperatures is not accompanied by strengthening metal, occur processes of creep [100, 179]. Deformation is realize/accomplished by the mutual displacement of grains and is accompanied by migraticn cf grain boundaries, by shaping of sub-structure [184]. Shift/shear cn slip planes under conditions of creep is negligibly small and to cause noticeable strengthening not can [190].

Change of mechanisms of deformaticn usually it is observed in certain temperature range for which the characteristically competing develppment of low- and high-temperature mechanisms.

In Conrad's work [183] are shown the predicted dislocation mechanisms of deformaticn in the range cf temperatures from absolute zero tc melting point (Table 31).

M. A. Zaykov [186, 191] it will propose to examine the
mechanical properties of materials in corresponding coordinates and
to introduce the concept of corresponding mechanical characteristics.
In this case for beginning, is accepted not absolute zero, but the
temperature of the appearance of this phase (the allotrope, etc.)
introduces the concept of relative temperature of material, which
instead of the temperature they set aside along the axis of the
abscissas:

$$\tau = \frac{T - T_{_H}}{T_{_K} - T_{_H}},$$  (5.14)

where $T_{_H}$ and $T_{_K}$ - temperatures, $^\circ K$, beginning and the end of the
existence of this phase;

T - the instantaneous value of temperature.

Page 248.

Along the axis of ordinates, utilizing the same principle, they
set aside the relation

$$\delta = \frac{e - e_{_H}}{e_{_H} - e_{_K}},$$  (5.15)

or in the logarithmic form:

$$\lambda = \frac{\ln e - \ln e_{_H}}{\ln e_{_H} - \ln e_{_K}}.$$  (5.16)

Table 31. Mechanisms of the deformation of metal [183].

| Тип (1) кристаллической решетки | (2) Металл | (3) Наиболее вероятный механизм | (4) Альтернативный механизм |
|---|---|---|---|
| | | $T<0.25\ T_{пл}$ | |
| Г. п. у. | Zn, Cd, Mg | Пересечение дислокаций (5) | (6) Неконсервативное движение порогов |
| Г. ц. к. | Al, Cu, Ag, Au, Ni | То же (7) | (8) Консервативное движение скользящих (10) порогов |
| О. ц. к. | V, Nb, Ta, Cr, Mo, W, Fe | (9) Преодоление барьеров Пайерлса—Набарро | Преодоление атомов внедрения и дисперсных выделений (11) Поперечное скольжение |
| | | $0.25\ T_{пл}<T<0.5\ T_{пл}$ | |
| Г. п. у. | Zn, Cd, Mg | (12) Пересечение дислокаций | (13) Неконсервативное движение порогов |
| Г. ц. к. | Al | (14) Поперечное скольжение | (15) Прорыв барьеров Ломера—Коттрелла |
| О. ц. к. | V, Nb, Ta, Cr, Mo, W, Fe | (16) Взаимодействие дислокаций с атомами внедрения | (17) То же |
| | | $T>0.5\ T_{пл}$ | |
| Г. п. у. | Be, Ti, Zn, Mg | (18) Переползание дислокаций $0.5T_{пл}<0.8T_{пл}$ Преодоление барьеров Пайерлса—Набарро призматическим скольжением $(T<0.8T_{пл})$ | (19) Неконсервативное движение порогов (20) Поперечное скольжение |
| Г. ц. к. | Al, Cu, Au, Pb | (22) Переползание дислокаций | (23) Неконсервативное движение порогов |
| О. ц. к. | Nb, Mo, Ta, Fe | (24) То же | (25) То же |

Key: (1). Type of crystal lattice. (2). Metal. (3). The most probable mechanism. (4). Alternative mechanism. (5). Intersection of dislocations. (6). Dissipative motion of thresholds. (7). the same. (8). Conservative motion of sliding thresholds. (9). Overcoming of Peyerls-Nabarro's barriers. (10). Overcoming of interstitial atoms

and dispersed liberation/isolations. (11). Cross slip. (12).
Intersection of dislocations. (13). Dissipative motion of thresholds.
(14). The cross slip. (15). Inrush/breach of lomera-Cottrell's
barriers. (16). Reaction of dislocations with interstitial atoms.
(17). The same. (18). Creeping of dislocations. (19). Dissipative
motion of thresholds. (20). Overcoming of Peyerls-Nabarro's barriers
by prismatic sliding. (21). Cross slip. (22). Creeping of
dislocations. (23). Dissipative motion of thresholds. (24). The same.
(25). The same.


Page 249.


Utilizing equation (5.10), M. A. Zaykov [186, 191] will be
obtained the following expressions:

$$\left.\begin{array}{l} \dfrac{\sigma}{\sigma_{\text{H}}} = \left(\dfrac{\sigma_{\text{K}}}{\sigma_{\text{H}}}\right)^{\tau}; \\[2mm] \dfrac{\sigma}{\sigma_{\text{K}}} = \left(\dfrac{\sigma_{\text{H}}}{\sigma_{\text{K}}}\right)^{1-\tau}, \end{array}\right\} \tag{5.17}$$

or in the logarithmic form:

$$\left.\begin{array}{l} \lg \sigma = \lg \sigma_{\text{H}} - \tau \lg \dfrac{\sigma_{\text{H}}}{\sigma_{\text{K}}}; \\[2mm] \lg \sigma = \tau \lg \sigma_{\text{K}} + \lambda \lg \sigma_{\text{H}}. \end{array}\right\} \tag{5.18}$$

The experimental results of the investigation of some refractory
metals and alloys for the limited temperature intervals, after
processing according to M. A. Zaykov, are represented in Fig. 205.

Some data on the temperature dependence of the strength of high-melting materials for the limited intervals are represented in common coordinates in Fig. 206 and 207, which testify to a good coincidence of calculated and experimental values.
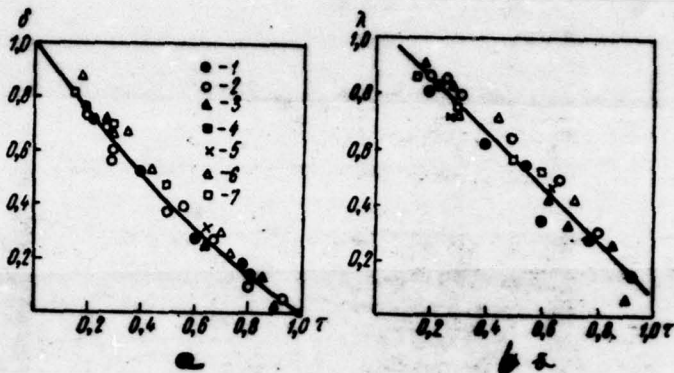
Fig. 205. The temperature dependence of the limit of the strength of refractory metals and some allcys cn their basis, presented in the coordinates:

$$a - \delta - \tau \left( \delta = \frac{\sigma - \sigma_{\kappa}'}{\sigma_{H} - \sigma_{\kappa}} ; \quad \tau = \frac{T - T_{H}}{T_{\kappa} - T_{H}} \right);$$

$$\delta - \lambda - \tau \left( \lambda = \frac{\lg \sigma - \lg \sigma_{\kappa}}{\lg \sigma_{H} - \lg \sigma_{\kappa}} \right);$$

1 - tungsten cermet; 2 - tungsten poured; 3 - tungsten recrystallized; 4 - W-3o/o Mo; 5 - W-27o/o Re; 6 - molybdenum allcyed; 7 - niobium.

Page 250.

It is necessary to alsc note existed ccmmunication/cpnnections between the characteristics of hardness and strength of tungsten, molybdenum and tantalum in the wide temperature range.

On the basis of dependences (5.9) and (5.12) it is possible to
find the relationship/ratio between hardness and limit of strength
[30, s. 7; 185]:

$$\frac{\sigma_b}{H} = \frac{m_n \dot{\sigma}_0}{k_n H_0} \, e^{(\varkappa_n - \vartheta_n) T}. \qquad (5.19)$$

to designate constants $\frac{m_n}{k_n}$ and $\frac{\dot{\sigma}_0}{H_0}$ respectively through $C_n$ and $C_0$,
the last/latter equation it is possible to record thus:

$$\sigma_s = C_0 C_n H e^{(\varkappa_n - \vartheta_n) T}. \qquad (5.20)$$

This exponential expression, apparently, will be valid for the
pure metals, immune to to the aging also of the not having allotropic
changes.

Dependence (5.20) in logarithmic coordinates must present the
graph, which consists of three line segments.

Figures 208-210 shows, as vary with temperature
communication/connection between the values of the limit of strength
and hardness for deformed tungsten, molybdenum and annealed tantalum.
In the logarithmic coordinates ln $\sigma_b$ -ln H of relationship/ratio, they
are real/actually depicted as three line segments.
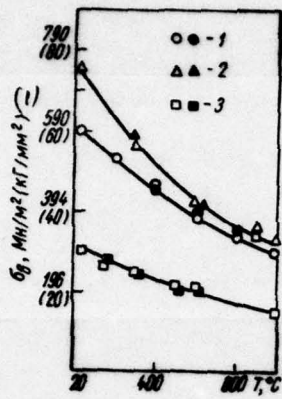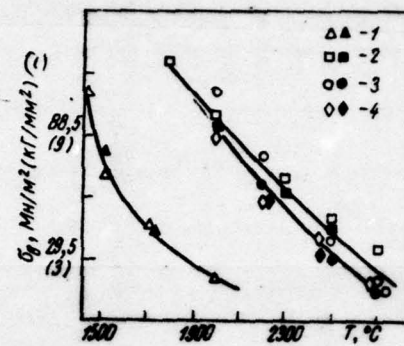
Fig. 206.        Fig. 207.

Fig. 206. The comparison of the calculated and experimental values of ultimate strength in the range of the elevated temperatures: 1 - tungsten fusion; 2 - molybdenum fusion; 3 - niobium (dark marks - computed values).

Key: (1). $MN/m^2$ ($kg/mm^2$).

Fig. 207. Comparison of calculated and experimental values of ultimate strength at high temperatures: 1 - Mo; 2 - W; 3 - W - Mo; 4 - W - Re (dark marks - computed values).

Key: (1). $MN/m^2$ ($kg/mm^2$).

Page 251.

For those sections of dependence to which correspond equal temperature coefficients of hardness and limit of strength $\alpha_n = \beta_n$, the relationship/ratio of the limit of strength and hardness is constant:

$$\sigma_s = C_0 C_n H. \qquad (5.21)$$

for sections, to which correspond the close values of temperature coefficients $\alpha_n$ and $\beta_n$, the graph of relationship/ratio (5.20) in coordinates $\sigma_s - H$ will present the slanting exponential curve which with sufficient reliability can be approximated by rectilinear cut.
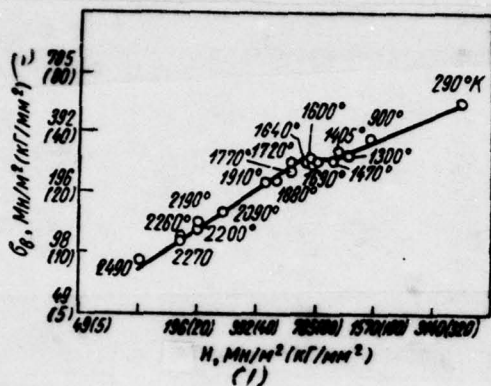
Fig. 208.



Fig. 209.

Fig. 208. Communication/connection between ultimate strength and hardness of tungsten (in curves is shown temperature, to °K).

Key: (1). MN/m² (kg/mm²).
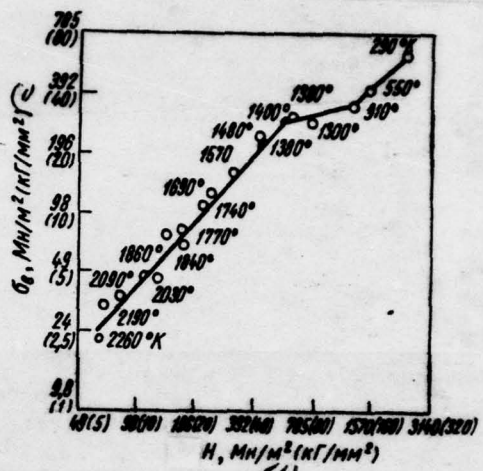
Fig. 209. Communication/connection between ultimate strength and hardness of molybdenum (designation - see Fig. 208).

Key: (1). MN/m² (kg/mm²).

Page 252.
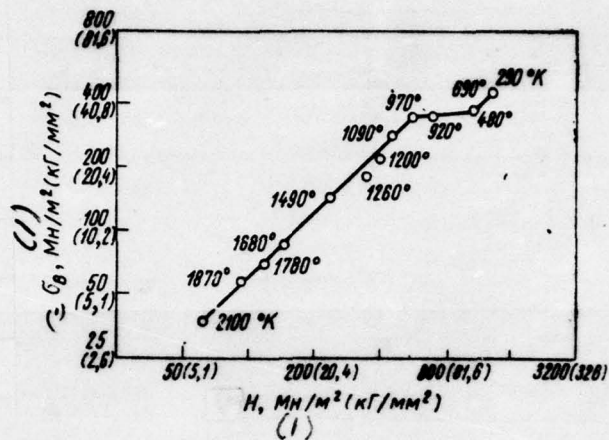


Fig.210. Communication/connection between ultimate strength and hardness for tantalum at different temperatures.
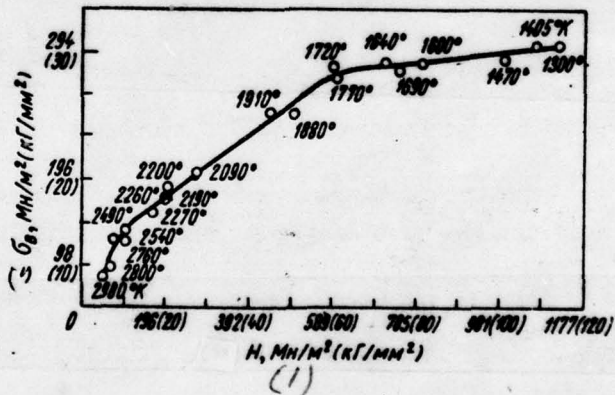
Key: (1). MN/m² (kg/mm²).



Fig. 211. Communication/connection between hardness and limit of strength of tungsten at different temperatures.
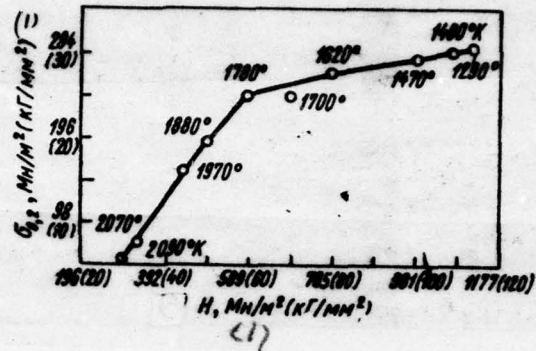
Key: (1). MN/m² (kg/mm²).

Fig. 212. Communication/connection between hardness and yield limit of tungsten at different temperatures.
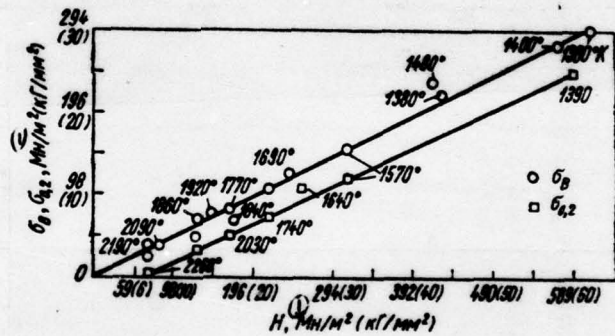
Key: (1). MN/m² (kg/mm²).



Fig. 213. Communication/connection between characteristics of hardness and strength of molybdenum at different temperatures.

Key: (1). MN/m² (kg/mm²).
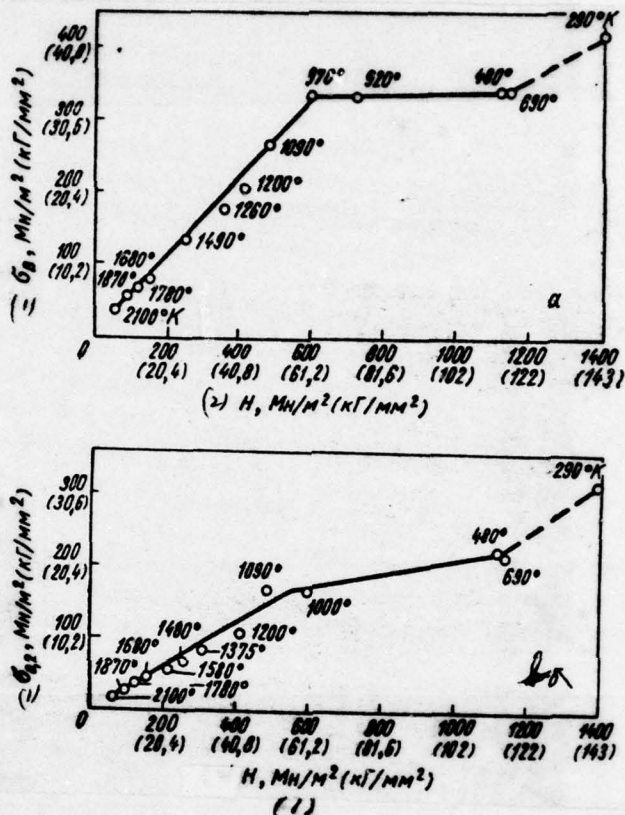
Page 253.



Fig. 214. Communication/connection between characteristics of hardness and strength of tantalum at different temperatures:

$$a - \sigma_b - H; \; b - \sigma_{0,2} - H$$

Key: (1). MN/m² (kg/mm²).

Page 254.

For the practical application/use to usefully obtain graphs and the analytical expressions of the relationship/ratios between hardness and the limits of strength and yield of refractory metals for the wide temperature range. This processing of experimental data have carried out we for deformed tungsten and molybdenum.

Communication/connection between hardness and limit of the strength of tungsten in the range of temperatures of 1000-2710°C is represented in Fig. 211, while communication/connection between hardness and yield limit $\sigma_{0,2}$ in interval of 1000-1820°C - in Fig. 212.

The graphs of the relationship/ratios between the limits of strength and yield, on one hand, and by hardness, on the other hand, for molybdenum at temperatures of 1100-2000°C are given to Fig. 213. Ultimate strength and yield point of molybdenum in the range of temperatures of 1100-2000°C are connected with hardness by the following relationship/ratios:

$$\sigma_a = 0,49H; \qquad (5.22)$$
$$\sigma_{0,2} = 0,45(H - 60). \qquad (5.23)$$

Communication/connection between hardness and strength of annealed tantalum at high temperatures is represented in Fig. 214.

If is calculated the relations of the yield point and hardness $\frac{\sigma_{0.2}}{H}$ for different temperatures, then it appears that for tungsten and for molybdenum they are included within limits from 0.20 to 0.41. Therefore for tentative calculations it is possible to utilize the averaged relationship/ratios:

for tungsten (from $20° \leqslant T \leqslant 1820°$ C)

$$\sigma_{0.2} = 0.307 H; \qquad\qquad (5.24)$$

for molybdenum (from $20° \leqslant T \leqslant 1760°$ C)

$$\sigma_{0.2} = 0.323 H. \qquad\qquad (5.25)$$

Page 255.

Chapter 6.

CREEP AND STRESS-RUPTURE STRENGTH OF REFRACTORY METALS.

Testing units and procedure.

Testing units.

During the laboratory tests of high-melting materials for creep and stress-rupture strength, are utilized in essence the specimen/samples of comparatively small size/dimensions. This fact conditioned some design features of testing units [157, 194, 195].

In the Institute of the problems of the strength of AS UkSSR for the test work of refractory metals for creep and stress-rupture strength, are created two installations: single-section ID-6V (Fig. 215) and six-section ID-6V6 (Fig. 216), intended for testing both of cylindrical (d=3-5 mm) and flat/plane ($\delta$=1-2 mm) specimen/samples in vacuum 1.33-0.399 MN/m$^2$ ($1 \cdot 10^{-5}$-$3 \cdot 10^{-6}$ mm Hg) at temperatures to 2500°C.

Single-section installaticn (Fig. 217) has the lever/crank
system of loading which makes it possible to increase external load
ten times, and it consists of loading device, vacuum chamber, systems
of heating specimen/sample and pumping cut of test chamber, control
panel and the temperature ccntrcl of specimen/sample. All elements of
construction/design, with exception of the unit of power transformer
and oil rotary pump, are scunted cr welded scunting.

On the struts of 11 loading devices, it is attached by traverse
5, on which is establish/installed upper capture by 4, which has
spherical support. Lower capture by 7 is ccnnected with thrust/rod by
10 through spherical self-adjusting hinge jcint 9. Cylindrical
specimen/sample with 6 is fastened in captures to thread, flat/plane
- with the aid of stud pins. Bcth cf captures are made from
molybdenum.

All cell/elements cf the mechanism of loading have the
demountable joints, allcwing easy to discornect them from the
conjugated assemblies of installation and cne from another; this
provides convenience in the assembly of specimer/sample and its rapid
centering.
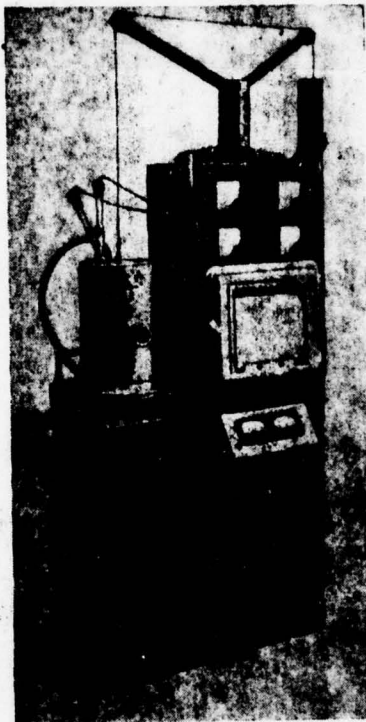
Page 256.



Fig. 215. General view of single-section installation ID-6V.
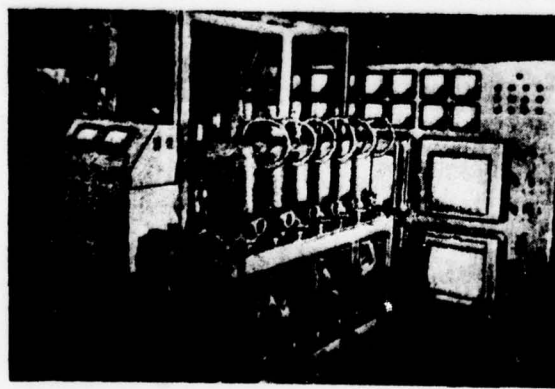


Fig. 216. General view of six-section installation ID-6V6.
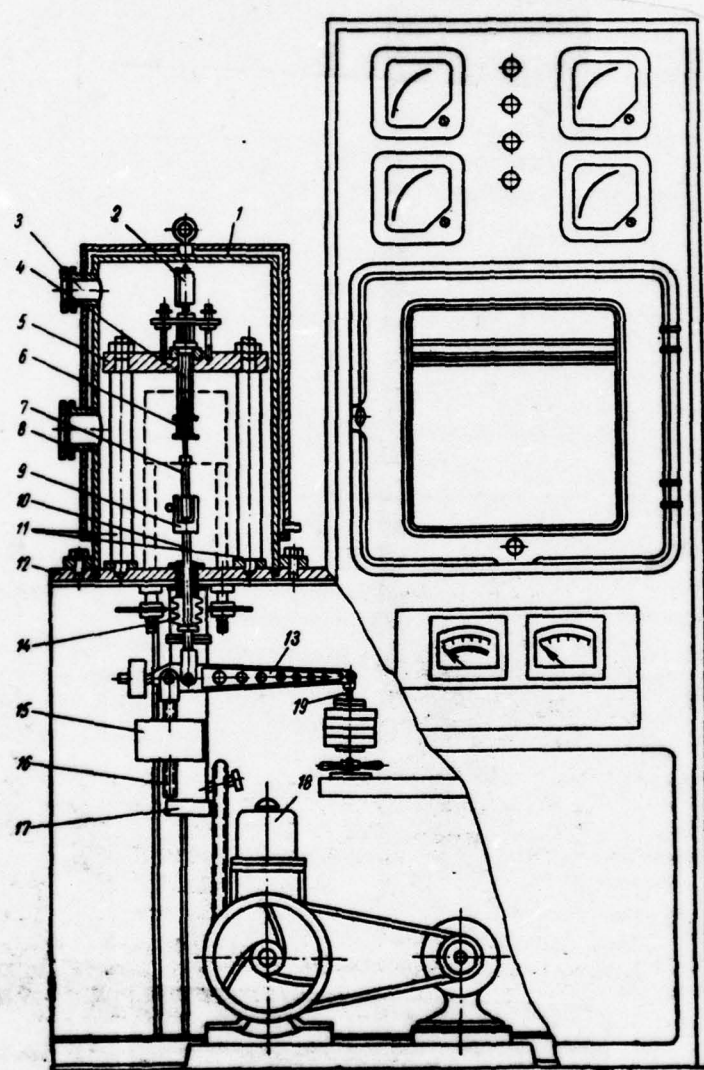
Page 257.



Fig. 217. Diagram of single-section installation ID-6V.

Fig. 217. Diagram of single-section installation ID-5V.

Page 258.

Loading lever 13 is suspend/hung from downdraft by 10 and it pivots on ball bearing ball-and-socket bearing. To the end of large lever arm, is fasten/strengthened suspension by 19, intended for the installation of interchangeable loads with the loading of specimen/sample. In the loading device enter also worm reducer 15 and screw/propeller 16. During the assembly of specimen/sample in captures also with its loading with the rotation of the worm of reducer it is possible to manufacture lift or lowering of lower capture together with lever. The construction/design of the mechanism of loading makes it possible for lower capture to be lower/omitted during the elongation of specimen/sample in the process of testing.

The mechanism of loading is placed into vacuum chamber, formed by water-cooled steel plate/slab 12 and by metallic cap/hood 1. Downdraft is introduced into the camera/chamber through the sealed joint with the aid of contac bellows 14.

In vacuum chamber there are two inspection window by 3 and 8. Window 8 is intended for observation after specimen/sample in the process of testing (measurement of strain cathetometer and the

measurement of temperature with the aid of pyrometer), window 3 - for relieving readings of indicator with the extensometric method of measurement of strain.

In the camera/chamber through the plate/slab, are passed copper conductors, cooled by running water, and thermocouples. All input/introductions have rubber gaskets.

Diffusion pump 17 (type $N-5S)$ ~~H-5C)~~ is connected with the camera/chamber by short connecting piece.

$T$ The forevacuum in the camera/chamber creates oil rotary pump to 18 (type VN-2MG).

Heater presents the tube with cut/sections, manufactured from molybdenum or tungsten. The length of heating tube 3-4 times exceeds the working length of specimen/sample, which provides uniform heating.

For decreasing heat losses, are used manufactured from molybdenum or tungsten. The length of heating tube 3-4 times exceeds the working length of specimen/sample, which provides uniform heating.

Bor decreasing heat losses, are used the laminated shields whose interior layer is made made of tungsten, subsequent - from molybdenum. Lower and side shields are establish/installed on separate cross beam attached on struts 11, but upper - on side shields.

The temperature of specimen/sample to 1300°C is measured by platinum-platinum-rhodium thermocouples, higher than 1300°C - by tungsten-rhenium thermocouples or a pyrometer of the type OPPIR-017.

The elongation of specimen/sample at temperatures to 1000°C is determined with the aid of indicator 2, adjustable directly in vacuum chamber. As the extenders serve four quartz rods, two of which lean on the supporting/reference pad, adjustable on specimen/sample of the lower mark of its working length, and two others - on the same pad, fastened of upper mark. Each pair of rods is finished with the framework: within the upper framework is fastened the indicator, the lower framework abut against the leg of indicator.

At the temperatures of testing higher than 1000°C strain are measured by a cathetometer of type KM-6. In this case to specimen/sample on the boundary/interface of its working length, are welded by spot electrostatic welding the pointed lug/lobes on disagreement of which in the process of testing they judge from the

strain cf specimen/sample.

Page 259.

Six-section installation (Fig. 218) makes it possible to conduct simultaneously the tests of six specimen/samples under the independent conditions.

On common/general/total welded mounting are mounted the elements cf vacuum chamber, and also systems of loading, heating and measurement of strain for all six sections. Is separately placed the electrical shield of control.

In the base of each camera/chamber, there are two holes for the conductors, thermocouples, downdraft, and also a grocves for fixation cf supporting cylinder. In chamber casing built in inspection window with quartz glass for the optical measurement cf strain with the aid cf cathetometer 1 and for measuring the temperature of specimen/sample with the aid of pyrometer. For preventing the precipitation of the condensate of evaporating particles on quartz glass, there is a shutter.
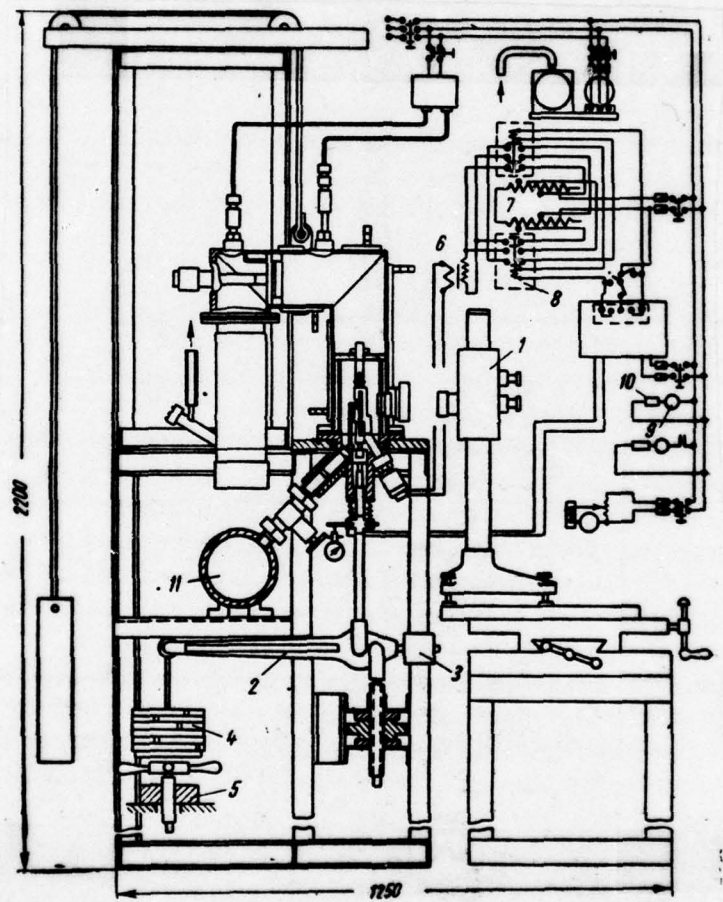
Fig. 218. Diagram of six-section installation ID-6V6.

Page 260.

    To chamber casing with the aid of ring, is fastened diffusion
pump. Unlike the common gates cf vacuum chambers, in the
camera/chamber of installation ID-6V6 is applied internalizations the
vacuum seal, which substantially decreases area of joint. The pumping
cut of air from each camera/chamber is manufactured by diffusion
pumps cf type TsVL-100 and by the common/general/total fore pump
VN-2MG.

    Lever/crank type loading mechanism is in each section; it makes
it possible to create the stretching force in specimen/sample to 5 kN
(515 kgf) and it consists cf the circuit of loading, loading lever of
the second kind with the relationship/ratio of arms 1:10 and of worm
reducer 5. The latter makes it possible to create pretensioning in
the circuit of the loading cf specimen/sample. Upper ball coupling of
the circuit of loading form the nuts also cf traverse with spherical
surfaces.

    Fastening specimen/samples in captures is realize/accomplished
just as in installation ID-6V.

Lower capture by means of adapter is connected with the downdraft to which through self-aligning ball bearing from link is suspend/hung loading lever 2 with counterweight to 3 from short arm and suspension for the installation of interchangeable loads 4 from long arm. For the safeguard for evenness of loading provided for special loading device 5.

Within vacuum chamber placed heating device: heater, current supplies and shields.

Heater is made made of molybdenum, tantalum or tungsten in the form of two parallel plates 0.5-1 mm in thickness from crosspiece. For the heat insulation of the working space of the camera/chamber, serve vertical and horizontal shields from tungsten, molybdenum and nickel tin 0.2-0.5 mm in thickness. Electric power to heater enters from step-down transformer 6 through copper busbar/tires and water-cooled copper conductors. The uniform heating of specimen/sample is provided because of the special form of heater.

Figures 218 gives also the schematic electric diagram of installation. The temperature of specimen/sample and the rate of its growth/build-up are regulated with the aid of the autotransformer of 7 types RNO-250-5 and of two electromagnetic contactors of voltage/stress 8.

Page 261.

The check of the temperature of specimen/sample is
realize/accomplished by platinum-platinum-rhodium ones and
tungsten-rhenium ones to the thermocouples through known electric
diagram [107] with the aid of the automatic electronic recording
potentiometer of the type EPP-09 which provides the automatic
maintenance of the assigned/prescribed temperature with
accuracy/precision $\pm 0.5$ deg; furthermore, is provided for the
measurement of temperature with the aid of a movable potentiometer of
the type PP.

Figures 218 shows the signaling system, which considerably
facilitates the maintenance of installation. So, during the supplying
of feed into the electric circuit of section lights up signal lamp by
9, connected through ballast resistance to 10. Analogous resistances
are included in the circuit of all signal lamps which are fired
respectively with the activation of an entire installation, the
output/yield of lever from horizontal position, the supply/feed of
maximum or minimum power to heater, etc.

The strain of specimen/sample in the process of creep determines

by optical and mechanical methods. The first method is instituted on
the measurement of the distances between the section/shear of the
welded to specimen/sample plates through inspection window with the
aid of cathetometer 1.

The small size of vacuum chamber makes it possible to approach
the telescope of cathetometer the specimen/sample up to the distance,
which makes it possible to utilize a maximum increase during the
measurement of strains. The second method of measuring the strains
consists in the determination of the displacement/movements of
thrust/rod with the aid of indicator.
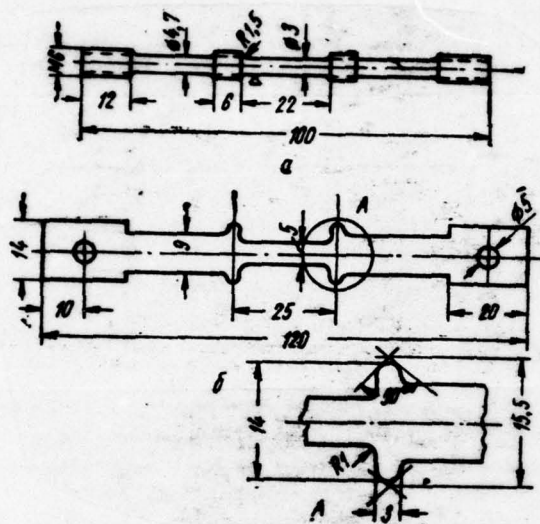
Fig. 219. Specimen/samples with special shoulders for creep tests: a) cylindrical specimen/sample; b) flat/plane specimen/sample.

Page 262.

Specimen/samples.

For studying of creep and stress-rupture strength for elongation, are used the specimen/samples of different types. This in

essence the so-called quintuple specimen/samples (Fig. 219, 220),
with the conventional relationship/ratio between the length of
working part $l_0$ and cross section $F_0$:

$$l_0 = 5.65 \sqrt{F_0} . \qquad\qquad (6.1)$$

Figures 219 and 220 depict cylindrical and flat/plane
specimen/samples with extended adapters. The size/dimensions
indicated and the forms of specimen/samples are most advisable for
the analysis of high-melting materials. During the tests of these
specimen/samples, the captures do not enter in the zone of heater,
which decreases the intense heat removal from specimen/sample and
provides the even distribution of temperature along the length of its
working part, and also decreases the expenditure/consumption of
electric power for heating of specimen/sample.
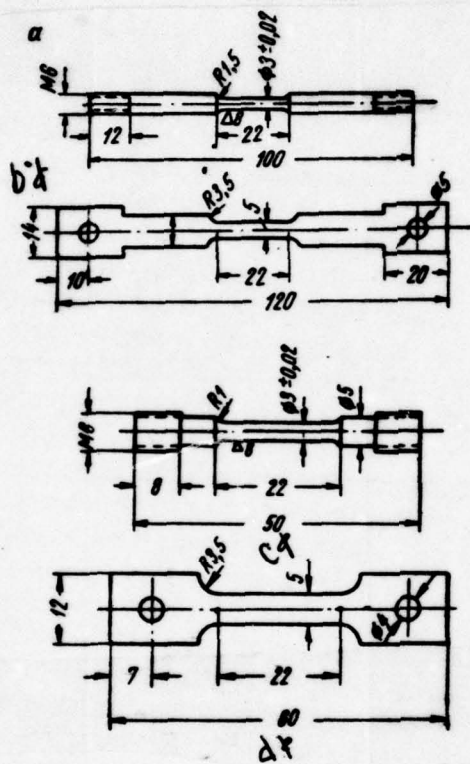
Fig. 220. Specimen/samples for creep test and stress-rupture strength: a) the extended cylindrical specimen/sample; b) the extended flat/plane specimen/sample; c) the shortened cylindrical specimen/sample; d) the shortened flat/plane specimen/sample.

Page 263.

The cylindrical specimen/sample (see Fig. 219a) on the boundary/interface between the worker and transient partly threaded but the flat/plane specimen/sample (see Fig. 219) - the shoulder/fillets, necessary for the installation of the supporting/reference area/sites on which lean the extensometers. For tests at the temperatures higher than 1000°C, are applied the specimen/samples, similar to those that are shown on Fig. 220a, b, not threaded and shoulder/fillets in the middle part. The measurement of strain in these cases manufactures with optical method with the aid of a cathetometer of type KM-6, with respect to a change in the distance between the plates which are welded to specimen/sample on the boundary/interface of its working part (Fig. 221).

During testing of scarce materials, were used short specimen/samples (Fig. 220c, d); the decrease of the length of specimen/samples is realized because of reduction in their adapters with the full/total/complete preservation/retention/maintaining of form and size/dimensions of working part.

Measurement of strain.

During endurance tests at high temperatures in vacuum or in the medium of inert gas they use extensively both devices for the direct measurement of strain (cathetometers, measuring microscopes and

special optical systems [107; 184; 196; 197] and of device for the
measurement of strain on shifting cf active thrust/rod
(extensometers, equipped mirror, interference and diffraction
systems, spring indicators and the like [194; 197, 198]. During the
measurement of strain with the aid cf optical systems, is determined
a change in the distance between standard points at the working
length of the specimen/sample through inspection windows in the
housing of reheating furnace and vacuum chamber. Is possible
automatic fixation of the results of measurement with the aid of
movie cameras or cameras [196]. However, in this case, the accuracy of
the measurement of strain is considerably lower than during the
utilization of cathetometers.

The method of determining the strain from the
displacement/movement of active thrust/rod has small
accuracy/precision; however, it is very simple and it is possible to
easily carry out automation of the process cf measurement [197].
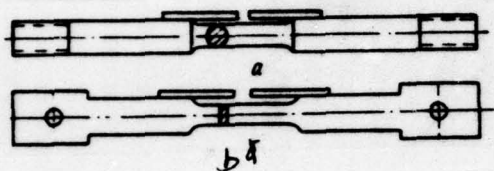
Fig. 221. Specimen/samples with the welded-cn plates for measuring
the strain with the aid of the cathetometer: a) cylindrical
specimen/sample; b) flat/plane specimen/sample.

Page 264.

For determining the creep strain, we put to use the method of
direct measurement with the aid of a cathetometer of type KM-6,
making it possible to record/fix the displacement of the graduation
marks, plotted/applied at the working length of specimen/sample, or
the plates, fasten/strengthened to adapter of the specimen/sample
(see Fig. 221), and also by the extensometric method, developed in
connection with tests at temperatures to 1000°C during installation
ID-6V.

D

During the utilization of each of the methods indicated in parallel was conductn the measurement of the strain of specimen/sample with the aid of the indicators, fixing the displacement of movable capture.

Construction/design of extensometer. With the aid of the extensometer of the developed by us copstruction/design, it is possible to measure creep strain both of flat/plane and cylindrical specimen/samples.

To thread or the recesses, available in the specimen/samples (see Fig. 219), are fastened nuts or dismountable/release clamping collars made of heat-resistant steel, employed with supporting/reference area/sites for the extenders of extensometer - rods from quartz glass 3 mm in diameter. The application/use of quartz extenders eliminates the error of measurement, connected with a change in the length of rods during heating.

The housing of indicator 1 (Fig. 222) is attached in disk by 2, which leans on two quartz rods and can be mcved on three guides 3, establish/installed on traverse 4. Quartz rods lean on pad by 6, establish/installed at the level of upper boundary of the working part of the specimen/sample.
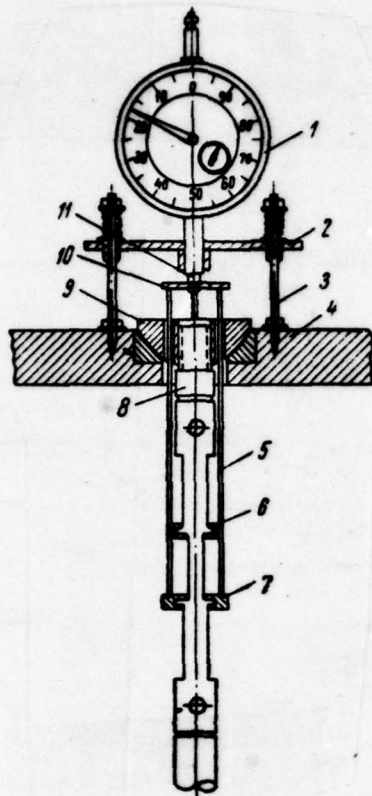
Fig. 222. Schematic of attachment for measuring the strain (extensometer).

Page 265.

The shaft of indicator with fastened/strengthened to it plate 10 leans on other two quartz rods 5, which they freely pass through holes in supporting/reference five of 9 upper captures by 8 and they lean on pad by 7, attached at the level of lower boundary of the

working length of specimen/sample.

Thus, to the rods, connected with upper supporting/reference clamping collar is establish/installed disk by 2 with the fastened/strengthened in it indicator, and to other rods, connected with lower clamping collar 11, leans the shaft of indicator with area/site 7.

This construction/design provides joint between the specimen/sample and rod- extenders and thereby it guarantees the precise measurement of the strain of specimen/sample.

Before the assembly of indicator the shaft is set in upper position - to the ground elevation of the red scale.

In the process of testing, as a result of the strain of specimen/sample, will step down lower supporting/reference area/site by 7, and together with it and the shaft of indicator; with this arrow/pointer of indicator it will show the strain of specimen/sample.

Because of the independent installation of extensometer during the measurement of the strain of the working part of the specimen/sample, are excluded the errors, caused by change in the

length of upper capture, by the strain adapter of the
specimen/sample, etc.

Error analysis for the measurement of strain.

The criteria, which determine the selection of one or the other
method of measuring the strain, are accuracy/precision, labor
consumption, the possibility of automatic recording.

First of all one should consider the degree of accuracy of the
measurement of strain.

For its determination is proposed the following dependence:

$$\dot{\varepsilon} \cdot t \cdot \delta = A, \qquad (6.2)$$

where $\dot{\varepsilon}$ - deformation rate;

$t$ - time between measurements, or control time;

$\delta$ - permissible error in determination $\dot{\varepsilon}$;

$A$ - an absolute error (accuracy/precision) in the measurement of
strain.

control time - time interval between measurements, during which at the rate of deformation $\dot{\varepsilon}$ can occur the accumulation of strain, sufficient, so that at the assigned/prescribed value of A the rate of deformation $\dot{\varepsilon}$ could be determined with accuracy/precision $\delta$. Consequently, if the deformation rate is changed during the time interval, which is lesser than the control, then with the selected accuracy of measurement this change in the velocity cannot be fixed.

Page 266.

For example, with $A=5\cdot10^{-3}$ mm and $\dot{\varepsilon}=10^{-2}$ mm/h (i.e. $4\cdot10^{-2}$ $^o/_o$/hour at the length of the working part of the specimen/sample $l=25$ mm) taking into account the fact that the process of creep influence different factors (technology of obtaining material, medium, the degree of evacuation/rarefaction, the value of the inleakages, etc.), which can cause a change in the deformation rate to 20 o/o, one should accept $\delta \leq 5$ o/o; then, accordingly (6.2), control time will be 10 h. But if $A=0.1\cdot10^{-3}$ mm, then t=0.2 h.

In this case, it is necessary to keep in mind that the increase of the absolute accuracy of the measurement of strain can significantly expand the possibilities of the analysis of the

factors, which influence process of creep.

Cathetometers (Fig. 223) must provide the accuracy of the measurement of strain to 1 $\mu$m, what to in practice attain is very difficult due to the effect of different errors in the optical measurement.

Accumulated error can be determined as follows:

$$\Delta l_1 + \Delta l_2 + \Delta l_3 + \Delta l_4, \qquad (6.3)$$

where $\Delta l_1$ - a reading error;

$\Delta l_2$ - error in the guidance/induction for the measured objective;

$\Delta l_3$ - error in the levelling;

$\Delta l_4$ - error caused by the insufficient mutual rigidity of supports 1, 2, 3 (see Fig. 223).
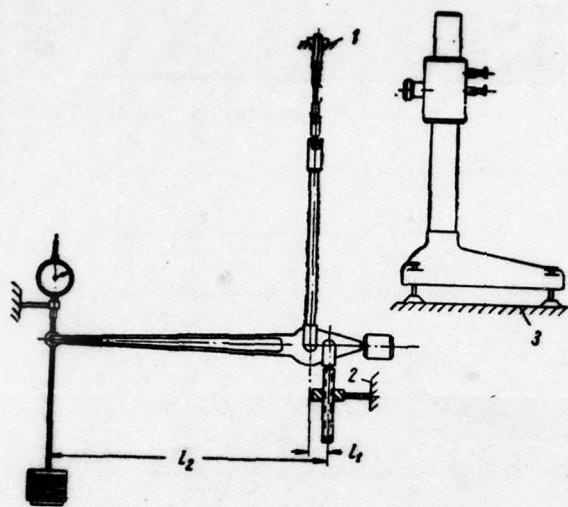
Fig. 223. Measuring circuit of strain with the aid of cathetometer.

Page 267.

For measuring the distance between standard points - the
section/shear of the welded-on to specimen/sample plates - the
telescope of cathetometer, rigidly connected with the system of
micrometric reading, alternately is aimed at each standard point.

The system of micrometric reading makes it possible to
record/fix the displacement of telescope with accuracy/precision 1

μm, although in this case it is difficult tc avcid the error for subjective character during the visual division of the side of reading parallelogram intc 10 parts.

More essential can be the errcrs, connected with the accuracy/precision of guidance/induction, which depends on an increase in the telescope, i.e., cn the distance between the telescope and the standard point. This distance is determined ty the size/dimensions of the camera/chamber; therefcre, an increase cannot be large. Furthermore, at the high temperatures of testing the bright brightness of specimen/sample impedes precise guidance/induction to standard pcint.

The accuracy of the measurement of strain, also substantially influence the mutual rigidity cf supports, the accuracy/precision of levelling, etc. Thus, the measurement of high-temperature strain by cathetometer with accuracy/precision 1 μm - the very labor-consuming frccess, which requires the breaking stress cf cperator.

Let us examine, the seccnd methcd of measuring the strain, which consists in the account of the displacement cf the active thrust/rod:

$$\Delta l_T = \Delta l_1' + \Delta l_2' + \Delta l_3' + \Delta l_4', \qquad (6.4)$$

where $\Delta l_T$ - displacement of active thrust/rod;

$\Delta l_1'$ - strain of the working part of the specimen/sample;

$\Delta l_2'$ - strain of adapters of the specimen/sample;

$\Delta l_3'$ - strain of the articulation of the circuit of the loading of specimen/sample;

$\Delta l_4'$ - strain, produced change in the temperature.

As is evident, a deficiency in this method is the fact that the displacement of active thrust/rod is determined not only amount of the strain of specimen/sample.

To the advantages of method, one should relate:

1) simplicity and convenience in the measurement;

2) a small labor consumption;

3) the possibility of the automation of the process of measurement.

Loads during the tests of high-temperature creep are small [$\sigma$=5-100 $\overset{M}{\text{m}}$N/m² (0.515-10.2 kg/mm²). Therefore with those selected by us form and the size/dimensions of specimen/samples the strain of adapters $\Delta l'_2$ either is negligible (since the stress in them 2-5 times less than in the working part of the specimen/sample), or it occurs with constant velocity, in consequence of which it ■ is possible to easily consider. On this same reason the strain in articulation $\Delta l'_3$ is also insignificant.

Page 268.

Numerous tests with the measurement of strain according to the schematic, presented in Fig. 223, they showed, that to the assigned/prescribed change in the temperature corresponds the completely specific displacement of active thrust/rod $\Delta l'_4$.

The systematic character of errors in the mechanical method of measuring the strain makes it possible to easily consider these errors.

Measurement and temperature control of testing.

During testing with heating of specimen/sample to 800°C the measurement of temperature usually manufactures with chromel-alumel

thermocouples, while at temperatures from 800 to 1300°C, are applied platinum-platinum-rhodium thermocouples.

For measuring the higher temperatures, are utilized tungsten-rhenium thermocouples of the type  II5/20.  *VR5/20.*  It should be noted that the characteristics of these thermocouples are slightly stable and are changed in the process of prolonged operation; therefore before each experiment it is necessary to manufacture the calibration of thermocouples.

Together with thermocouples for measuring high temperatures (2100-2600°C) we applied the optical pyrometers of the type OPPIR-09 and OPPIR-017.

During the measurement of the temperature of specimen/sample by optical pyrometers it is necessary to bear in mind, that in the process of endurance tests on sight glass of installation appears the film as a result of precipitating the material, which vaporizes from the surface of heater and specimen/sample. With an increase in the thickness of film, the transparency of glass is decreased, which can introduce essential errors into the measurement of the real temperature of specimen/sample. Therefore, sight glasses must have the safety devices which are open/disclosed only during the measurement of temperature.

During the utilization of pyrometers, they occur of error during the comparison of the brightness of body and filament, and also the error, caused by absorption in the medium between the telescope and the emitting body whose temperature is measured. The first of the errors indicated usually does not exceed 1c/o; the second - increases with an increase in the measured temperature and at 2500°C it reaches values by 1-1.5o/o. Precise values of temperature determine, introducing the appropriate corrections whose values install by measuring the temperature of special specimen/samples with the holes, which imitate the conditions of blackbody radiation [197].

A control of the temperature in the process of endurance tests realize/accomplish with the aid of temperature controllers and automatic electronic potentiometers of the type EPP-09M, which ensure accuracy/precision with $\pm 0.5$o/o from the maximum limit of the scale of measurement, that for tools with the calibration of the scale KhA, PP and VR composes $\pm 5.5$, $\pm 8$ and $\pm 17$ deg with respect [194, 198].

Page 269.

Accuracy analysis of temperature control.

The dependence of creep rate $\dot{\varepsilon}_T$ for alloy VN-2 at stress $\sigma=75$ MN/m² (7.65 kg/mm²) that of the temperature, can be represented by the formula

$$\lg \dot{\varepsilon} = -3.5 + 0.015 \cdot \Delta T$$

at temperatures from 1180°C to temperature of 1320°C. To Fig. 224 is represented the dependence

$$\eta = \frac{\dot{\varepsilon}_T}{\dot{\varepsilon}_{T+\Delta T}} = f(\Delta T), \qquad (6.5)$$

where $\dot{\varepsilon}_T$ - a creep rate at temperature T;

$\dot{\varepsilon}_{T+\Delta T}$ - creep rate at temperature T+ΔT;

ΔT - interval of the oscillations of temperature.

Utilizing formula (6.5), it is possible to show, as depends the accuracy/precision of the determination of creep rate A on the oscillation of the temperature:

$$A_1 = \frac{\dot{\varepsilon}_{T+\Delta T} - \dot{\varepsilon}_T}{\dot{\varepsilon}_{T+\Delta T}} = 1 - \frac{\dot{\varepsilon}_T}{\dot{\varepsilon}_{T+\Delta T}}; \qquad (6.6)$$

$$A_2 = \frac{\dot{\varepsilon}_{T+\Delta T} - \dot{\varepsilon}_T}{\dot{\varepsilon}_T} = \frac{\dot{\varepsilon}_{T+\Delta T}}{\dot{\varepsilon}_T} - 1. \qquad (6.7)$$
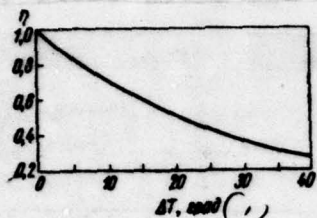
Fig. 224. Effect of an interval of the oscillation of temperature on a change in the deformation rate.

Key: (1). ΔT, deg.

Table 32. Effect of an interval of the oscillations of temperature on the accuracy/precision of the determination of the deformation rate.

| $\Delta T$, $град$ (1) . . . | 5 | 10 | 15 | 20 | 25 | 30 | 35 |
|---|---|---|---|---|---|---|---|
| $A_1$, % . . . . . . | 15 | 28 | 39 | 48,5 | 57 | 63 | 68 |
| $A_2$, % . . . . . . | 18 | 39 | 64 | 95 | 132 | 170 | 214 |

Key: (1). ΔT, deg.

Page 270.

Magnitudes of error in the measurement of the deformation rate, calculated according to formulas (6.6) and (6.7), are given in Table

32, which gives the sharp representaticn atout the fact that an increase in the interval of the oscillations of temperature strongly **affects** the accuracy/precisicn cf the determination cf creep rate $\dot{\varepsilon}_T$, moreover with a temperature rise the error it is increased.

Given data place in doubt the possibility cf the wide application of electronic faders cf the temperature during high-temperature tests with the application/use of high(ly)-inertia heaters.

Heaters.

For heating of specimen/samples during the tests of high-melting materials for creep and stress-rupture strength, is utilized in essence the radiation method of heating.

With wish it is possible to heat specimen/sample by the direct transmission of electric current. This methcd of heating is very simple, do nct require substantial changes in the heating system, used for radiation heating, and easily there can be realized in all construction/designs of the testing machines: fcr this it is necessary one of the captures to electrically insulate from the mass of installation and with the aid of flexible busbar/tires to bring stress to captures.

It was shown [199, 200], that the direct transmission of the current through specimen does not have this effect on the physical, mechanical and chemical properties of material which would differ from the effect of radiation heating.

However, for direct heating by electric current the characteristically parabolic temperature distribution over the working length of specimen/sample. With the increase of temperature, this law considerably is reinforced. Furthermore, in the region of neck as a result of the local increase of electrical resistance, as a rule, occurs the hot spot of specimen/sample.

For heating of specimen/samples by emission/radiation are prepared the heaters from plates or rods of refractory metals - tungsten, molybdenum, tantalum or niobium.

As the criteria of a comparative evaluation of construction/designs of heaters can serve such characteristics as expenditure of power on heating of specimen/sample for obtaining the assigned/prescribed temperature, the possibility of obtaining the even distribution of temperature of the working part of the specimen/sample, the reliability of their continuous operation and

the labor consumption of manufacture.

In our practice are applied in essence laminated heaters (Fig. 225) in the form of cut tube - for heating of cylindrical specimen/samples, and the strip heaters - for flat/plane specimen/samples.

Page 271.

Basic advantage of the construction/design of such heaters is minimum distance (1-2mm) between its walls and the specimen/sample, which provides a comparatively small difference in the temperatures of specimen/sample and heater and leads to a sharp reduction in the expenditure of power in comparison with other forms of heaters [158, 198]. Figure# 226 depicts the dependence of the expenditure of the power of electric power, necessary for heating of the specimen/sample to the assigned/prescribed temperature with the aid of the heaters of our construction/design, manufactured from tantalum.

For an increase in the rigidity of heater, is provided for special bracket 1 with insulator by 2 (Fig. 227), which provides the invariability of the form of heater in the process of endurance tests.

The even distribution of temperature along the length of the working part of the specimen/sample is achieved because of the barrel-shaped form of heater or because of the special form of the working plates (see Fig. 227b). The distance between the heater and the specimen/sample is minimal, since the captures are arrange/located out of heater.
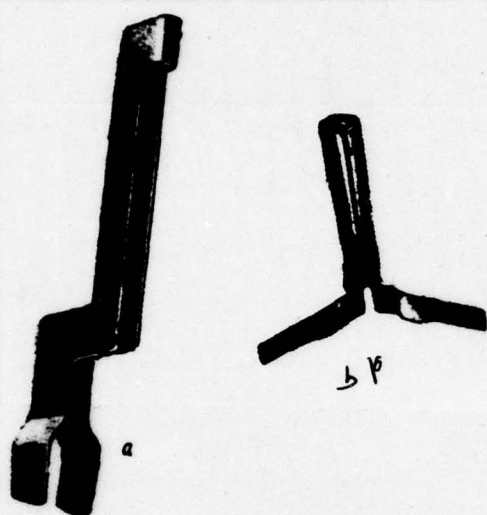
Fig. 225. Heating elements: a) for flat/plane specimen/samples; b) for cylindrical specimen/samples.
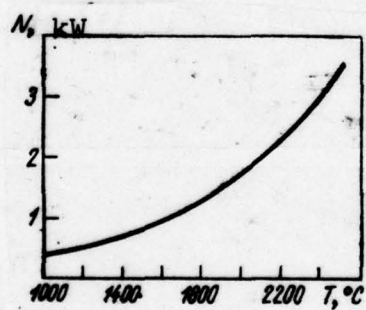
Fig. 226. Dependence of power, consumed by flat/plane heater from tantalum, on temperature.

Page 272.

In the majority at present of the construction/designs of
heaters used is provided for the input/introduction of captures into
the cavity of heater [157, 158, 198], which leads to a considerable
increase in the distance (to 15-25 mm) between the heater and the
specimen/sample, and consequently, to a sharp increase in the power
consumption, spent on heating of specimen/sample. This conclusion
confirm the results of the conducted by us investigation of the
effectiveness of ray heat exchange between the surfaces of flat/plane
heater and specimen/sample in dependence on the distance between them
(Fig. 228).

On   Fig. 228 it follows that with an increase in distance h
between the surfaces of specimen/sample and heater (Fig. 229) from 1
to 5 mm the effectiveness of ray heat exchange $\eta$ between them sharply
falls, but with further increase in this distance, it is changed
insignificantly and remains low.
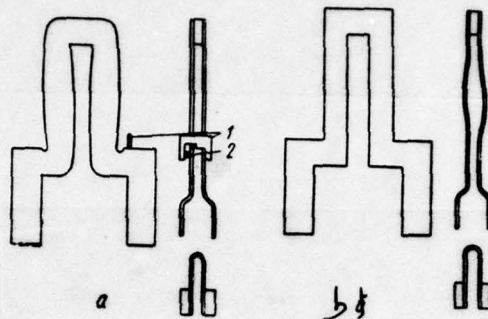
Fig. 227. The scan/development of the flat/plane heater, which ensures the uniform heating of the working part of the specimen/sample: a) the plates of heater have special form; b) barrel-shaped heater.
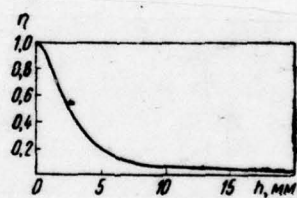


Fig. 228. Dependence of effectiveness of heat exchange ($\eta$) on distance (h) between heater and specimen/sample.
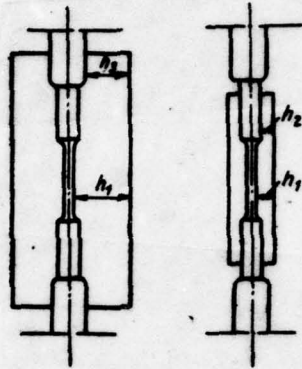
Fig. 229. Diagram of mutual layout of specimen/sample and heater.

Page 273.

For the majority of known heating systems [157, 158, 198] characteristic ones are the high values $h_1$, order 20-25 mm, and $h_3$=15-20 mm (see Fig. 229a). In these cases, as it follows from Fig. 228, on heating of specimen/sample, is expend/consumed the insignificant part of thermal energy, its basic part is spent on the heating of massive thrust/rods for purpose of the decrease of temperature differential along the length of specimen/sample.

From the point of view of the increase of the effectiveness of

heating systems more rational is the schematic, presented in Fig. 229, characteristic feature of which is the fact that the massive thrust/rods do not enter in the heating zone, but heater is considerably approximated to specimen/sample. Values $h_2$ in such cases can compose 1-2 mm, and $h_1 = 4-7$ mm.

In such systems of heating because of the considerable size decrease of heater and increase of the effectiveness of ray heat exchange between the heater and the specimen/sample 4-5 times, are reduced the expenditures of electric power on heating of specimen/sample to the assigned/prescribed temperature during the safeguard for uniform heating of its working part.

Emission/radiation of the temperature distribution along the length of specimen/sample.

Temperature contrast along the length of the working part of the specimen/sample causes the nonuniform strain of its separate sections, which can lead to essential errors during determining of the characteristics of creep.

Let us isolate on the working part of the specimen/sample with the aid of the graduation marks three sections by length on 2mm, as shown in Fig. 230, and let us assume, that mean temperature and the

average speed of strain on sections 1, 2, 3 are respectively equal to: $T_1, \dot{\varepsilon}_1; T_2, \dot{\varepsilon}_2; T_3, \dot{\varepsilon}_3$.

If is considered that in the presence of uneven heating along the length of the specimen/sample which is characterized by the distribution of temperatures $T_1 = T_3 < T_2$, will occur the distribution of the rates of deformation $\dot{\varepsilon}_1 = \dot{\varepsilon}_3 < \dot{\varepsilon}_2$, then it is possible to determine error $A_1$ for measurement $\varepsilon$ as follows:

$$A = \frac{\varepsilon - \varepsilon'}{\varepsilon} = \frac{\frac{\Delta l}{l} - \frac{\Delta l - \delta}{l}}{\frac{\Delta l}{l}} = \frac{\delta}{\Delta l} = \frac{3\dot{\varepsilon}_2 t - 2\dot{\varepsilon}_1 t - \dot{\varepsilon}_2 t}{3\dot{\varepsilon}_2 t} =$$

$$= 0.66 - 0.66 \, (\dot{\varepsilon}_1 / \dot{\varepsilon}_2), \qquad (6.8)$$

where $\delta$ - decrease $\Delta l$ because of the nonuniformity of the strain

$$\dot{\varepsilon}_1 = \dot{\varepsilon}_3 < \dot{\varepsilon}_2.$$

Page 274.

The value of error $A$ in dependence on the ratio of the velocities of strain $\dot{\varepsilon}_1 / \dot{\varepsilon}_2$ is represented graphically in Fig. 231. In Fig. 224 was represented the dependence $\dot{\varepsilon}_1 / \dot{\varepsilon}_2$ on $\Delta T$ for alloy VN-2 with stress 75 MN/m² (7.65 kg/mm²). With the aid of Fig. 224 and 231 it is possible to determine $A$, by knowing the temperature

differential along the length of specimen/sample $\Delta T$. For example, for $\Delta T=10$ deg value A composes 19o/o. In this case, it must be noted that at one and the same value $\Delta T$ for different materials of the value of relation $\dot{\varepsilon}_1/\dot{\varepsilon}_2$ are different, and consequently, are distinguished values A.

The given calculation, in spite of the averaging of the values of velocities for individual sections, convincingly shows that even an small (~ 10 deg) temperature differential leads to the significant errors in determining of the characteristics of creep. The degree of evacuation/rarefaction and the inleakage in test chamber, the composition of medium and material of heaters, and also other factors have to a greater or lesser extent effect on the rate of creep strain of refractory metals. Under these conditions the nonuniformity of the temperature distribution along the length of specimen/sample must be brought to minimum.

At present the nonuniformity of heating specimen/sample, as a rule, they determine with the aid of thermocouples by measuring the temperature in different point of the heated specimen/sample. Unfortunately, the higher the temperature, those less sensitive thermocouples it is necessary to utilize. This leads to the fact that the accuracy of the measurement of temperature actually exceeds the permissible gradient. In connection with this is developed the method

cf determining of temperature differential along the length of specimen/sample, instituted on the account cf a change in the length cf different sections of its working part after strain.
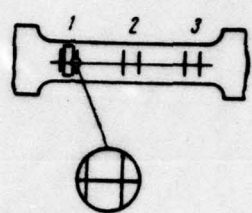
Fig. 230. Specimen/sample for measuring the strain of individual sections.
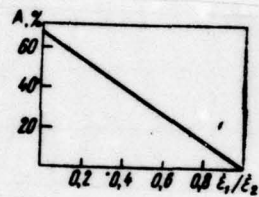
Fig. 231. Effect of nonuniformity of distribution of rate of deformation of specimen/sample on accuracy/precision of its determination.

Page 275.

If temperature in all points of the working part of the specimen/sample is identical, then also the rate of deformation of its separate sections will be one and the same. Knowing the dependence of the rate of deformation of this material on temperature, on a difference in the strain of individual sections, it

is possible to determine the temperature differential along the
length of specimen/sample. However, in this case, one should consider
the error, caused by the local character of plastic deformation.
Figures 232 depicts the graph of strain distribution for the
specimen/sample of alloy on the basis of niobium on section 5 mm in
long at temperature of 1300°C (overall strain composed 9.8o/o). The
strain of sections 0.2 mm in long oscillates within limits from
8.6o/o to 11o/o; for sections 2 mm in long oscillation it is less -
within limits of 9.6-10c/o.

At the length of sections l=2 mm and their during relative
strain 10o/o, amount of the strain of each section during the even
distribution of temperature (without the account the locality of
strain) is 200 μm. A difference in the strains for individual
sections composes 10o/o-9.6c/o=0.4c/o, i.e., 8 μm. Then from equation
(6.8) it follows that $A$ =4o/c. Putting to use graphs in Fig. 224 and
231, we find that the same error in the determination of the
deformation rate can be caused the temperature differential along the
length of specimen/sample, equal to 2 deg.

Absolute accuracy p, from which one should measure the distances
between grooves in specimen/sample during the study the temperature
differential, can be determined from the relationship/ratio:

$$p = \Delta d, \qquad (6.9)$$

where $\Delta$ - the permissible error during measurement;

$\varepsilon$ - amount of relative strain;

$l$ - distance between grooves.

In our case ($\Delta=1o/c$,   $\varepsilon = 10o/o$   $l = 2000$ $\mu m$) p=2 $\mu m$. We determined the distances between grooves with the aid of the microscope, built in into tool PMT-3, which provides the absolute accuracy of the measurement ~0.3 $\mu m$.
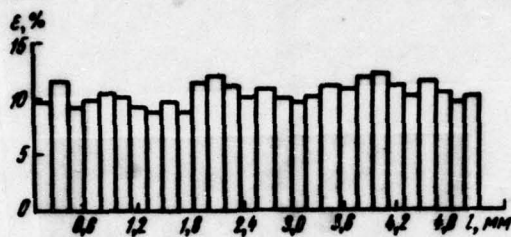
Fig. 232. Strain distribution according to specimen/sample made of alloy on the basis of niobium at temperature of 1300°C.

Page 276.

Characteristics of strength and plasticity of refractory metals under the prolonged effect of load and temperature.

In the Institute of the problems of the strength of AS UkSSR, are carried out the investigations of creep and stress-rupture strength of molybdenum, niobium, tantalum and some alloys on their basis whose results are given in present paragraph.

All the investigations were conducted in vacuum (1.38-0.399 MN/m² [1·10⁻⁵-3·10⁻⁶ mm Hg]) during the testing units, described in the preceding/previous paragraph. For the tests of tantalum and alloys of tantalum and niobium, were applied the planes (see Fig.

220b), while for the tests cf molybdenum - cylindrical (see Fig. 220c) specimen/samples. Basis of tests was 10-500 h.

Tantalum [1].

FOOTNOTE [1]. Composition - see Table 3. ENDFOOTNOTE.

Together with tungsten tantalum is the refractory metal (melting point composes 2996°C); however, its strength during short-term and endurance tests is lower than the strength of tungsten.

Fig. 233. The stress-rupture strength of tantalum: 1 - at 800°C; 2 - at 900°C.

Key: (1). MN/m$^2$ (kg/mm$^2$). (2). h.

Table 33. Creep rates of tantalum.

| Температура испытания, °С (1) | Напряжение, Мн/м$^2$ (кГ/мм$^2$) (2) | Время до разрушения, ч (3) | Скорость ползучести, %/ч (4) |
|---|---|---|---|
| 800 | 107,8 (11) | 239 | 0,030 |
|     | 117,6 (12) | 67  | 0,180 |
| 900 | 78,4 (8)   | 99  | 0,190 |
|     | 83,3 (8,5) | 37  | 0,525 |
|     | 93,1 (9,5) | 4   | 4,800 |

Key: (1). Testing temperature, °C. (2). Stress, MN/m² (kg/mm²). (3). Time to failure, h. (4). Creep rate, c/c per hour.

Page 277.

Figures 233 depicts the results of the tests of unalloyed annealed tantalum for stress-rupture strength with 800 and 900°C.

Stress-rupture strength (base 100 h) at 800°C is equal to 115 MN/m²

(11.7 kg/mm²), and at 900°C it is 80 MN/m² (8.2 kg/mm²). Follows to

note that an incidence/drop in the stress-rupture strength with an

increase in the duration of tests is small (angle of the slope of

curved stress-rupture strength to time axis is small).


The values of the creep rates of tantalum they are brought in

Table 33.

Alloy Ta-10% W[1].

FOOTNOTE [1]. Composition - see Table 3.  ENDFOOTNOTE.


The stress-rupture strength of pure tantalum can be raised, by

alloying by other its refractory metals. One of the most widely used

alloys of tantalum with tungsten it is Ta-10c/o W.


The investigation of creep and stress-rupture strength of this

alloy were conducted with 800, 900, 1300 and 1800°C. Figures 234

depicts the results of the test of stress-rupture strength.


From given data follows that the stress-rupture strength of

alloy Ta-10o/o W with 800 and 900°C falls into time insignificantly,

whereas at temperatures 1300 and 1800°C imeet a powerful reduction in

the strength with an increase in the duration of tests.
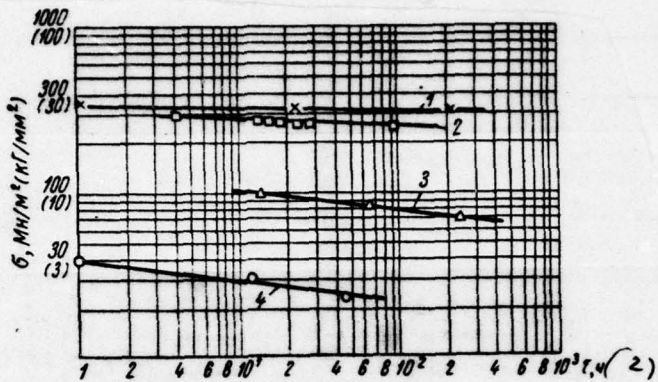
Fig. 234. The stress-rupture strength of alloy Ta-10o/o W. 1 - at 800°C; 2 - at 900°C; 3 - at 1300°C; 4 - at 1800°C.

Key: (1). $\sigma$, MN/m² (kg/mm²). (2). $\tau$, h.

Page 278.

The comparison of the results of the test of the stress-rupture strength of pure tantalum (see Fig. 233) and of alloy Ta+10o/o W (see Fig. 234) it shows that the alloy considerably stronger than pure tantalum: its stress-rupture strength proves to be 3-3.5 times higher.

Table 34 gives the results of measuring the creep rate of alloy Ta-10o/o W.

Molybdenum. The results of the test of the unalloyed molybdenum'

for stress-rupture strength with 1400°C are given to Fig. 235,
where along the axis of ordinates is plotted stress, and along the
axis of abscissas, - a logarithm of time to failure.

FOOTNOTE [1]. Composition - see Table 3. ENDFOOTNOTE.

All experimental points well fit a straight line, therefore, the
functional dependence between stress and time to failure for
molybdenum can be represented in the following form:

$$t = Ae^{-\alpha\sigma}, \tag{6.10}$$

where t - time to the failure

$\sigma$ - stress;

$A$, $\alpha$ - constant coefficients.

Table 34. Creep rates of alloy Ta-10o/o H.

| Температура испытания, °C (1) | Напряжение, Мн/м² (кГ/мм²) (2) | Время до разрушения, ч (3) | Скорость ползучести, %/ч (4) |
|---|---|---|---|
| 900 | 294,0  (30) | 283,0 | 0,011 |
|  | 313,6  (32,5) | 96,0 | 0,033 |
|  | 333,2  (34,2) | 86,0 | 0,070 |
|  | 352,8  (36,3) | 14,5 | 0,250 |
| 1300 | 68,6   (7,0) | 244,0 | 0,055 |
|  | 82,32  (8,4) | 65,0 | 0,300 |
|  | 98,98 (10,1) | 14,0 | 1,35 |
| 1800 | 22,54  (2,3) | 46,0 | 0,860 |
|  | 29,4   (3,0) | 12,0 | 1,500 |
|  | 39,2   (4,0) | 1,0 | 16,000 |

Key: (1). Testing temperature,        °C. (2). Stress, MN/m² (kg/mm²).

(3). Time to failure, h. (4). Creep rate, % per hour.



Fig. 235. Stress-rupture strength of molybdenum at temperature of
1400°C.

Key: (1). $\sigma$, MN/m² (kg/mm²). (2). $\tau$, h.

Page 279.

The values of the creep rates of molybdenum for different
stresses are given in Table 35.

Alloy VM-1 [1] in initial state is characterized by the noticeable
structural heterogeneity: together with the sections of the

relatively even distribution of fibrous structure, there were whirlpools of filaments.

FOOTNOTE 1. Composition - see Table 3. ENDFOOTNOTE.

It turned out that the whirlpools had large hardness [H=3500-5000 MN/m² (357-408 kg/mm²)], than remaining material [H=2300-2700 MN/m² (235-276 kg/mm²)]. This is one of the confirmation of the heterogeneity of strain distribution after rolling in this alloy; the presence of sections with different hardness affects the course of recrystallization, strain and the decomposition of material.

Table 35. Creep rates of molybdenum with 1400°C.

| Напряжение, Мн/м² (кГ/мм²) (1) | Время до разрушения, ч (2) | Скорость ползучести, %/ч (3) |
|---|---|---|
| 19,6 (2,0) | 94,0 | 0,133 |
| 24,5 (2,5) | 32,5 | 0,475 |
| 39,2 (4,0) | 4,5 | 3,500 |
| 49,0 (5,0) | 0,5 | 18,400 |

Key: (1). Stress, MN/m² (kg/mm²). (2). Time to failure, h. (3). Creep
rate, o/o per hour.
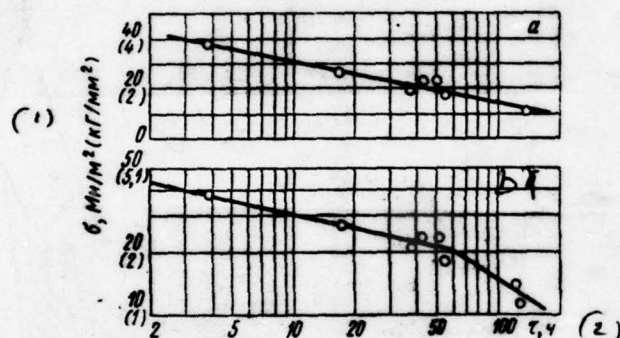


Fig. 236. Stress-rupture strength of alloy VM-1 at 1600°C: a) in
coordinates σ - lg t; b) in coordinates lg σ - lg t.

Key: (1). MN/m² (kg/mm²). (2). h.

Page 280.

The curve of the stress-rupture strength of alloy VM-1 at 1600°C

is represented in semi-logarithmic coordinates in Fig. 236a. From curve/graph it follows that the dependence between stress and time to failure can be described by equation (6.10), as in the case of pure molybdenum.

The results of the test of alloy VM-1 are represented also in the logarithmic system of coordinates (Fig. 236b). In this case on the graph of stress-rupture strength, there is a break. Judging by curves of creep, to the onset of break (50 h) still occurs an increase in the strain, and then gradually it ceases. This gives grounds to assume that the break corresponds to the replacement of the mechanisms of creep - to transition from shift mechanism to diffusion.

Thus, it can be assumed that the power dependency between stress and time to the failure

$$t = B\sigma^{-\beta},\qquad\qquad (6.11)$$

where $B$, $\beta$ - constant coefficients, characterize the physical processes, which occur in material; however for the facilitation of extrapolation to conveniently put to use exponential dependence (6.10).

Table 36 gives corrected values of creep rates for different stresses with 1600°C.

Allcys on the basis of niobium [1].

FCCTNOTE [1]. Composition - see Table 3. ENDFCCTNCTE.

Niobium and its alloys possess good plasticity and comparatively high heat resistance, having in this case low specific gravity/weight in comparison with refractory metals - molybdenum, by tantalum and tungsten.

I carried out the investigation of creep and stress-rupture strength of alloys VN-2, Nb - 9.8o/o Mo (alloy 1), Nb - 9o/o Mo (alloy 2).

Table 36. Creep rates of alloy VM-1 at 1600°C.

| Напряжение. Мн/м² (кГ/м.м²) (1) | Время до разрушения, ч (2) | Скорость ползучести, %/ч (3) |
|---|---|---|
| 11,0 (1,12) | 133 | 0,0065 |
| 13,0 (1,32) | 124 | 0,0200 |
| 18,0 (1,84) | 54 | 0,0575 |
| 22,5 (2,26) | 49 | 0,1690 |

Key: (1). Stress, MN/m² (kg/mm²). (2). Time to failure, h. (3). Creep rate, o/o per hour.

Page 281.

According to their structure niobium alloys are solid solutions and are not strengthened by temper hardening. Niobium alloys can be strengthened by the dispersed particles of carbides, oxides and other compounds, which are generated during the reaction of the cell/elements of implementation with zirconium, titanium, hafnium and other additions. In this case, it is possible within considerable limits to vary strength and plasticity of alloys.

Alloy VN-2. The results of the tests of alloy VN-2 for stress-rupture strength are given to Fig. 237 and in Table 37.

As can be seen from Fig. 237, test results satisfy well power dependency (6.11) in the investigated temperature and time intervals.
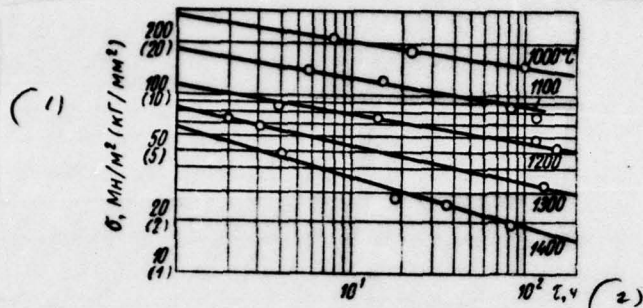
Fig. 237. The stress-rupture strength of alloy VN-2.

Key: (1). MN/m² (kg/mm²). (2). h.

Table 37. Creep rates of alloy VN-2.

| Температура испытания, °C (1) | Напряжение, Мн/м² (кгГ/мм²) (2) | Скорость ползучести, %/ч (3) |
|---|---|---|
| 1000 | 196,0 (20,0) | 1,92 |
|  | 176,4 (18,0) | 0,5 |
|  | 135,24 (13,8) | 0,11 |
| 1100 | 117,6 (12,0) | 1,56 |
|  | 79,38 (8,1) | 0,286 |
|  | 66,64 (6,8) | 0,113 |
| 1200 | 73,5 (7,5) | 2,0 |
|  | 68,6 (7,0) | 1,32 |
|  | 55,86 (5,7) | 0,188 |
|  | 52,92 (5,4) | 0,168 |
| 1400 | 26,46 (2,7) | 1,9 |
|  | 23,52 (2,4) | 1,06 |
|  | 18,13 (1,85) | 0,4 |

Key: (1). Testing temperature, °C. (2). Stress, MN/m² (kg/mm²).

(3). Creep rate, o/o per hour.

Page 282.

For an alloy is characteristic high strength. Minimum plasticity occurs with 1000°C; permanent elongation in this case composes 20-25o/o. Higher than 1100°C is observed the considerable increase of plasticity (δ=45-50o/o) and at 1200°C plasticity is maximum (δ=70-75o/c). At this temperature occurs an increase in the plastic deformation with an increase in the time tc failure during the decrease of load.

At 1300-1400°C plasticity somewhat descends; however, all the same is sufficiently high (δ=50-6Cc/o).

The values of the rates of the steady-state creep, designed on the basis of primary curves of creep, are given in Table 37.

Alloy 1 differs significantly from alloy VN-2 in the content of molybdenum (9.8o/o and 3o/o, respectively). The results of the tests of alloy 1 are represented in Fig. 238a and in Table 38. Ccmmunication/connection between stress and time to failure for alloy 1, as for alloy VN-2, characterizes power dependency (6.11). The characteristics of the heat resistance cf alloy 1 at high temperatures are somewhat higher than fcr alloy VN- 2 (see Table 37), at the same time the plasticity of alloy 1 lower than the plasticity cf alloy VN-2.
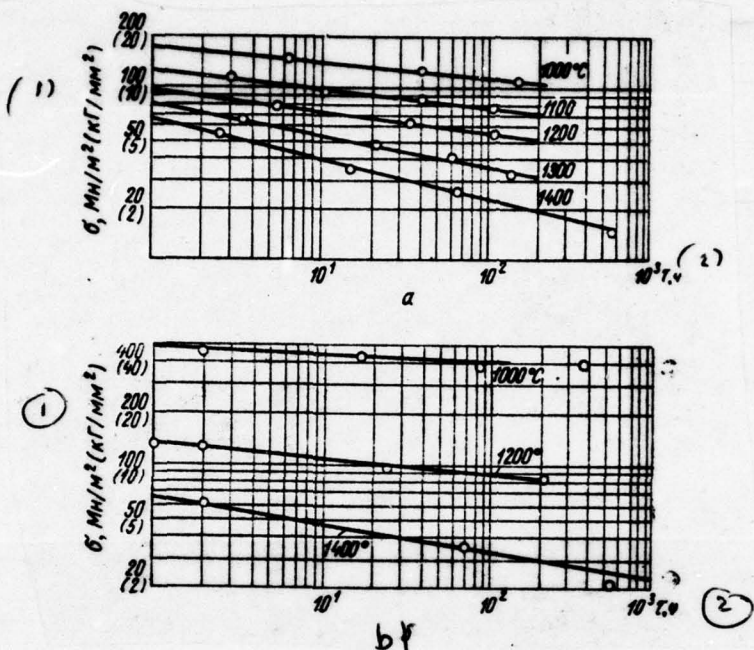
Fig. 238. The stress-rupture strength of alloys on the basis of the niobium: a) alloy 1; b) alloy 2.

Key: (1). MN/m² (kg/mm²). (2).  h.

Page 283.

At 1000°C plasticity with decrease stress and an increase in the time to failure remains the virtually constant/invariable (permanent elongation per unit length after decomposition composes 34-36o/o), at

1200°C value δ=35-40o/o, while at 1400°C value δ=45-50o/o.

The values of the creep rates of alloy 1 are given in Table 38.

Alloy 2. Test results for this alloy are represented in Fig. 238b and in Table 39.

Stress and time to the failure of alloy 1 are connected by exponential equation (6.11). The characteristics of the plasticity of alloy 2 are considerably lower than for VN-2 and alloy 1. So, at 1000°C the elongation per unit length of the specimen/sample of alloy 2 composes a total of 5-7o/c, at 1200°C 9-11c/c and at 1400°C 12-15o/o. However, on heat resistance alloy 2 considerably exceeds two first alloys.

For the comparison of the characteristics of the investigated alloys of niobium Fig. 239 and 240 depict the temperature dependences of hour stress-rupture strength [lg $\sigma_0 = f_1(T)$] and the coefficient, which determines the slope/inclination of the graph of stress-rupture strength in the logarithmic system of coordinates [$\beta = f_2(T)$]. The first dependence characterizes the strength, the second - creep strength.

The greatest stress-rupture strength with 1000°C has alloy 2

[469 MN/m² (48 kg/mm²) with holding 1 h]; hcur stress-rupture strength of alloy VN-2 and cf alloy 1 is respectively equal to 276 and 165 MN/m² (27 and 17 kg/mm²) (Table 39).

Table 38. Creep rates of alloy 1.

| Температура испытания, °C (1) | Напряжение, Мк/м² (кГ/мм²) (2) | Время до разрушения, ч (3) | Скорость ползучести, %/ч (4) |
|---|---|---|---|
| 1000 | 146,02 (14,9) | 6,5 | 2,780 |
|      | 122,50 (12,5) | 41,0 | 0,510 |
|      | 102,90 (10,5) | 137,0 | 0,125 |
| 1200 | 77,42 (7,9) | 5,5 | 4,100 |
|      | 63,70 (6,5) | 35,0 | 0,530 |
|      | 53,90 (5,5) | 110,0 | 0,190 |
|      | 49,98 (5,1) | 117,0 | 0,152 |
| 1400 | 52,92 (5,4) | 2,5 | 10,250 |
|      | 24,50 (2,5) | 63,0 | 0,286 |
|      | 14,70 (1,5) | 583,0 | 0,058 |

Key: (1). Testing temperature,    °C. (2). Stress, MN/m² (kg/mm²). (3). Time to failure, h. (4). Creep rate, c/o per hour.

Page 284.

Given data show that for niobium fusions because of alloying with different cell/elements can be obtained the essentially different values of strength and plasticity; however, with a temperature rise, these differences in certain cases are leveled. So, at 1400°C value of hour stress-rupture strength for alloy 2 is 66 MN/m² (6.7 kg/mm²), for alloy VN-2, it is equal to 63 MN/m² (6.4 kg/mm²) and for alloy 1 - 69 MN/m² (7 kg/mm²).

Table 39. The stress-rupture strength of niobium fusions at different temperatures.

| Сплав (1) | Темпера- тура испытания, °C (2) | $\sigma_1$, Мн/м² (кГ/мм²) (3) | | $\sigma_{100}$, Мн/м² (кГ/мм²) (3) | | $\sigma_{200}$, Мн/м² (кГ/мм²) (3) | | $\sigma_{500}$, Мн/м² (кГ/мм²) (3) | |
|---|---|---|---|---|---|---|---|---|---|
| ВН-2 | 1000 | 276 | (28,2) | 143 | (14,6) | 129 * | (13,1) | 114 * | (11,6) |
| | 1100 | 167 | (17) | 82 | (8,4) | 74 | (7,55) | 64 * | (6,5) |
| | 1200 | 114 | (11,6) | 50 | (5,1) | 44 | (4,5) | 37 * | (3,75) |
| (4) | 1300 | 84 | (8,6) | 29 | (3,0) | 26 | (2,63) | 22 * | (2,22) |
| | 1400 | 62 | (6,3) | 17 | (1,72) | 14 * | (1,42) | 10 * | (1,02) |
| Сплав 1 | 1000 | 165 | (16,8) | 111 | (11,3) | 105 | (10,7) | 96 * | (9,8) |
| | 1100 | 126 | (12,85) | 77 | (7,85) | 72 | (7,35) | 66 * | (6,75) |
| | 1200 | 94 | (9,6) | 50 | (5,1) | 45 | (4,6) | 40 * | (4,1) |
| (4) | 1300 | 79 | (8,1) | 34 | (3,46) | 30 | (3,06) | 26 * | (2,65) |
| | 1400 | 68 | (6,95) | 24 | (2,45) | 20 | (2,02) | 16 | (1,63) |
| Сплав 2 | 1000 | 469 | (47,8) | 387 | (39,5) | 376 | (38,35) | 361 * | (36,8) |
| | 1100 | 231 * | (23,6) | 180 * | (18,4) | 173 * | (17,65) | 165 * | (16,8) |
| | 1200 | 130 | (13,3) | 93 | (9,5) | 88 | (9,0) | 83 * | (9,0) |
| | 1300 | 87 * | (8,9) | 56 * | (5,7) | 53 * | (5,4) | 48 * | (4,9) |
| | 1400 | 65 | (6,6) | 35 | (3,56) | 32 | (3,26) | 28 * | (2,85) |

Key: (1). Alloy. (2). Testing temperature,     °C. (3). MN/m²

(kg/mm²). (4). Alloy.

------

FOOTNOTE [1]. Data are acquired by extrapolation. ENDFOOTNOTE.

MICROCOPY RESOLUTION TEST CHART
NATIONAL BUREAU OF STANDARDS-1963-A
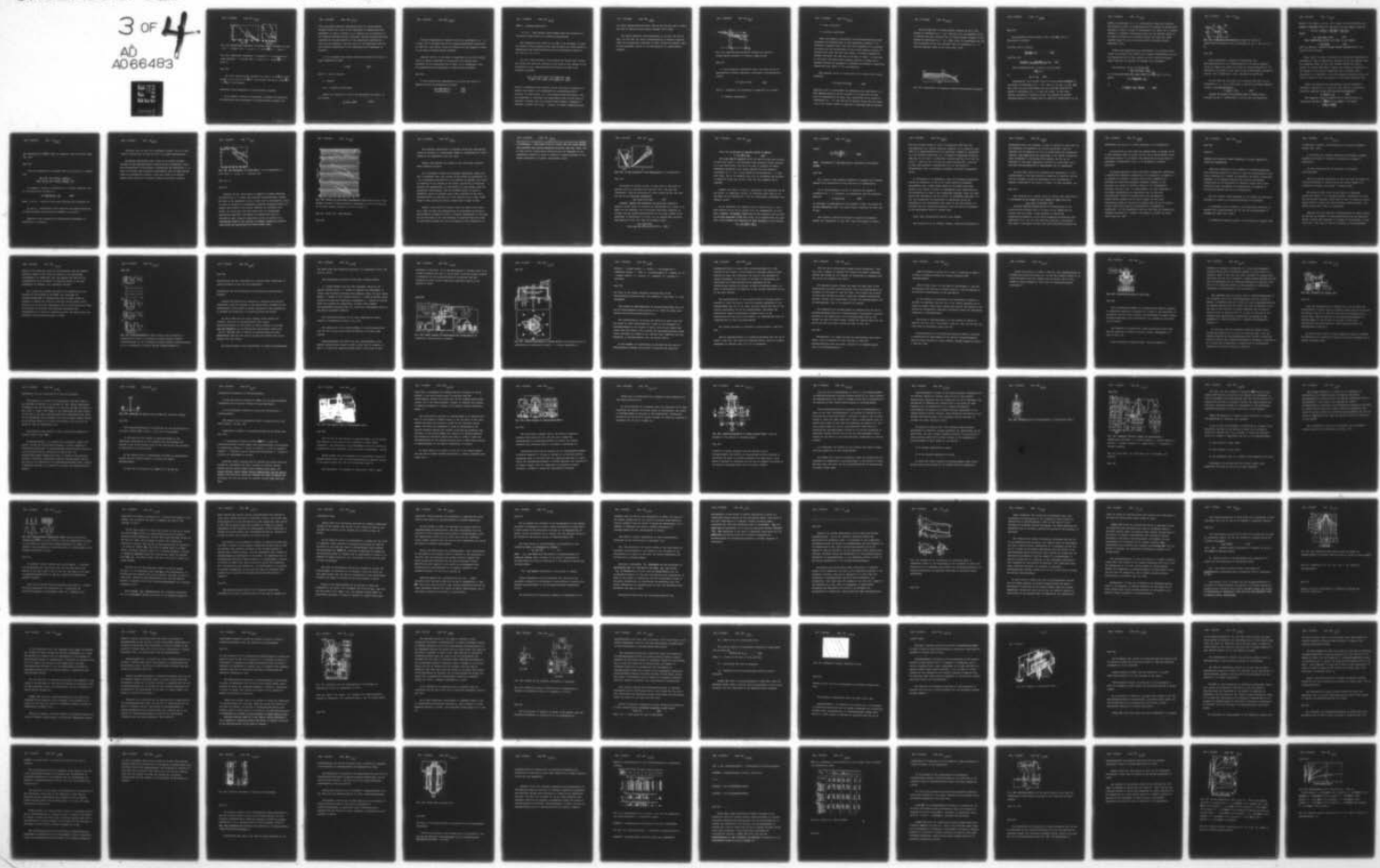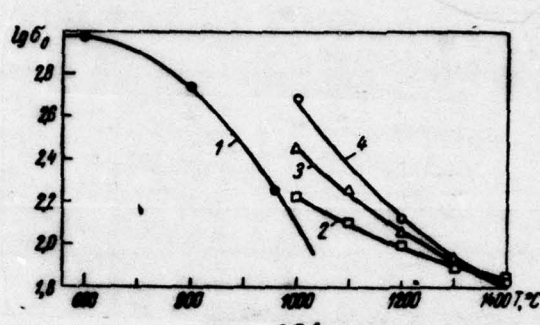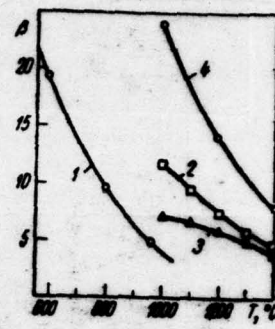
Fig. 239.    Fig. 240.

Fig. 239. Temperature dependence of stress-rupture strength (on base 1 h): 1 - Inconel 700; 2 - alloy 1; 3 - alloy VN-2; 4 - alloy 2.

Fig. 240. Temperature dependence of parameter $\beta$, of characteristic creep strength: 1 - Inconel 700; 2 - alloy 1; 3 - alloy VN-2; 4 - alloy 2.

Page 285.

500- hour stress-rupture strength for alloy 2 is 28 MN/m² (2.85 kg/mm²), for an alloy 1-16 MN/m² (1.63 kg/mm²) and for an alloy VN-2 - 10 MN/m² (1.02 kg/mm²).

Temperature-time dependences of stress-rupture strength.

Is at present a series of expressions, proposed for describing the temperature-time dependences of stress-rupture strength [201,

202 ]. Processing numerous experimental data the stress-rupture strength showed that none of the expressions of temperature-time dependence is general purpose, i.e., suitable for all materials in the unlimited temperature-time intervals. Meanwhile, temperature-time intervals of the applicability of the expressions indicated as a rule, are not imparted. From our point of view preferable ones are the following expressions of the temperature-time dependence of strength.

1. It is assumed that between stress and service life there is power dependency of form

$$t = B\sigma^{-\beta},$$
     (6.12)

where t - time to failure;

$\sigma$ - stress;

B, $\beta$ - constant coefficients.

Taking the logarithm of (6.12) and designating lg $B/\beta = \sigma_0$, we will obtain

$$\lg \sigma = \lg \sigma_0 - \frac{1}{\beta} \lg t.$$
     (6.13)

From the curve/graph of equation (6.13) in coordinates lg $\sigma$ - lg T (Fig. 241) it follows that for the assigned/prescribed temperature of value lg $\sigma$ and $1/\beta = tg\ \alpha$ they are constants in the absence of break on the graph of stress-rupture strength.

Equation (6.13), if are known to dependence lg $\sigma_0 - f_1(T)$ and $\beta = f_2(T)$, it makes it possible to extrapolate test results both according to the temperature and on time, and it represents, thus, the temperature-time dependence of stress-rupture strength.

Page 286.

It was accepted that dependences lg $\sigma_0 = f_1(T)$ and $\beta = f_2(T)$ in general form can be presented as follows:

$$lg\ \sigma_0 = a_1 T^2 + b_1 T + c_1, \qquad (6.14)$$

$$\beta = a_2 T^2 + b_2 T + c_2. \qquad (6.15)$$

where T - testing temperature;

$a_n, b_n, c_n$ - the constant coefficients which they calculate on the basis of test results at different temperatures.

For determining the values $a_1$, $b_1$, $c_1$, it is necessary to solve the system of three equations with three unknowns for three values of temperatures and established/installed from experiments values lg $\sigma'_0$; lg $\sigma''_0$; lg $\sigma'''_0$.

So, for a heat-resistant alloy Inconel 700 (46.5o/o Ni; 29.4o/o Co; 14.8o/o Cr) [205] you obtained on the basis of the results of six experiments by the common/general/total duration of 600 h the following equations:

$$lg\,\sigma_0 = -4.44 \cdot 10^{-6}T^2 + 46.11 \cdot 10^{-4}T + 88.99 \cdot 10^{-2}, \quad (6.16)$$
$$\beta = 60.29 \cdot 10^{-6}T^2 - 1342.2 \cdot 10^{-4}T + 78.254 \cdot 10^{-2}, \quad (6.17)$$

which, in combination with equation (6.13) they made it possible to predict the results of 50 experiments by common/general/total duration, 20 times larger ($\sigma_0$ - hour stress-rupture strength). From the comparison of calculated and experimental data for the alloy in question it follows that the proposed method makes it possible to determine stresses with error ±10o/o, if testing temperature does

not exceed assign/prescribed more than on 100-120 deg, and to reduce the time of testing stress-rupture strength 10-15 times.

One should emphasize that dependences $\lg \sigma_0 = f_1(T)$ and $\beta = f_2(T)$ (Fig. 239 and 240) are strict characteristics of concrete material, since the insignificant deviation of their values from nominal leads to the significant errors in the determination of stress-rupture strength.
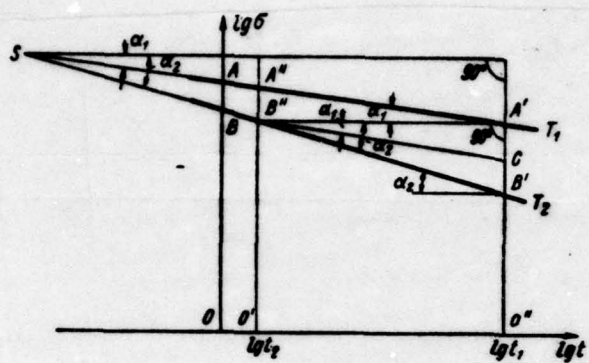
Fig. 241. Communication/connection between the curves of stress-rupture strength at different temperatures.

Page 287.

2. From parametric dependences [201, 202] test of all is experimentally checked dependence, determined by Larson-Miller's formula

$$T(C + \lg t) = p = F(\sigma), \qquad (6.18)$$

where p - parameter, not depending on temperature at $\sigma$=const;

T - absolute temperature;

t - time to failure;

C - constant coefficient.

There are numerous contradictory conclusion/derivations about advantages and disadvantages in this expression. However, it is accepted to consider [203, 204] that this dependence it is possible to utilize for the extrapolation of the stress-rupture strength of material with error not more than $\pm 10o/c$, if testing temperature differs from given one less than by 50 deg, but time - is less than to one order. The given below analysis allowed to refine and to somewhat develop the dependence in question and thereby to expand the temperature-time limits of its applicability.

From equation (6.18) it follows that with $\sigma$=const also P=const, therefore,

$$T_1(C + \lg t_1) = T_2(C + \lg t_2). \qquad (6.19)$$

Equation (6.19) is recommended for determining the coefficient of C. Thus, Larsona-Miller's method consists in the fact that the base curve of decomposition ab (Fig. 242), constructed in the system of coordinates $\lg \sigma$ - P, with the aid of equation (6.18) for any values $\sigma$ and T with known C makes it possible to determine time to failure.

From the equation of stress-rupture strength (6.13) in the system of coordinates lg $\sigma$ - lg t (see Fig. 241) and equation (6.18) it follows that each straight line of stress-rupture strength in the system of coordinates lg $\sigma$ - lg t (Fig. 243a) is transformed with the aid of equation (6.18) into straight line in coordinates lg $\sigma$ - P with the specific angle of the slope (Fig. 243b).
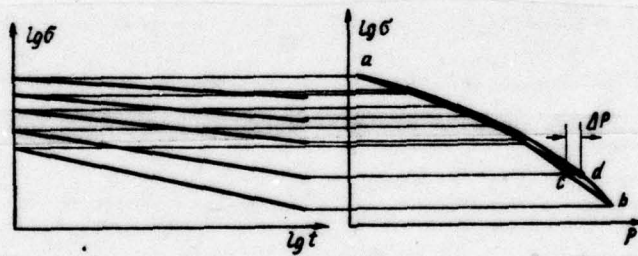
Fig. 242. Construction of parametric curved stress-rupture strength.

Page 288.

The dependence between angles α and γ (see Fig, 243) is determined as follows:

from Fig. 243a it follows

$$\frac{\lg \sigma_1 - \lg \sigma_2}{\lg t_2 - \lg t_1} = \operatorname{tg} \alpha, \qquad (6.20)$$

from Fig. 243

$$\frac{\lg \sigma_1 - \lg \sigma_2}{P_1 - P_2} = \frac{\lg \sigma_1 - \lg \sigma_2}{T(C + \lg t_2) - T(C + \lg t)} = \lg \gamma. \qquad (6.21)$$

After dividing (6.20) on (6.21), we will obtain

$$\frac{\operatorname{tg} \alpha}{T \cdot \lg \gamma} = 1,$$

or

$$\operatorname{tg} \alpha = T \cdot \operatorname{tg} \gamma. \qquad (6.22)$$

Consequently, the straight lines of stress-rupture strength in the system of coordinates lg σ - lg t with $T_1$, $T_2$, $T_3$, ..., $T_n$ (see Fig. 242a) they are transformed also into straight lines in the system of coordinates lg σ - P (see Fig. 242b). In this case, several, according to equation (6.22), are changed the relative slope/inclination of straight lines at different temperatures. In the

system cf coordinates lg σ - P, each straight line, as it follows from equation (6.18), is shift/sheared by in parallel to itself along axle/axis P during a change in coefficient cf C. Thus, for a concrete material at different temperatures there are the specific values C, at which is obtained the continuous broken line (see Fig. 242b), variable curve. In this case Larscn-Miller's method is valid, ctherwise is not.

Ecrmula for determining the coefficient C. In a series of the works, it is noted, that coefficient C depends substantially both on the temperature and on time; however are not given the formulas, which would make it possible tc consider this dependence.

From equation (6.19) it follows that

$$C(T_2 - T_1) = T_1 \lg t_1 - T_2 \lg t_2.$$

If is designated $T_2 - T_1 = \Delta T$, then $C \cdot \Delta T = T_1 \lg t_1 \lg t_2 - \Delta T \lg t_2,$ whence

$$C = \frac{T_1 (\lg t_1 - \lg t_2)}{\Delta T} - \lg t_2,$$

cr

$$C = \frac{T_1}{\Delta T} \left( \lg t_1 - \lg t_2 - \frac{\Delta T}{T} \lg t_2 \right). \qquad (6.23)$$
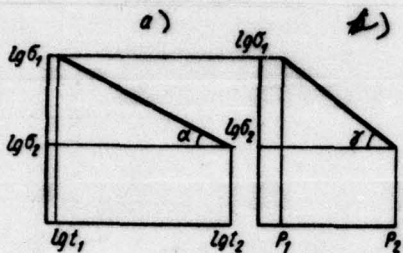
Fig. 243. Communication/connection between the curves of stress-rupture strength in the coordinates: a) lg σ - lg t; b) lg σ - V.

Page 289.

Since coefficient C depends on temperature, the accuracy/precision of its determination with the aid of equation (6.23) is higher, the lesser the value ΔT. During processing of the obtained by us results of the tests of the stress-rupture strength of alloys 1 and 2 coefficient C they calculated for ΔT=10 deg.

In this case the value ΔT/T lg t₂ composed less than 1o/o of difference lg t₁ - lg t₂, which made it possible to present equation (6.23) in the following form:

$$C = \frac{T_1}{\Delta T}(\lg t_1 - \lg t_2). \qquad (6.24)$$

Figures 241 depicts the straight lines of stress-rupture strength and BB' at temperatures T₁ and T₂ with the appropriate

angles of the slope $\alpha_1$ and $\alpha_2$. With $\sigma=\text{const}$ (to this condition, for example, correspond cuts O'B'' and A''O''). we will obtain following:

$$\text{tg}\,\alpha_1 = \frac{1}{\beta_1} = \frac{A'B'}{\lg t_1 - \lg t_2} = \frac{A'O' - B''O'}{\lg t_1 - \lg t_2} = \frac{\lg \sigma_{01} - \lg \sigma_{02}}{\lg t_1 - \lg t_2},$$

whence

$$\lg t_1 - \lg t_2 = \beta_1 (\lg \sigma_{01} - \lg \sigma_{02}). \qquad (6.25)$$

After substituting (6.25) in (6.24), we will obtain

$$C = \frac{T_1}{\Delta T} \beta_1 \lg \frac{\sigma_{01}}{\sigma_{02}}, \qquad (6.26)$$

where $\sigma_{01}$ and $\sigma_{02}$ - value of stress-rupture strength with $T_1$ and $T_2 = T_1 + \Delta T$ (with t=const).

Thus, (6.26) it makes it possible to determine the dependence of coefficient C only on temperature. Equation (6.26) was obtained under the assumption about the fact that between tension and time to failure is a power dependency. However, the essence of conclusion is not changed, if the form of dependence will be another. For a conclusion it is important so that the dependence between tension and time to failure it would be possible to approximate straight line.

Widest use together with exponential obtained exponential dependence. Therefore it is useful to note that for a last/latter dependence equation (6.26) will take the following form:

$$C_1 = \frac{T_1}{\Delta T} \beta_1 (\sigma_{01} - \sigma_{02}). \qquad (6.27)$$

From equation (6.26) it follows that $\Delta C$ with $T_1$=const and transition from one $t_1$ to next it is caused by the change

$$\left[\lg \frac{\sigma_{01}}{\sigma_{02}}\right]_{t_1} - \left[\lg \frac{\sigma_{01}}{\sigma_{02}}\right]_{t_2}$$

and, therefore, if $B''C \| A''A'$, then by difference $A'B' - A''B'' = C'B'$ (see Fig. 241).

Page 290.

From the examination of triangles $A'B''C$ and $A'B''B'$, it follows that

$$CB' = A'B' - A'C = A'B'' \, \mathrm{tg}\, \alpha_2 - A'B'' \, \mathrm{tg}\, \alpha_1 =$$
$$= (\lg t_1 - \lg t_2) \frac{1}{\beta_2} - (\lg t_1 - \lg t_2) \frac{1}{\beta_1} = \lg \frac{t_1}{t_2} \left( \frac{1}{\beta_2} - \frac{1}{\beta_1} \right).$$

In summary, a change of coefficient of $C$ during transition from $T_1$ to $T_2 = T_1 + \Delta T$ will be equal to:

$$\Delta C = \frac{T_1}{\Delta T} \beta_1 \lg \frac{t_1}{t_2} \left( \frac{1}{\beta_2} - \frac{1}{\beta_1} \right), \qquad (6.28)$$

where $t_1$ and $t_2$ - values of time whose difference is determined $\Delta C$;

$\beta_1$ and $\beta_2$ - coefficients, which determine the slope/inclination of direct/straight stress-rupture strength of $T_1$ and $T_2$.

Equation (6.28) expresses the time/temporary dependence of coefficient C of $T = \mathrm{const}$.

From Fig. 244, in which are represented values C for $r=1$ h and $r=100$ h, follows that in this case of C is changed substantially.

Processing experimental data. There are at present diverse variants of the representation of Larson-Miller's dependence, which are characterized by the methods of determining the coefficient C. In spite of the fact that processing experimental data by these methods leads to contradictory results, until now, there is no unified opinion about which of the methods indicated should be utilized.
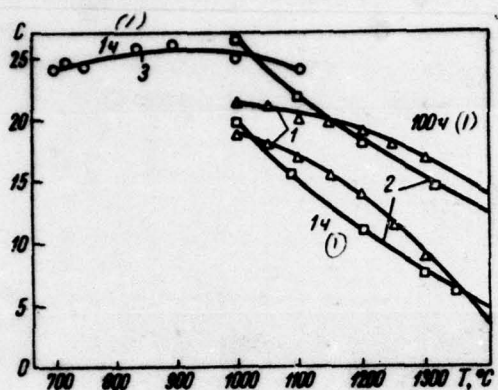
**Fig. 244.** The dependence of coefficient C on the temperature: 1 -
alloy VN-2; 2 - alloy 1; 3 - *Inconel* 700.

Key: (1). h.

Page 291.

Equation (6.19), which makes it possible to simply determine
coefficient of C, it found wide practical application/use. Brought
out from (6.19) expression (6.26) we have used in calculations, since
it makes it possible to considerably precisely determine values of C.
Figures 245a depicts test results, machined in accordance with
(6.26). As can be seen from the figure, for the investigated
high-melting materials this method of treating test data is
unsuitable, since separate temperature curves are proved to be
considerably moved by one relative to another; method is plausible
when curves are approximated by common broken line.
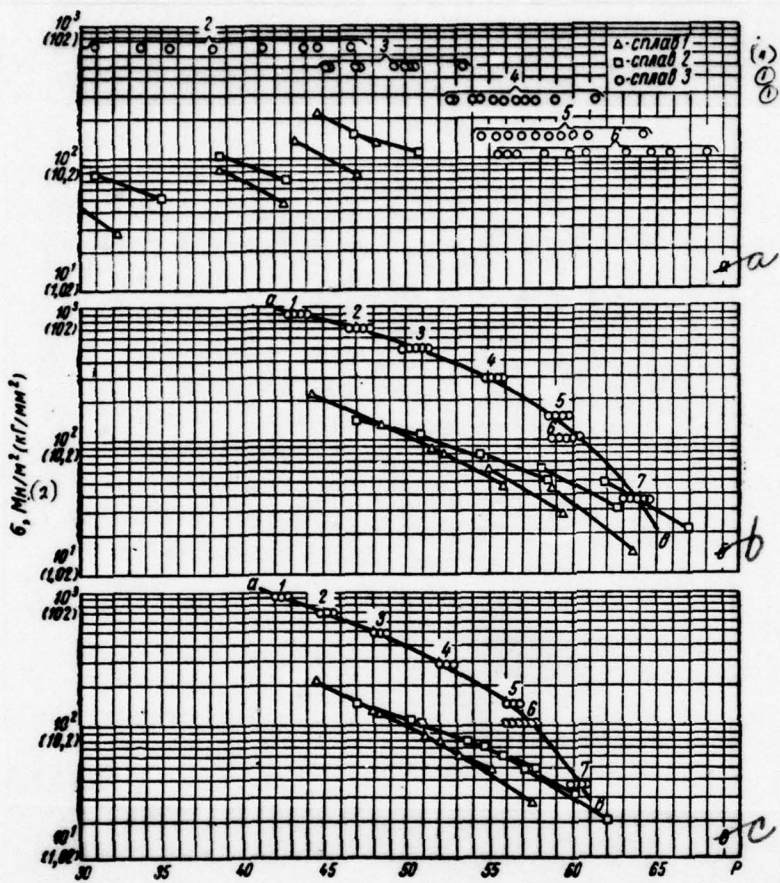
Fig. 245. Results of processing experimental data with the aid of the diverse variants of Larson—Miller's dependence: a) P=1.8 T (C+lg τ); b) the same, another version; c) P=1.8 T (K+lg τ).


Key: (1). alloy. (2). MN/m² (kg/mm²).


Page 292.

The essential shift/shears of separate curves for high-melting alloys are caused by a considerable change in coefficient of C with a change in the temperature (see Fig. 244).

Figures 245b depicts the results of the same tests, machined under condition C=const.

It is necessary to make the following observation. Larson and Miller considered that with $\sigma$=const in the system of coordinates $1/T$ - lg t dependence $f(\sigma)=T(C+\lg t)$ is expressed by straight line [201]. If according to the results of the tests, carried out at different tensions and temperatures, is constructed for each stress level the appropriate curve/graphs, then the obtained family of lines is frequently pencil of straight lines, that intersect in one point, arrange/located on axle/axis lg t with ordinate C=-lg t (Fig. 246a). Based on this, Larson and Miller assumed that C=const ($\sim$C=20).

However, the predicted straight lines can prove to be curves (Fig. 246b) and then the determination of coefficient according to the procedure, proposed in [201], it becomes meaningless. At the same time on the basis of the vast analysis of empirical data the author of work [206] confirms that for the increase of the reliability of

the results of calculation one should utilize precisely this method
of determing C. From Figure 245b it follows that the latter method
more plausible than method presented previously (see Fig. 245a), and
in this case for high-melting materials with the expansion of the
temperature interval of tests is observed a regular increase in the
mutual shift/shear of separate temperature curves.
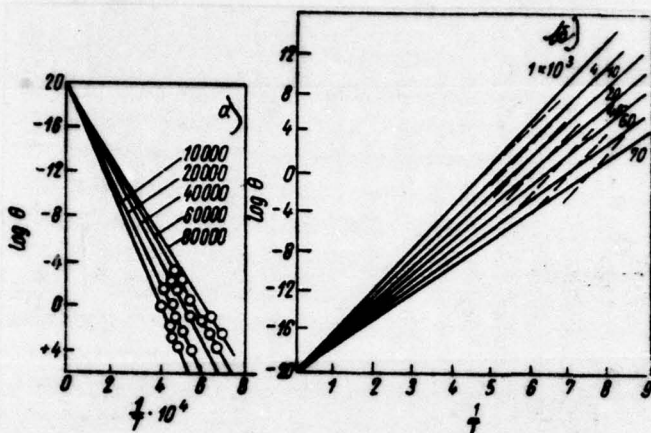
Fig. 246. To the procedure of the determination of coefficient C.

Page 293.

Derivation of formula (6.18). In work [204] on the basis of analysis [207] is expressed the assertion about the fact that coefficient C must be determined not from formula (6.19), but with the aid of the following expression:

$$T_1(C_1 + \lg t_1) = T_2(C_2 + \lg t_2). \qquad (6.29)$$

However, without the acceptance of additional conditions equation (6.29) cannot be utilized for determining of C, since in it there are two unknowns. Let us determine additional condition as follows. For the exception/elimination of the error, caused by the dependence of coefficient C on time, let us suppose that $t_2$=const. Then equation (6.29) will take the following form:

$$T_1(C_1 + \lg t_1) = T_2 C_2,$$
$$T_1 C_1 + T_1 \lg t_1 = (T_1 + \Delta T) \cdot C_2 = T_1 C_2 + \Delta T \cdot C_2. \qquad (6.30)$$

After the conversions of equation (6.30) we obtain:

$$C_1 - C_2 = \frac{\Delta T}{T} C_2 - \lg t. \qquad (6.31)$$

The right side of equation (6.31) is equal to zero with $C_1 = C_2 = C$. In this case values C are determined from equations (6.26). However, as it was shown above, this does not make it possible to obtain continuous parametric curve during passage from the system of coordinates $\lg \sigma$ - $\lg t$ to the system of coordinates $\lg \sigma$ - P (see Fig. 245a). But if is accepted $C \neq C_2$ [i.e. is recognized the validity of equations (6.29) and (6.31)], then the line segments can be combined.

However, the sense of values C, determined from equations (6.19) and (6.29), is completely various. In connection with this let us introduce the new designation K for the coefficients, determined from equation (6.29).

Let us substitute into equation (6.31) value of $\lg t_2 - \lg t_2$ from equation (6.24) let us accept $t_2 = 1$, and consequently, $\lg t_2 = 0$. After assuming $K_1 = \max(C_n)$ [therefore of many values $C_1$ and $C_2$ which can satisfy equations (6.29) and (6.30), we is selected the only pair which characterizes the properties of this material], we will obtain:

$$K_{n-1} - K_n = \frac{\Delta T}{T} K_n - \frac{\Delta T}{T_n} C_n.$$

whence

$$K_n = \frac{K_{n-1} + \frac{\Delta T}{T_n} C_n}{1 + \frac{\Delta T}{T_n}}, \qquad (6.32)$$

where   $K_1 = \max\{C_n\}$; $C_n$ — the coefficient, determined from equation (6.26).

Page 294.

As a result of the analysis conducted is proposed the following method of the construction of the base curve of decomposition.

If is valid dependence (6.12), is selected the system of coordinates lg $\sigma$ - P. Parameter P is determined from the following equation:

$$P_n = T_n(K_n + \lg t), \qquad (6.33)$$

in this case $K_n$ they determine from equation (6.32); the values $\Delta T$ during computation K and C one should select identical not more than 10 deg.

Test results, machined according to recently the examined method, are represented in Fig. 245c. From this figure it follows

that the proposed method is valid in temperature (500 deg) and
time/temporary (4-5 orders) intervals accepted. It is turned out that
there is a common/general/total law governing a change in coefficient
of K for different materials. So, in identical temperature intervals
(400 deg) for an alloy 1 coefficient K varied from 18.8 to 17.36; for
alloy 2 - from 19.9 to 17.9; for the alloy Inconel 700 - from 26.0
to 24,5. The decrease of coefficient of K for all alloys is
insignificant, what is necessary continuity condition of parametric
curve,

In conclusion it is necessary to make the following observation.
During the evaluation of one or the other method of processing
experimental data, rarely divide errors in the method and error,
caused by the scatter strictly of experimental data. Deficiencies in
this estimation can lead to the unjustified disputes, since the first
errors bear systematic, and the second - an accidental character. So,
Fig. 242 illustrates the utilization of dependence (6.18) for
processing of the experimental data, which do not have scatter. At
the same time the calculated parametric curve ab does not correspond
to the experimental points of broken line.

Thus, cd→ΔP characterizes errors in the method.

The carried out by us analysis (errors, caused by the scatter of

experimental data, are excluded) it made it possible to show that for
the continuity of parametric the curved coefficient C must be
constant, but be decreased by 1.5-2 in sufficiently wide temperature
interval. This underscores the empiricism of the method in question,
since coefficient C, determined from equation (6.19), can be
decreased in this same temperature interval by 15 and more, and in
that case the extrapolation of experimental data is impossible.

In works [204, 208] it is confirmed that coefficient C is the
characteristic of the heat-resistant properties of material, and are
made the attempts to find its dependence on the composition of
melting, conditions of the strain of blank, its heat treatment, etc.

Page 295.

From obtained by us formula (6.26) it follows that coefficient C
is determined by the product of the values of three functions:

$$\lg \sigma_0 = f_1(T); \quad \beta = f_2(T); \quad \frac{T}{\Delta T} = f_3(T)$$

The first function characterizes an incidence/drop in the
stress-rupture strength with an increase in the temperature for
t=const, and the second - creep strength. To search for
communication/connection of the noted properties of materials with
coefficient of C, but not with functions $f_1(T) = \lg \sigma_1$ and $\beta = f_2(T)$ -
that means to disregard the fact that three functions indicated are

independent, but this as it showed analysis, it is inadmissibly.

It should also be noted that the extrapolation on formula (6.18) is less reliable, than on formula (6.12), due to the existence of the noted above errors in the method. When selecting of one of them for processing of experimental data, it is necessary to consider following.

As already mentioned, Larsen and Miller assumed that coefficient C unessentially depends on temperature, in consequence of which it is possible to consider a constant value. This assumption was confirmed for some heat-resistant materials; however, it was disproved as a result of further analyses of the high-melting materials (see Fig. 244). It render/showed, for them coefficient C can depend substantially on temperature, and in this case Larsen-Miller's method is inapplicable. Data processing on stress-rupture strength for an alloy Inconel 700 and three high-melting alloys on the basis of niobium with the aid of formula (6.26) showed that essential differences the dependence of coefficient C on the temperature (see Fig. 244) they are explained by different character of a change in functions $\lg \sigma_0 = f(T)$ for these alloys (see Fig. 239).

Page 296.

Chapter 7.

STRENGTH AND PLASTICITY UNDER CONDITIONS OF CYCLIC VARIATION IN
STRESS AND TEMPERATURE.

Operating conditions of the elements of construction/designs
from refractory metals in a series of cases are characterized by the
cyclic recurrence of a change in temperature and value of mechanical
stresses. It is completely obvious that without the detailed
investigation of the properties of refractory metals under these
conditions their utilization for manufacturing the elements of
construction/designs will not be substantiated.

The most typical conditions/modes of the thermal and mechanical
loadings of a series of construction/designs are following:

1. Mechanical load is constant, and temperature cyclically is
changed. This conditions/mode let us call the conditions/mode of
thermocyclic creep (Fig. 247a).

2. Temperature remains constant, and cyclically is changed value

cf mechanical stresses, conditions/mode of low-cycle isothermal fatigue (Fig. 247b).

3. Cyclically are changed temperature and stresses, moreover emergence and change in stresses are explained by change in temperature.

Are most characteristic two versions of last/latter conditions/mode.

The first version corresponds to that case when the element of construction/design is rigidly hooked and heating causes in it compression stresses, and cooling - tensile stress.

The second version occurs during heating of laminated cylindrical shells. If the thermal-expansion coefficient of filler more the thermal-expansion coefficient of shell of refractory metal, during heating in shell will appear thermal tensile stresses, and during cooling (Fig. 247c) of compression.

Together with the enumerated conditions/modes of cyclic loading and heating the elements of construction/designs of the refractory metals, by which the frequency of a change in the stresses is small (less than 1 Hz), many of them are subjected to the simultaneous

effect of the mechanical loads of high frequency (ten and hundred
hertzes), caused by the forces of inertia of the oscillating
cell/elements. In connection with this appears the need for the
investigation of the strength of refractory metals at the high
frequencies of loading, i.e., mechanical fatigue.

For solving the problems indicated in the Institute of the
problems of the strength of AS UkSSR, were developed the
construction/designs of installations and procedure, making it
possible to conduct the tests of refractory metals during cyclic
variation in the load and temperature, and are also carried out works
on the study of the basic laws governing deformation and
decomposition of a series of refractory metals and alloys during the
enumerated above conditions/modes of tests.

Page 297.
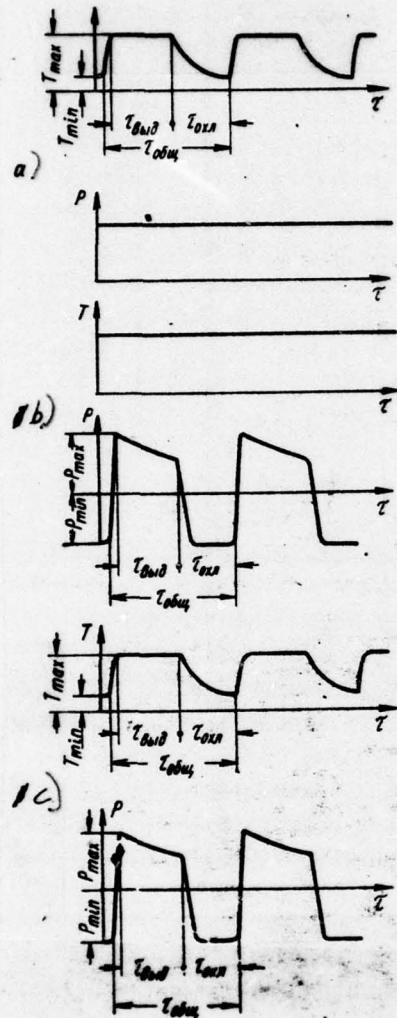


Fig. 247. Conditions/modes of tests during cyclic variation in temperature and load: a) thermocyclic stress-rupture strength (conditions/mode A); b) isothermal low-cycle fatigue (conditions/mode B); c) nonisothermal low-cycle fatigue (conditions/mode C).

Page 298.


Installations for the investigation of strength under conditions of cyclic variation in the load and temperature.

Installation for the investigation of thermocyclic stress-rupture strength.


Figures 247a depicts the diagram of a change in the load and temperature, which is realized in the installation, intended for the investigation of the effect of cyclic variations in the temperature to strength and plasticity of refractory metals and alloys.


As can be seen from the given diagram, which stretch the stresses, which act in specimen/sample, they remain constant/invariable in the process of entire testing, at the same time the temperature of specimen/sample periodically varies from $T_{min}$ to $T_{max}$. The time of holding of specimen/sample at these temperatures, and also the rate of heating and cooling they can be changed over wide limits.


The block diagram of the installation, in which are manufactured

the tests under the conditions indicated, is represented in Fig. 248
[119, p. 343].

The installation consists of five basic building blocks:

1 - vacuum chamber with the test specimens, placed in the
special loading device; 2 - system of creation and measurement of
vacuum, that includes forevacuum and diffusion pumps, and also vacuum
gauge; 3 - system of the automatic drive; 4 - block of heating, which
consists of power and regulating transformers; 5 - system of control,
check and recording of temperature, in which enter command
electropneumatic apparatus KEP-12U, electronic potentiometer EPP-0.9,
the optical pyrometer OPPIR-09.

The construction/design of the basic assemblies of vacuum
chamber is schematically shown on Fig. 249.

The pumping out of the camera/chamber is realize/accomplished
with the aid of fore pumps VN-2MG and diffusion oil-vapor pump
N-5S-MI.

Specimen/samples are placed into the camera/chamber in the
special loading device which is shown on Fig. 249. It consists of
disk 7, to which are fastened loading levers with 10 and 14 with

extenders 12 and grips 11 for specimen/samples 8. Loading lever 10 is
rigidly connected with disk 7, while lever 14 can be rotated relative
to axle/axis 15. The application/use of cylindrical and ball
couplings in power circuit completely eliminates slants in the
process of tests.

Page 299.
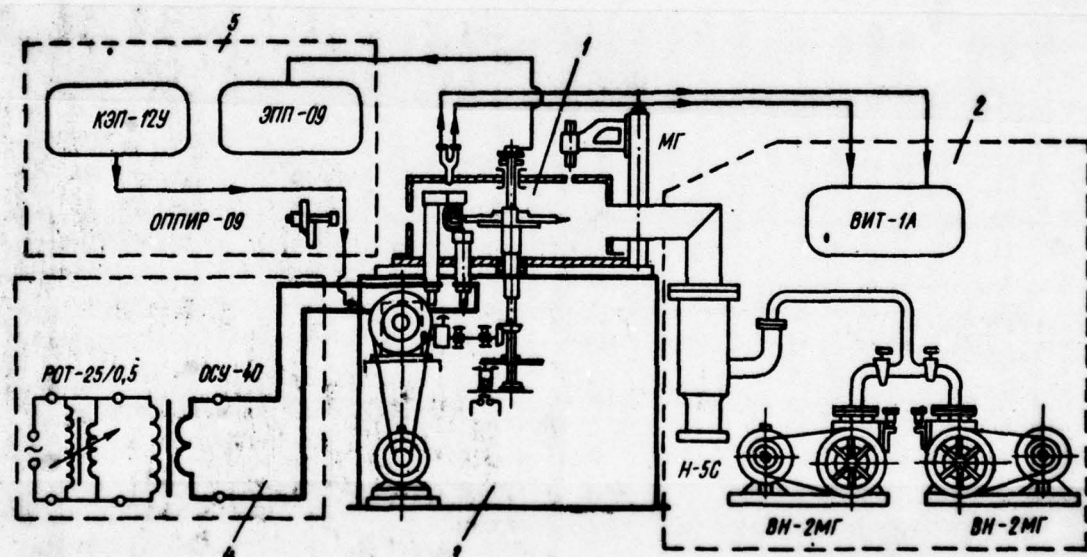


Fig. 248. Block diagram of installation for investigation of
thermocyclic stress-rupture strength.

Page 3C0.
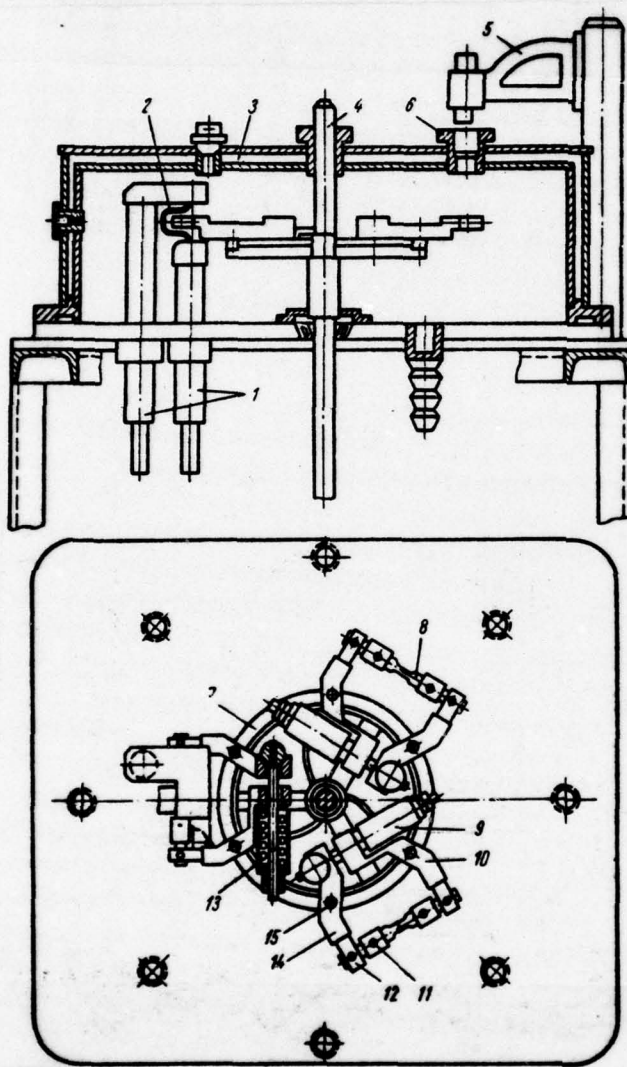


Fig. 249. Construction/design of vacuum chamber and loading device of installation for thermocyclic tests: 1 - current conductors; 2 -

heater; 3 - vacuum chamber; 4 - shaft; 5 - microscope MG; 6 - inspection window; 7 - disk; 8 - specimen/sample; 9 - sleeve; 10, 14 - loading levers; 11 - capture; 12 - extender; 13 - spring; 15 - axle/axis.

Page 301.

All parts of the loading mechanism are made made of the heat-resistant stainless steel, and extenders 12 and grips 11 - from molybdenum.

The loading of specimen/sample is realize/accomplished with the aid of interchangeable coiled springs by 13, which are placed into special water-cooled beaker/sleeves by 9.

The characteristics of springs are selected in such a way that the change in their size/dimensions, caused by the elongation of specimen/samples in the process of tests, prove to bes itself much lesser than that strain, that provides the assigned/prescribed stress level; therefore the change in the external load, connected with the elongation of specimen/sample, does not exceed 3-4o/o.

In the assembly of installation, is provided for the batch of interchangeable springs, which makes it possible with identical

accuracy/precision to assign load cn specimen/sample in a wide
interval of its values. In the process cf operating (pricr to each
testing and after its ccmpleticn) the spring, they calibrate on
special attachment. On the basis of the data cf calibrating, are
constructed the graph/diagrams of the dependence of the
effort/forces, created by springs, on their preliminary strain, on
which is manufactured the selection of the springs, necessary for one
cr the cther testing.

   The application/use of the examined method cf loading makes it
possible tc avoid the errcrs, caused by pressure difference in the
camera/chamber and out cf it, which can occur during the room of the
loading cell/element out of the camera/chamter, and create the
sufficiently compact multiposition loading device. In our
installation with the aid of this device, are ccnducted the tests of
simultaneously of three specimen/samples.

   The loading mechanism is fastened to special shaft 4 (see Fig.
249).

   Heating specimen/samples is realize/acccmplished with the aid of
heater 2 (see Fig. 249) frcm the refractory metal, which is tungsten,
molybdenum or tantalum plate 0.5-1 mm in thickness.

With the aid of water-cooled copper current conductors 1 (see Fig. 249) to heater is supplied the current from power transformer OSU-40; the voltage in the windings of transformer is regulated with the aid of the regulator RGT 25/0.5.

The minimum distance between the upper and lower part of the heater where is placed specimen/sample, limit the size/dimensions of extenders 12 and grips 11 (see Fig. 249), which during the rotation of shaft pass through the heater. Since this distance sufficiently greatly (~20 mm), the temperatures of heater and specimen/sample will be distinguished, that it is necessary to consider.

The temperature of specimen/sample is measured with the aid of platinum-platinum-rhodium or tungsten-rhenium thermocouple, connected directly to the working part of the specimen/sample and by that brought out made of vacuum chamber through the running shaft with the aid of the slip ring whose drawing is shown on Fig. 250.

Page 302.

Thermocouple 1 is passed through the plug/silencer from vacuum rubber 7 and is connected to slip rings by 9, which are isolate/insulated from each other. Cap/cover 8 is pressed against base 6 by screw/propellers 3.

Base is placed on special nut 5, that is installed to shaft 4, on which is rigidly attached the loading mechanism with specimen/samples.

From the ball races 9 cf readings cf thermccouple 1, they are remové/taken with the aid of sliding ccntacts 2 and are supplied to an electronic potenticmeter of the type BPF-C9.

In the process of investigaticn the temperature of heater in parallel is controlled with the aid cf the cptical pyrometer and on stress on heater, which gives, taking into acccunt the results of the carried out calibrating, additicnal infcrmaticn about the temperature conditions of specimen/sample.

The length of specimen/samples in the process of testing is measured with the aid of microscope 5 (see Fig. 249) type MG with the scale value of micrcmeter gauge 0.CC2 mm.

Application/use of a lcng-distance objective makes it possible tc manufacture the meastrements of the strain of specimen/sample, which is found directly in vacuum chamber, through inspection window 6 (see Fig. 249).

During the rotation of shaft 4 (see Fig. 249) specimen/sample is periodically moved from heater by 2 to the free position (where it is cooled because of the heat removal into captures), also, to the window of vacuum chamber 6, about which is establish/installed microscope 5.
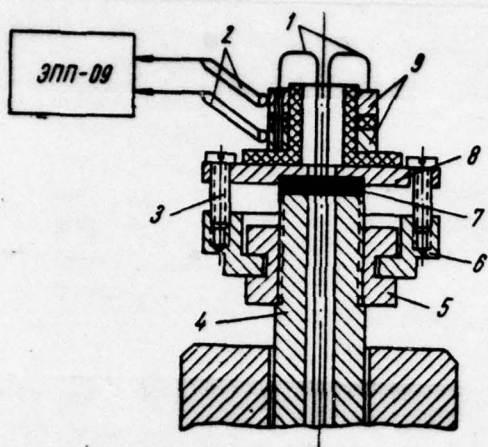
Fig. 250. Construction/design of slip ring.

Page 303.

This displacement/movement of specimen/sample makes it possible to completely reproduce the diagram of a change in the temperature in accordance with Fig. 247a, moreover the temperature of heater remains constant/invariable, which contributes to an increase in the period of its service.

The schematic of program unit, which periodically turns shaft from one position to another (heating, cooling, measurement), is given to Fig. 251.

Device consists of electric motor 1 and worm reducer 2,

connected by textrope transmission 11; 3 types electromagnetic couplings EM-32; pair of bevel-gear wheels 5, one of which it is mounted to shaft 4 (see also Fig. 249); solenoid 10; program disk 6 with holes for the rod of solenoid; 7 types command apparatus KEP-12U with the periodicity of the connection/inclusion of contacts from 3 min to 18 h; auxiliary device 8, which consists of resistances, capacities and relay MKU-48; final microswitch 9.

The operating cycle of program unit is realize/accomplished in this sequence. One of the specimen/samples, which is located in heater, is age/held there for a period of time, assign/prescribed by the command apparatus KEP-12U. After this time is closed by one of the pairs of the contacts of command apparatus and is supplied electric pulse on solenoid coil 10. Is drawn in the core of the solenoid which free/releases program disk and presses on the knob/button of final microswitch 9, including electromagnetic coupling 3.

In this case with the constantly connected electric motor through the conical pair, is given in rotation shaft 4 with the loading mechanism and specimen/samples. With the aid of auxiliary device 8, time of the connection/inclusion of solenoid is selected so as to ensure the displacement of program disk in circumference relative to the rod of solenoid on 20-25 mm.
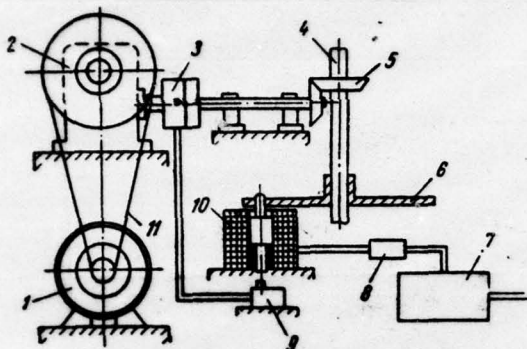
Fig. 251. Schematic of program unit.

Page 304.

After the disconnection of solenoid coil, its rod under the action/effect of return spring is pressed against disk and slips over its surface, thus far it does not fall into the following hole on program disk, which corresponds to the displacement/movement of specimen/sample to the position of cooling. In this case, wear/operates final microswitch 9, which disconnect/turns off electromagnetic coupling 3.

In certain time, given by command apparatus, again is included the solenoid and is repeated the cycle of the work of program unit in sequence described above.

Installation for the investigation of low-cycle fatigue.

The program of a change in the temperature and load, which it was possible to realize in the process of tests during experimental installation for the investigation of low-cycle fatigue, was shown on Fig. 247b, c. Figure 247c change in the temperature and load depicts in the form of the most common/general/total trapezoidal cycle which can be transformed into triangular cycle during tests without holding at the extreme levels or in cycle with holding only on one of the levels of load and temperature, etc.

Load change in the process of tests provides the schematic of loading, shown on Fig. 252.

To specimen/sample 1, is applied the preliminary tension from spring 2 during the displacement/movement of helical supports 3. Alternating effort/force in specimen/sample appears during imposition on the constant tension, determined by spring sag, the alternating/variable compressive force P, created by the hydraulic machine of one-sided action/effect UMM-10. Changing spring sag and the value of the amplitude of the alternating/variable force, created by hydraulic machine, it is possible to obtain the required cycle of loading.
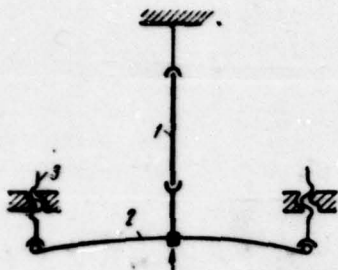
Fig. 252. Schematic of loading during tests for low-cycle fatigue.

Page 305.

The construction/design of installation for the investigation of low-cycle fatigue UTUV-1 [119, p. 322; 215, 216] provides:

1) test work via the loading of specimen/samples by the alternating effort/force of low frequency with the safeguard for holding of the varied duration both on the effort/force and according to temperature at extreme levels;

2) the reliable work of installation according to predetermined program with the synchronization of loading and heating specimen/sample;

3) test work in vacuum to 13.33 MN/m² (10⁻⁴ mm Hg) for

preventing the oxidation of specimen/samples;

4) the high rates of heating to 2000°C via the direct/straight transmission of the current through the specimen/sample;

5) the continuous recording of strain and effort/force in specimen/sample.

The general view of installation UTUV-1 is shown on Fig. 253, block diagram - on Fig. 254.

Installation consists of following systems and the blocks (see Fig. 254):

1 - experimental hydraulic machine UMM-10, in which is establish/installed vacuum chamber with specimen/sample and mechanism of preliminary loading; 2 - block of heating; 3 - unit of automatic control; 4 - recording unit of strain and effort/force; 5 - system of creation and measurement of vacuum.

Universal testing machine UMM-10, intended for static tests for elongation, compression and bend, consists of strictly testing machine and the control panel, which includes force gauge, the pumping station, which creates working effort/force, and the control system, with the aid of which are assigned the rates of loading and unloading, and also the levels of constant working loads (see Fig. 253).
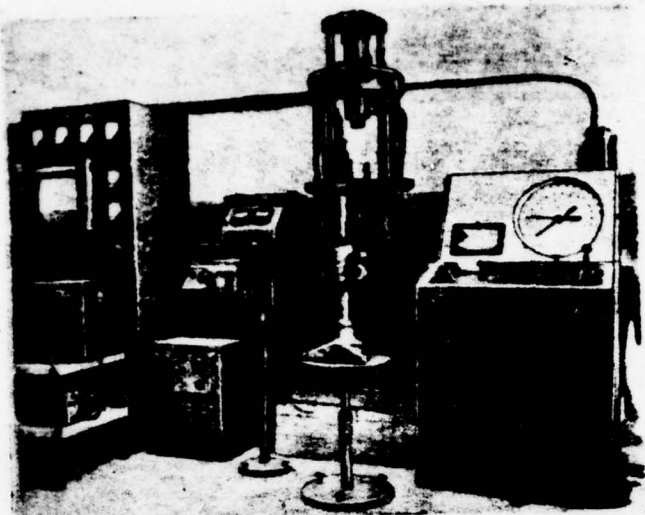
Fig. 253. The general view of installation LTUV-1.


Page 306.


With the aid of this machine to specimen/sample, can be applied only tension. In our tests it was necessary to ensure cyclic elongation - the compression of specimen/sample. This was reached by introduction to the kinematic chair of elastic cell/element - spring.

Vacuum chamber with the assembly of the preliminary loading of specimen/sample (Fig. 255) is establish/installed on machine instead of its lower capture with the aid of actuating screw 11.

Specimen/sample 1 is fastened in clamp grips 5 and 6. Upper

fixed grip 5 is connected by welding with the cap/cover of vacuum chamber 2, and lower movable grip 6 is derived from the camera/chamber through the vacuum seal. To the movable water-cooled capture out of the camera/chamber, rigidly is fastened the traverse of measuring brackets 10, spring 8 and flexible current-conducting busbar 9.

The water-cooled cap/cover of camera/chamber 2 is fastened with bolts to the flange of chamber casing 7, and the place of the joint between cap/cover and housing is packed by the ring from vacuum rubber, the value of compression of which is determined by the initial clearance between the flanges of housing and cap/cover. The cap/cover of the camera/chamber and captures are isolate/insulated from housing by textolite packing and rings in order to avoid the closing/shorting of the current-carrying parts to mass during heating of specimen/sample by the direct transmission of current.

To upper capture the current is fed out of the camera/chamber with the aid of copper flexible busbar/tire 4, which is fastened with copper nut 3.
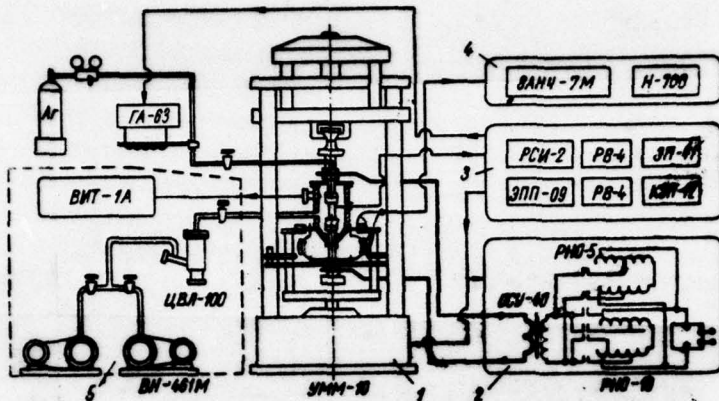
Fig. 254. Block diagram cf installation UTUV-1.

Page 307.

The water-cooled chamber casing 7 ty electric welding is connected with base plate 19, with the aid cf which the camera/chamber is establish/installed cn ccluars 13, rigidly connected with actuating screw 11 by means cf plate/slab 12.

Preliminary spring sag is assigned by the displacement/movement of helical supports 17. Spring is carried cut in the form uniform resistance beam, at its ends there are spherical bearings 15, which absorb the displacement/movement of helical supports. The brackets 18 of helical support have the capability to accomplish rotation relative to columns 13 during the installation of spring.

Spring sag is record/fixed from readings of dial indicators 16
with scale value 0.01 mm.

In the plate/slab 19 of chamber there are area/sites of 24 small
rigidities for glueing the strain gauges of effort/force. The strain
of specimen/sample is measured by the extensometer, structurally
carried out in the form of pliable brackets 14, which are fastened to
crosshead with 10 and to holders 20.
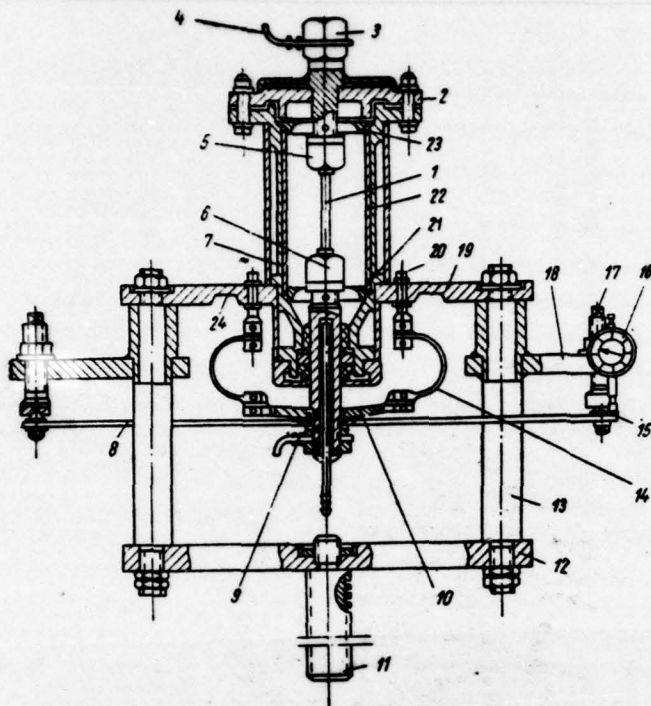
Fig. 255. Construction/design of vacuum chamber UTUV-1 with the assembly of the loading of specimen/sample.

Page 308.

Traverse is rigidly connected with the movable grip of specimen/sample, and holders are fix/recorded by bolts relative to plate/slab 19, which is rigidly connected with upper grip 5. This makes it possible to determine with the aid of brackets the amount of the strain of specimen/sample with its cyclic loading.

With the aid of beaker/sleeves 21 and 23 in the camera/chamber, is establish/installed polished aluminum shield by 22, which prevents the superheating of the walls of chamber casing and it contributes to the decrease of heat losses during heating of specimen/sample.

The construction/design of fastening solid specimen/sample is shown on Fig. 256. Specimen/sample 1 is fastened to connecting rod 7 with the aid of cut clamp insert 4 (conicity 12 deg.), ring 2, slide blocks 3, cover and which fixes nuts 5 and 6. Clamp inserts enter in conical bore holes of rods with the tightening of adapter nut 5 and they tightly press the stem of specimen/sample. They serve for centering the specimen/sample relative to rod and the protection of electrical contact between the rod and the specimen/sample during heating of the latter by the direct/straight transmission of electric current.

In fastenings, are drilled the air escapes from closed volumes with the pumping out of the camera/chamber.

In chamber wall, there is inspection window for observation and measuring the temperature of specimen/sample in the process of tests, and also there are holes for the input/introduction of thermocouples and vacuum gauge lamps.

Specimen/sample is heated by the direct/straight transmission of the current, applied to captures with the aid of the flexible busbar/tires, collected from the copper foil 0.1 mm in thickness. The section/cut of busbar/tires, contact area in the places of their fastening and the section/cut of the current distributing cell/elements of captures is selected from the calculation of the optimum specific current density, which eliminates the heating of the current distributing parts. For preventing heating captures, is provided for their cooling by water.

The system of heating (Fig. 257) includes power step-down transformer Tr1 (OSU-40), voltage regulators $RN_1$ (RNO-10-250) and $RN_2$ (RNO-5-250), and also voltage regulator (S-5000). In the process of tests, heating system must provide a change in the temperature of specimen/sample at three stages of the heating:

1) at minimum temperature of cycle;

2) at the maximum temperature of cycle;

3) during the forced heating of specimen/sample, which occurs during passage from minimum to the maximum level of temperature.
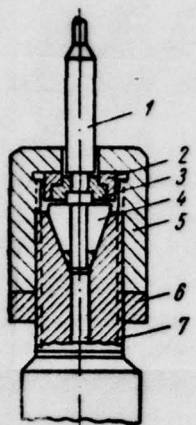
Fig. 256. Fastening solid specimen/sample in installation UTUV-1.

Page 309.
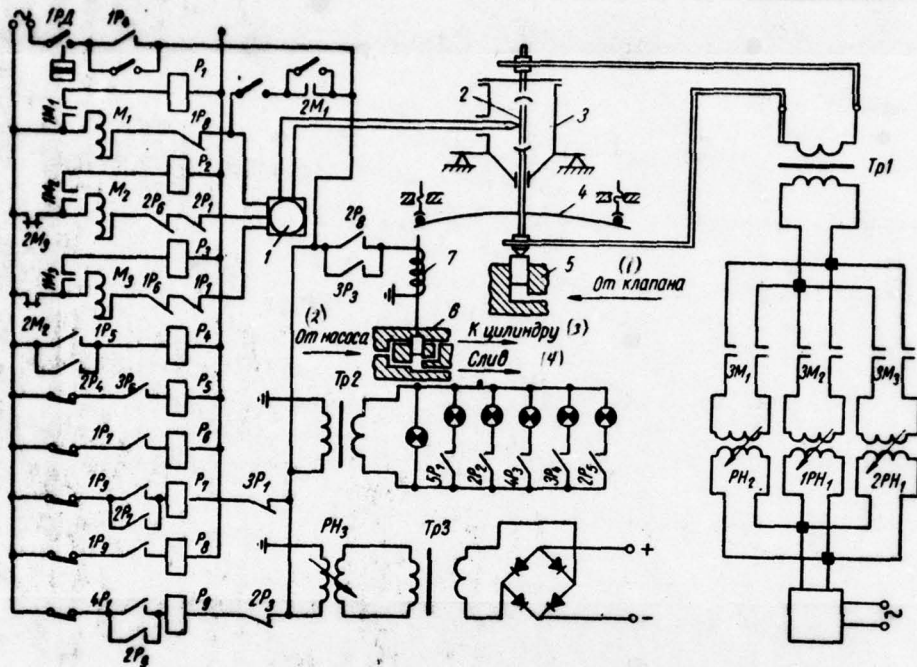


Fig. 257. Schematic electric diagram of installation: 1 - potentiometer EPP-09M2; 2 - specimen/sample; 3 - vacuum chamber; 4 - spring; 5 - loading cylinder; 6 - bypass valve; 7 - solenoid; 8 - voltage regulator.

Key: (1). From valve. (2). From pump. (3). To cylinder. (4). overflow.

Page 310.

For this, two exit windings of regulator RNO-10-250 and one winding RNO-5-250 are connected to the entrance of transformer on turn in accordance with test program, with the aid of contacts K on command from the unit of automatic control. The application/use of electrical interlock excludes the possibility of the simultaneous connection/inclusion of heating along two or three channels.

Figure 258 depicts the diagram of the recording of a change in the temperature at different test programs:

As can be seen from diagrams, the character of a change in the temperature and load in the process of tests can be different. Varying the holding time, it is possible to obtain the following cycles of a change in temperature and load of the specimen/sample:

a) with holding at upper level;

b) with holding at lower level;

c) the triangular cycle of a change in the temperature and load.

Furthermore, is provided the out of phase change in the temperature and load for any of the cycles indicated.

The maximum frequency cf a change in the temperature is determined by the allowable speeds of heating and cooling specimen/sample in vacuum and for the greatest temperature range is approximately 1 cycle after 2 min. Heating and cooling specimen/sample in accordance with predetermined program is fulfilled on command from the automatic control system of temperature. The rates of heating, loading and unloading specimen/sample, And also the levels of temperatures and loads are assigned during the presetting of this system.

Let us examine the cycle of the operation of the automatic control system of the installation (see Fig. 257).
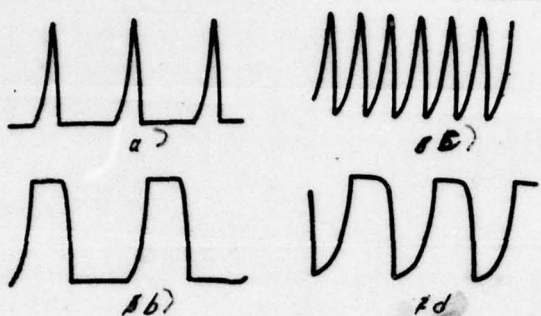
Fig. 258. Characteristic temperature cycles during tests during installation UTUB-1: a) with holding at minimum temperature of cycle; b) with holding at maximum and minimum temperature of cycle; c) a change in the temperature on triangular cycle; d) with holding at the maximum temperature of cycle.

Page 311.

In automatic control system, enter potenticmeter 1 - EPP-09M2 with thermocouple PP, auxiliary relay B of the type "EP-4? "and MKU-48, of the time relay R₇ and B₉ (RV- 4), the relay of the count of momentum/impulse/pulses F₅ (RSI-2), command tool KEP-13U and magnetic starters.

Cycle can be divided into the following four parts: I - holding with high temperature and elongation; II - cooling and the application/appendix of compression load; III - holding at low

temperature and during compression; IV - heating and increase in the tension. Let us observe the work of schematic for each of the sections of cycle.

On the first section of cycle, the circuit of coil $M_3$ is closed and contacts $3M_3$ provide the connection/inclusion of heating at constant maximum temperature. Contact $1R_3$ closes the relay circuit of the time $R_7$, which, being blocked by contact $2R_7$, begins the countdown of holding. The circuit of the solenoid coil of control of 7 is closed by contact $3R_3$, the valve of bypass valve 6 is moved upward, providing pressure relief oil in loading cylinder 5. Tension is applied to specimen/sample only from spring. After the holding time when $T_{max}$ is closed contact $1R_7$ and on the coil of relay $R_6$ it passes current.

Contacts $1R_6$ and $2R_6$ disconnect circuit $M_3$ and $M_2$ (second section). It is simultaneous with this $3R_3$, being disconnected, it de-energizes the solenoid coil of the control: the valve of valve it steps down, connecting high-pressure main line with the working cylinder of machine, and to the cooling specimen/sample it is applied compression load.

Upon reaching $T_{min}$ (third section) the electronic regulating unit of potentiometer closes the circuit of the magnetic starter $M_1$

whose contacts $3M_1$ connect heating specimen/sample with holding at lower level. During the start of auxiliary relay $R_1$, the contact $3R_1$ de-energizes coil $R_7$ and disconnects $R_6$; $4R_1$ closes the relay circuit of the time $R_9$, which begins the countdown of holding at minimum temperature of the compressed specimen/sample. At the termination of holding, $R_9$ closes contact $1R_9$, wear/operates relay $R_8$, breaking up circuit $M_1$ and $R_1$ and preparing for work $M_2$ and $M_3$.

The circuit of the solenoid of control is closed by contact $2R_8$, the valve of valve is moved upward, connecting the main line of high oil pressure with overflow. Pressure in the working cylinder of machine falls (fourth section), and the compression load, applied to specimen/sample, is decreased. In this case, the regulating unit of potentiometer EPP-09-M2 closes circuit $M_2$, specimen/sample is heated. On leaving to upper level (first section of cycle) the regulating unit disconnects $M_2$ and includes $M_3$ - specimen/sample it is age/held at constant temperature, but by the time relay $R_7$, connected with contact $1R_3$, it begins the countdown of holding. Then cycle is repeated.

Page 312.

The normally-closed contact 1BD of pressure relay water disconnects the feed of control circuit in the case of stopping the

supply/feed water.

During tests with alternating load and the constant temperature instead of the contacts $2R_8$ and $3R_3$ in the circuit of valve 6, are included the contacts of the command tool of KEE-12U (Fig. 257 shows).

On the electric circuit of installation, is shown also the block of signaling, which consists of step-down transformer $Tr_2$ (MTO-50) and bulbs LS, and also the block of straightening, which includes autotransformer $RN_3$ (LATR-10), step-down transformer $Tr_3$ (OSO-0.25) and rectifying bridge of diodes D-305 at output/yield of which it is possible to obtain current by 10 A and voltage of 30 V for the feed of loop oscillograph.

The tests of high-melting alloys are conducted in vacuum. The camera/chamber is evacuated by oil diffusion pump N-5S and by two fore pumps VN-2MG. The need for the installation of two periodically included fore pumps is dictated by the high duration of tests.

Vacuum in the camera/chamber in the process of tests was maintained at the level 13.3-1.33 mN/m² ($10^{-4}$-$10^{-5}$ mm Hg), leak rate did not exceed 0.2-0.4 $\mu$l/s, i.e., the examined vacuum system is sufficiently airtight, it makes it possible to conduct tests under

conditions, which eliminate the possibility of appearing the oxide films on the surface of specimen/samples at maximum temperature.

In the process of tests, was measured the overall strain of specimen/sample and effort/force. For such measurements it is not possible to stick resistance strain gages or specimen/sample, since the temperature of tests is very high. Were used the resistance strain gauges, outlying from the zone of high temperatures and vacuum and placed to elastic cell/elements.

Strain and effort/force for specimen/sample 1 were record/fixed at the signal of the sensors, stuck to brackets 14 and plate/slab 19 (see Fig. 255) and collected into bridge circuits. Signals from strain gauges were reinforced by the strain measuring station 8ANCh-7M and were supplied to the trails of oscillograph N-700. Oscillogram was record/written in the special cassette of the retarded rewinding 2.5 mm/s in a velocity of.

Measuring system they calibrated with the aid of needle indicators with the scale value 0.01 mm and of dynamometers of type DS-1 with scale value 25 N (2.5 kgf). During calibrating occurred the linear dependence between the values of strain (effort/force) and of the signal, entering from sensors to oscillograph.

Page 313.


Let us examine the procedure of the determination of the plastic

component of deformation in cycle, during utilization by which rests

a whole series of the deformation criteria of the decomposition of

metals. During calculation let us operate with the absolute values of

the strains of the working section of specimen/sample ($\delta$).


The total strain of specimen/sample, record/written in the

process of tests, is determined as follows:

$$\delta^c_{\text{сум}} = \delta^c_{\text{мех}} + \delta^c_{\text{тепл}}. \qquad (7.1)$$

where     $\delta^c_{\text{мех}}$ — the mechanical deformation of specimen/sample and

system of loading, which consists of the plastic deformation of

specimen/sample and elastic deformation of the system of loading and

specimen/sample;


$\delta^c_{\text{тепл}}$ — the thermal deformation of the system of loading.


Thermal deformation can be determined with the aid of the

equipment, available in the assembly of installation, by heating the

unloaded specimen/sample to the assigned/prescribed temperature

limits.


For determining the mechanical component of deformation it is

necessary from the amount total deformation to deduct the value of the thermal deformation of the system of loading. After deducting elastic component from the amount of mechanical deformation, it is possible to determine the absolute plastic deformation of specimen/sample for each torque/moment of testing.

The amount of plastic deformation in cycle experimentally determined by the construction of hysteresis loop.

Fig. 259 illustrates the graphic method of the construction of hysteresis loop according to the results of the recording of the oscillograms of a change in the total and thermal deformation and effort/force in specimen/sample.

Mechanical deformation $\delta^c_{Mex}$ determined via the coincidence of oscillograms with the recording by the total $\delta^c_{cyм}$ and thermal $\delta^c_{тепл}$ of deformations, but the value of effort/force R for the corresponding moments of time they read directly from oscillogram. In terms of the values of effort/force and the corresponding values of mechanical deformation, was constructed the hysteresis loop. The plastic deformation of specimen/sample in cycle was determined from hysteresis loop with no load.

Calculations showed that the accuracy/precision of the

determination of the amount of plastic deformation in cycle to a
considerable degree depends on the accuracy/precision, from which of
the total deformation is eliminated thermal component. For a
comparison Fig. 259 gives hysteresis loop in coordinates $\delta^c_{cym}$ — $R_e$
which can be constructed, if is does not eliminated thermal component
$\delta^c_{remn}$. The comparison of two types of hysteresis loops shows that for
determining the actual value of the plastic deformation of
specimen/sample the exception/elimination of thermal component is
compulsory.

Page 314.

Equality the thermal deformations of the loaded and unloaded
specimen/sample - one of the important conditions during the
construction of hysteresis loops - is provided, if the temperature
distribution along the length of specimen/sample and the gradients of
the temperature in the case of application/appendix and in the
absence of load are identical. In our experiments this condition was
observed; therefore during the determination of the absolute plastic
deformation of specimen/sample, it was admissibly utilize a value of
the thermal deformation of the unloaded specimen/sample.

Hysteresis loop during tests under conditions of a combined
change in the temperature and load is not symmetrical relative to the
axle/axis of strain. This can be explained by the fact that the
elongation of specimen/sample occurs at high temperature, and
compression - with lower (see the diagram of the cycle of a change in
the temperature in Fig. 259), in consequence of which during
elongation and compression are proved to be different the
module/moduli of elasticity, yield points and other characteristics.
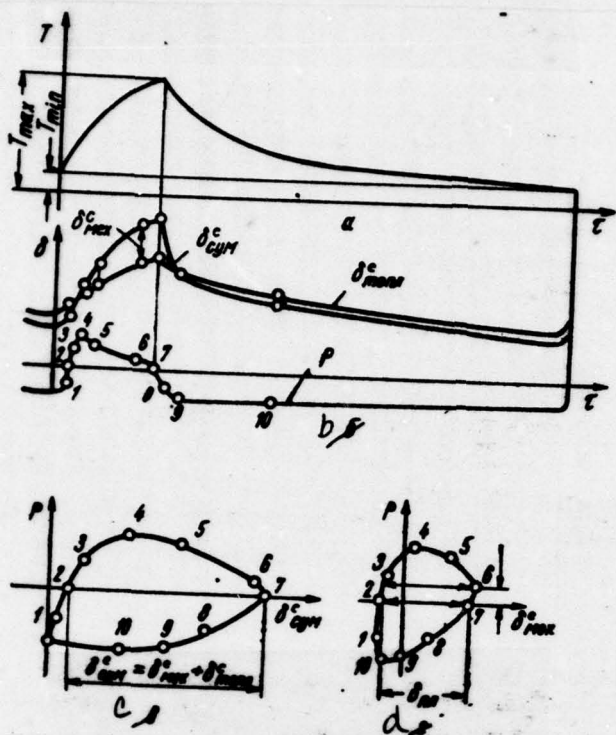
Fig. 259. Diagram of the construction of hysteresis loop: a) temperature cycle; b) the oscillogram of the recording of strain and effort/force; c) hysteresis loop without the exception/elimination of thermal deformation; d) hysteresis loop with the excluded thermal deformation.

Page 315.

Under isothermal test conditions of hysteresis loop, they constructed on oscillograms of the recording of total strain and effort/force of specimen/sample, since in this case it is not necessary to eliminate thermal deformation. For these conditions the hysteresis loop is virtually symmetrical relative to the axle/axis of abscissas.

The values of the plastic deformation, determined with the aid of the described above procedure, are integral ones. For determining the local relative plastic deformation, it is necessary to know the law of a change in the plastic deformation along the length of the specimen/sample being investigated which depends on stresses and the temperature distribution along the length of specimen/sample. It should be noted that the character of the temperature distribution and, consequently, also plastic deformations other conditions being equal (identical material, the condition of fastening specimen/sample, medium), depend first of all on the rates of heating and cycling specimen/sample.

At high rates of heating the zone of specimen/sample, distant from its center section, are heated insignificantly and plastic deformation is localized in the limited volume, which has maximum temperature. During the tests with by the low speeds of heating or with holding at the maximum value of temperature, its distribution

along the length of specimen/sample more uniform, and plastically is strained the considerably larger volume of metal.

Figure 260 shows the distribution curves of temperature along the length of solid specimen/sample made of molybdenum alloy at different heating rates. The heating rates changed, varying power in the circuit of heating. Thermocouples were fastened in special drillings in the body of specimen/sample; the diameter of holes corresponded to the diameter of the working junction. Each thermocouple they connected with separate potenticmeter ПП-1, in the process of heating, was manufactured simultaneous reading of all thermocouples.

The recrystallization of this alloy begins at ~1370°C; therefore during tests with holding at the maximum temperature more than 8 min, the temperature at an entire working length of specimen/sample exceeds the temperature of recrystallization; at high heating rates, the zone with the temperature, which exceeds recrystallization, substantially is decreased (see Fig. 260).

Consequently, if tests are conducted at the different heating rates, it is necessary to consider difference in the extent of the zones wrought metal during the determination of the amount of the relative plastic deformation of specimen/sample.

The boundary/interfaces of these zones can be determined in each individual case with the aid of the methods of structural analysis.

Page 116.

The calculations, carried out for one of the alloys on the basis of molybdenum, showed that for test conditions accepted occurs the following dependence:

$$\Delta\varepsilon_{max} = 2.25 \frac{\delta_{пл}}{l}, \qquad (7.2)$$

where $\Delta\varepsilon_{max}$ - relative plastic deformation of material in cycle in the center of specimen/sample;

$l$ - working length of specimen/sample whose temperature is higher than the temperature of recrystallization;

$\delta_{пл}$ - the integral absolute plastic deformation of specimen/sample, determined made of hysteresis loop in coordinates $P - \delta^c_{мех}$.

From formula (7.2) it follows that the maximum deformation in the center of specimen/sample considerably (2.25 times) exceeds the averaged value; therefore test results, machined without the account to localization of deformation, they will give the decreased values of maximum plastic deformations.
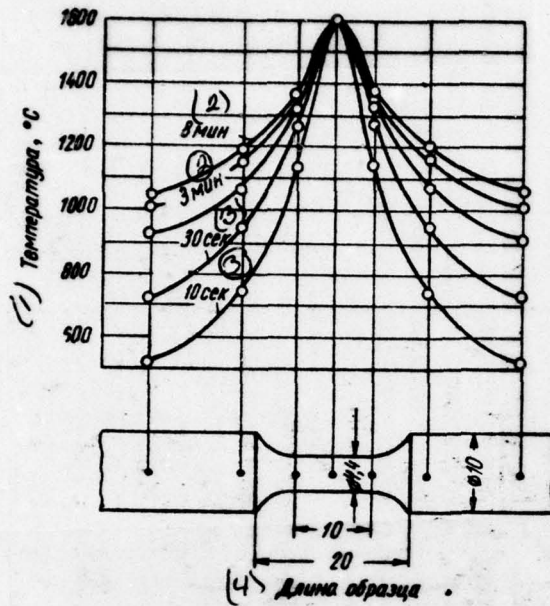
Fig. 260. The temperature distribution along the length of specimen/sample at different heating rates (in curves is shown value $\cdot$)

Key: (1). Temperature, °C. (2). min. (3). s. (4). Length of specimen/sample.

Page 317.

Setting up for the investigation of mechanical fatigue with expansion-compression.

In the literature [213, 214] described large number of settings up, intended for metal testing for fatigue (durability). As a rule, the settings up, intended for the investigation of the fatigue of heat-resistant metals at temperatures to 700-900°C, in principle they in no way differ from stands at room temperatures. In these high-temperature settings up the specimen/samples are heated in resistance furnaces with the heating elements, manufactured from heat-resistant alloys.

For the test work of high-melting materials with t>2000°C in the vacuum of the settings up, developed for testing of structural steels and heat-resistant alloys, are unacceptable, and it is necessary to design special settings up.

Figure 261 shows the construction/design of the setting up, developed in the institute of the problems of the strength of AS UkSSR, for test work for fatigue of refractory metals in vacuum at temperatures to 2000°C [212].

Setting up consists of vacuum chamber and evacuating system, the system of heating specimen/sample and automatic temperature control,

system of loading, measuring system the stress and strains in specimen/sample in the process of tests. Last/latter system makes it possible to investigate the dissipation of energy in metals in the process of fatigue tests with the aid of the construction of dynamic hysteresis loop - the method which will be examined below.

Specimen/sample by 7 is placed into that establish/installed on mounting 1 water-cooled vacuum camera/chamber 6, manufactured from the stainless steel. Vacuum in the camera/chamber creates fore pump VN-2MG and diffusion pump N-5S.

Heating the specimen/sample is realize/accomplished with the aid of tungsten heaters, throughout which it passes current from power transformer; stress on its primary winding is regulated with the aid of autotransformer. For an increase in the calorific efficiency and prevention of the superheating of the walls of vacuum chamber, the heater is encircled by shields 8.

Temperature is controlled and is automatically is maintained at the assigned/prescribed level with the aid of thermocouples and the block of automatic control. The loading of specimen/sample is realize/accomplished from electric motor by 4 with the aid of the exciter of displacement/movements 14 with by the continuously adjustable over the course amplitude. The exciter of

displacement/movements strains the elastic spring of 5 levers 3, realize/accomplishing thus the loading of specimen/sample.

Page 318.

Via the selection of the corresponding size/dimensions of springs and value of load 9 on the arm of spring 5 it is possible to attain the coincidence of frequency of induced oscillations with the natural frequency of oscillation of spring, i.e., to change to the resonance operating mode and to unload from mechanical effort/forces the bearing of vibration exciter.

The effort/force, which acts in specimen/sample in the process of tests, is determined with the aid of the optical system, which consists of mirror 12, fasten/strengthened to spring 5, illuminator 13 scale 11, taking into account the results of the carried out dynamic calibrating of setting up.

Taking into account that in the process of tests the temperature of specimen/sample can oscillate, which may change the character of the cycle of loading, the exciter of displacement/movements with electric motor 4, which gives it in rotation, are fasten/strengthened to plate/slab by 2, which is moved relative to hinged bearing edges.

Rotating steering wheel by 10 and thereby moving plate/slab 2, it is possible to completely remove the effect of thermal elongation on the characteristics of the cycle of loading.
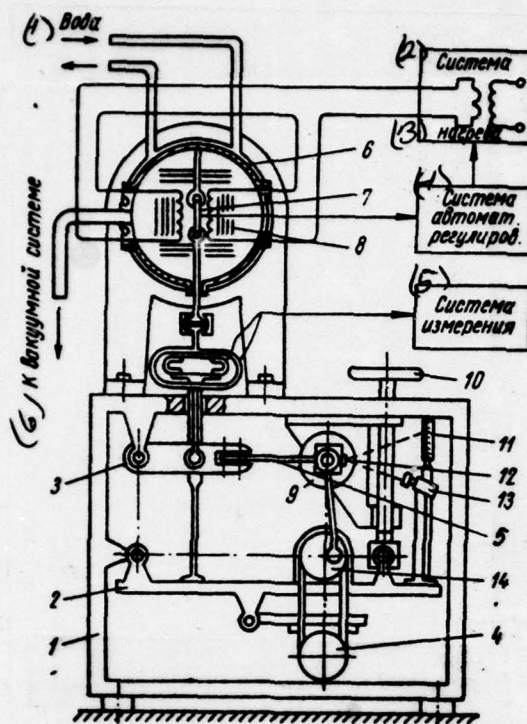
Fig. 261. Setting up for the investigation of the fatigue of high-melting alloys at frequencies to 50 Hz.

Key: (1). Water. (2). System. (3). heating. (4). System automatic machine of regulation. (5). Measuring system. (6). To vacuum system.

Page 319.

The described setting up will make it possible to also investigate structural transformations in metals, utilizing a method of dynamic hysteresis loop [194], which assumes the reproduction of the dependence between the stress and the strain within the limits of one cycle of loading. In such a case, when material is strained by completely elastic ones, the line of the load application will coincide with the line of unloading, which indicates the absence of the irreversible losses in material; with an increase in the stress level, the line of loading will not coincide with the line of unloading (Fig. 262) and within the limits of one cycle the process of the deformation of material will be characterized by closed loop whose area is proportional irreversiblly scattered in material energy, but width - inelastic deformation in cycle.

In the setting up of hysteresis loop in question they are reproduced with the aid of the unit of electronic equipment, shown on Fig. 263.

In it enter electronic oscillograph 1, frequency filters 2 and 3, intermediate low-frequency amplifier 4, phase inverter 5, strain measuring station 6, switch 7 and resistance strain gages to 8, 9 and 10.
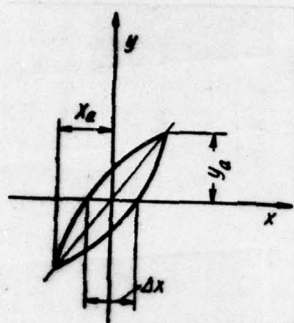
Fig. 262.
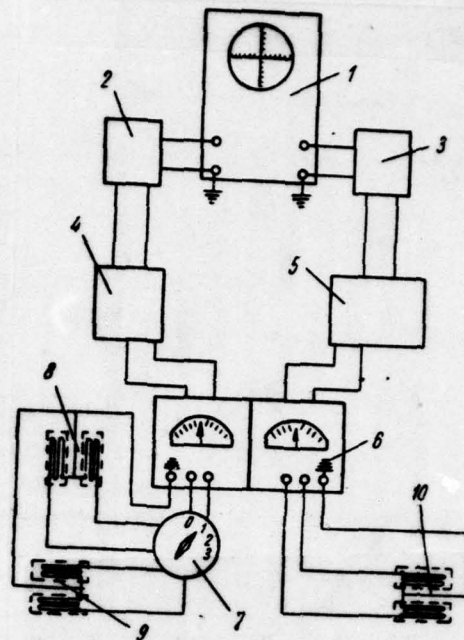


Fig. 263.

Fig. 262. Diagram of the inelastic deformation of material.

Fig. 263. Measuring circuit of setting up for investigation of
fatigue of high-melting alloys at frequencies to 50 Hz.

Page 320.

One of the pairs of sensors 8 is stuck on the bracket (see Fig.
261) whose deformation is proportional to the deformation of

specimen/sample, two other pairs of sensors 9 and 10 are stuck on the
elastic dynamometer (see Fig. 261) whose deformation is proportional
to the accompanying to specimen/sample effort/force.

With repeating-alternating loading the signal from sensors in
the specimen/sample through the strain measuring station, through
repeater and the filter enters the tangential channel of oscillograph
and is caused the deviation of electron beam with respect to
horizontal which will be proportional the deformation of
specimen/sample; signal from sensors to the dynamometer through the
strain measuring station, the phase inverter and the filter enters
the uptake of oscillograph and is caused the deviation of electron
beam with respect to vertical line, proportional to effort/force.

With cyclical loading the displacement/movement of ray/beam
continuously and on oscilloscope face we will obtain the line which
will characterize the dependence between effort/force and deformation
within the limits of one cycle (see Fig. 262).

Amount of inelastic deformation in cycle during the utilization
of this procedure can be calculated according to the formula

$$\Delta \epsilon = k_r \cdot \Delta x, \qquad (7.3)$$

where  $k_x$ - a scale along the axis of abscissas;

$\Delta x$ - width of loop on oscilloscope face.

The value of specific irreversibly scattered in cycle energy will be equal to:

$$D = k \cdot k_x \cdot \Delta x \cdot k_y \cdot y_a. \qquad (7.4)$$

where k - a factor of the form of loop (k ≈ 1.33);

$k_y$ - scale along the axis of ordinates;

$y_a$ - amplitude of the beam deflection along the axis of abscissas.

Figure 264 gives the specimen/samples of hysteresis loops for different stress levels, obtained during investigation of one of the materials with the utilization of the described above procedure.
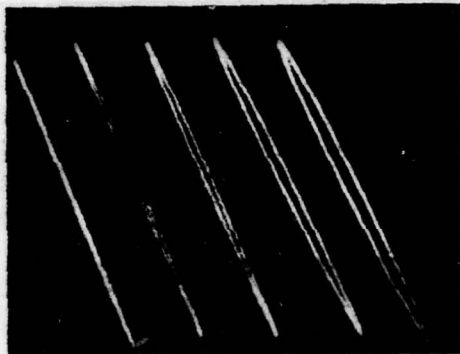
Fig. 264. Examples of dynamic hysteresis loops.


Page 321.


Setting up UVV-1 for the investigation of mechanical fatigue with bend.


The diagram of installation UVV-1 is given to Fig. 265.


Specimen/sample 1 is fastened in two struts with 2 to crosshead 3. Vibrations from moving coil of dynamic loudspeaker are transferred traverse (and, correspondingly, to specimen/sample) through power duct by 4, which rigidly is fastened to crosshead with the aid of

conical clamp.

Bearings 5 provide strictly the vertical displacement/movement of duct 4; they are establish/installed on eccentrics, which makes it possible to conduct their control.

Specimen/samples are heated by the transmission of the electric current through heating rods 6 cf tungsten or molybdenum, feed to which is supplied from a power transformer of the type the OSU-40 on special copper cooled current supplies 7, cne of which it is made movable for the compensaticp the thermal expansion of heating rods. On drillings, made inside current conductors is fed water for cooling some parts within the camera/chamber.

The amplitude of transverse vibrations of specimen/sample is measured with the aid of tele-sicrcscope with the micrometer eyepiece through window 8.
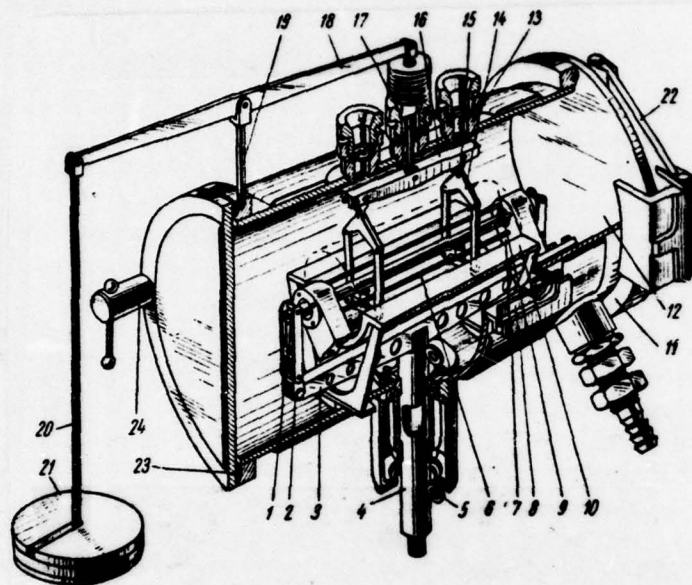
DOC = 78133011



Fig. 265. Diagram of installation UVV-1.

Fig. 265. Diagram of installation SVT-1.

Page 322.

For decreasing heat losses, the specimen/sample and heating rods
are closed by system from nine heat shields 9, made from laminated
molybdenum 0.1 mm in thickness.

Between external chamber walls and shields 9, is located
water-cooled shield by 10, that consists of two parts.

Vacuum chamber consists of housing by 11 and cap/covers 12,
which are equipped by water jackets for preventing heating of vacuum
chamber.

In the housing of chamber are provided three windows 13 for the
conclusion/derivation of thermocouples, lead/ducts strain gauge, for
the introduction of the packing/seal of the system of power
calibrating, setting up of vacuum gauge lamps.

Figure 265 shows also system for power calibrating. It consists

of two hinged framework by 14, that have saddle detents for pipes, slide blocks 15, traverses 16, connecting rod by 17 with vacuum seal, lever 18, strut 19, connecting rod 20 with the plate, to which are placed loads 21. The vertical connecting rods of hinged framework 14 pass through special cuts in the system of shields.

For calibrating are utilized the wire-strain gauges, stuck on specimen/sample, strain measuring station and oscillograph.

The sense of calibrating consists in the fact that is found communication/connection between the amplitude of the oscillations of specimen/sample, measured with the aid of tele-microscope, and the stress in it at normal temperature.

Stresses at high temperature are determined analytically taking into account the temperature distribution along the length of specimen/sample and dependence of the modulus of elasticity on temperature for this material. The system of power calibrating allows for to check the correctness of the analytical determination of the stresses in specimen/sample by additional calibrating at temperature of 700-900°C with the utilization of high-temperature wire-strain gauges.

The cap/covers of camera/chamber 12 are fastened to housing with

the aid of special links 22 with adjuster bolts, which ensure the uniform reduction of sealing rubber packing 23. Clamps 24 are equipped end-thrust bearing.

For high-temperature tests was created the new type of fastening specimen/sample-tubes, which was shown on Fig. 266. Jet with 11 is pressed by prism 3 and by finger/pin 13, fasten/strengthened between two connecting rod 1. Spring 4 by upper end abut against strut 5, and lower - into finger/pin 6, which can be moved in the groove/slots of strut, In order to spring by the capture not flatten tubes, into last/latter is inserted insert 12.

Struts 5 form with crosshead 10 movable connection. Bearing clearances 9 of this connection are selected by conical nuts 7 and by screw/propellers 8.

For decreasing the contact surface between the strut and connecting rods 1, to avoid additional energy losses in the process of testing, are establish/installed the disks.

Page 323.

For preventing the displacement/movement of tested tube along horizontal axis in time of tests on prisms 3, there are pins 2 by

diameter 2 mm which enter in holes in the tubes 2.5-2.8 mm in diameter.

For the elimination of the clearances, which appear in the work of the load-bearing elements of assembly, and the prevention of percussive attenuation it is necessary that the interference for fastening of specimen/samples would be 1.5-2 mm; this provide hard springs with 4.

The practice of tests showed the reliability of the operation of this fastening of jets. One of the advantages of this form of fastening was the insignificant heat removal due to low contact surface between prism 3 and specimen/sample 11. On Fig. 267 shown vacuum seal of power duct.

Rubber bellows 2 by upper flange of insert 3 is pressed with the aid of screw/propellers by 6 against insert 7, housing 1 and saddle 8. Bracket 4 forces the bottom edge of bellows against power duct 5. The elasticity of bellows depends on its height and the thickness of side walls (in our setting up their thickness was 6 mm).

For visual monitoring of the oscillating specimen/sample and measurement of amplitude in the camera/chamber, there is inspection window with molybdenum glass and shutter from laminated molybdenum

0.1 mm in thickness, which can be turned on 90 deg. from vertical position under the action/effect of the magnet, arrange/located from the outer side of the camera/chamber. The advantage of a shutter of such type lies in the fact that there is no need for for drilling holes for the housing of window and manufacture of special packing/seals for the cylinder of the mechanism of the opening of shutter.
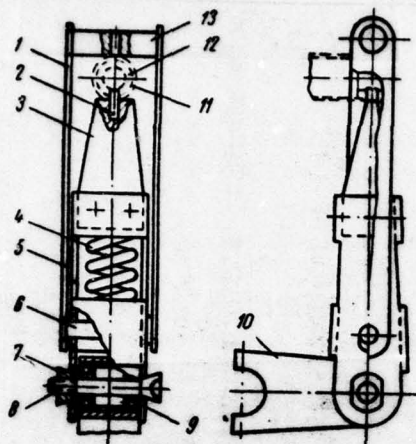
Fig. 266. Clamp for fastening of tubular specimen/sample.

Page 324.

As vibration exciter in the cell/elements being investigated is used the vibration table of the type VU-10/3000 (EV-1M) with the following characteristics: operating frequency 50-3000 Hz; maximum acceleration - 20 g. Maximum weight of test specimens - 98 N (10 kgf). Were selected the following size/dimensions of specimen/sample: $D_{\text{нар}} = 11,6\ мм;\ D_{\text{вн}} = 10,4\ мм;\ l = 300\ мм.$

Calculations show that in the case of hinged anchorage of the

specimen/sample its natural frequency will be 230-400 Hz, depending
on the material of specimen/sample and temperature of tests.

The measurement of temperature is manufactured with the aid of a
platinum-platinum-rhodium (tungsten-rhenium) thermoccuple, and its
control during testing - with the aid of the gauging electronic
potentiometer of the type EPP-09.

During this setting up it is possible to experience/test on it
got tired also the specimen/samples of other construction/designs.

Furthermore, with the aid of this setting up it is possible to
conduct vibration tests of the series of elements of
construction/designs, in particular joints refractory metal -
ceramics with the control of vacuum tightness of connection in the
process of testing.
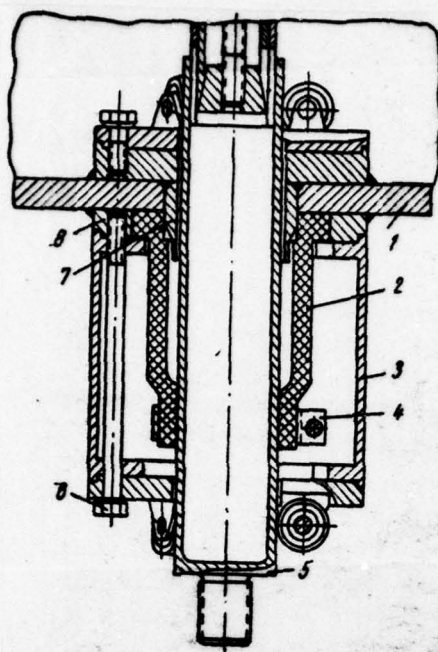
Fig. 267. Vacuum seal of power duct.

Page 325.

For this, in the camera/chamber are provided for the corresponding attachments.

During this setting up was finished also the procedure of the test of the shortened specimen/samples by the size/dimensions: $D_{нар}=13.5$ мм; $D_{вн}=13.0$ мм; $Z=150$ mm.

Characteristics of strength and law governing deformation and
destruction of refractory metals under conditions of cyclic variation
in the load and temperature.


Research of the laws governing deformation and decomposition of
high-melting alloys on the basis of tantalum, niobium and molybdenum
was conducted through three programs of a change in the temperature
and load - see Fig. 247 and Table 40. In the table indicated also
corrected values of the gradient of temperature along the length of
specimen/sample for different conditions/modes of tests, the type of
specimen/samples and the characteristic of the cycle of loading.

Table 40. Characteristics of the conditions/modes of thermocyclic loading.

| (1) Режим изменения нагрузки и температуры | $^\tau$общ | $^\tau$выд | $^\tau$охл | $T_{min},$ °C | $T_{max},$ °C |
|---|---|---|---|---|---|
| (2) Режим А — термоциклическая ползучесть *1 (P=const) | | | | | |
| I | 11 мин | 30 сек | 10 мин | 250 | 1600 |
| II | 109 мин | 30 мин | 78 мин | 250 | 1600 |
| III | 721 мин | 240 мин | 481 мин | 250 | 1600 |
| IV | 12 мин | 3,5 мин | 8 мин | 250 | 1500 |
| V | 105 мин | 30 мин | 74 мин | 250 | 1500 |
| VI | 11 мин | 30 сек | 10 мин | 250 | 1200 |
| VII | 39 мин | 10 мин | 28 мин | 80 | 900 |
| VIII | 108 мин | 30 мин | 77 мин | 80 | 900 |
| (4) Режим Б — изотермическая малоцикловая усталость *2 (T=const) | | | | | |
| I*3 | 52 сек | 28 сек | 20 сек | — | 1600 |
| II*4 | 52 сек | 28 сек | 20 сек | — | 1600 |
| (6) Режим В — неизотермическая малоцикловая усталость *5 (e₀=const) | | | | | |
| 1 | 105 сек | 12 сек | 89 сек | 250 | 1600 |

Key: (1). Conditions/mode of a change in the load and temperature.

(2). Conditions/mode A - thermocyclic creep1.

FOOTNOTE 1. Specimen/sample flat/plane, $\Delta T$=50 deg. ENDFOOTNOTE.

(3). min. (4). Conditions/mode B - isothermal low-cycle fatigue 2.

FOOTNOTE 2. specimen/sample circular $\Delta T$=200 deg. ENDFOOTNOTE.

(5). s. (6). Conditions/mode C - ncnisothermal low-cycle fatigue[5].

FOOTNOTE [5]. Specimen/sample circular, $\Delta T = 450$ deg.

------

FOOTNOTE [3]. $r \approx -1.5$, $\sigma_a$-const. ENDFOOTNOTE.

FOOTNOTE [4]. $r \approx -1.5$, $\sigma_a$-const. ENDFOOTNOTE.

Page 326.

During tests under conditions of cyclic variation in the
temperature with the constant tension (conditions/mode a) utilized
flat/plane laminated specimen/samples with the size/dimensions of
working part 25x5x(0.5-1) mm. Circular bar specimen/samples of
working part 10 mm in length and 4.4 mm in diameter utilized during
tests under conditions b and c (low-cycle isothermal and
ncnisothermal fatigue). Figure 268 shows form and the
size/dimensions of test specimens. The mechanical properties of the
investigated alloys are given in table 41.

Table 41. Mechanical characteristics of the wrought alloys, selected for thermocyclic tests.

| (1) Сплав | T, °C | (2) $\sigma_{в}$, MN/м² (кГ/мм²) | (2) $\sigma_{0,2}$ MN/м² (кГ/мм²) | ψ, % | δ, % |
|---|---|---|---|---|---|
| Ta — 10% W | 20 | 820 (83,5) | 715 (73,0) | 90 | 31 |
| | 200 | 820 (83,5) | 560 (57,1) | 86 | 19 |
| | 900 | 490 (50,0) | 340 (34,7) | 43 | 16 |
| ВН-2: 96,05% Nb, 3,8% Mo, ≤0,01% Cr, ≤0,05% C, ≤0,03% O₂, ≤0,04% N₂ | 20 | 656 (67,0) | 532 (54,3) | 63 | 30 |
| | 250 | 493 (50,3) | 389 (39,6) | 68 | 27 |
| | 1200 | 170 (17,3) | 114 (11,6) | ~100 | 33 |
| | 1600 | 43,8 (4,45) | 21,6 (2,2) | ~100 | 57 |
| ВМ-1: 98,8% Mo, ≤0,6% W, ≤0,4% Ti, 0,15% Zr, ≤0,01% C, ≤0,003% O₂ | 20 | 760 (77,5) | 497 (50,7) | 54 | 25 |
| | 250 | 572 (58,3) | 435 (44,5) | 77 | 30 |
| | 1200 | 252 (25,7) | 203 (20,35) | 90 | 22 |
| | 1600 | 59,7 (6,1) | 38,5 (3,9) | 100 | 54 |
| ЦСДМ: 99,87% Mo, 0,02% Al, 0,004% Ni, 0,005% Ti, 0,005% Cr, 0,001% Mg, 0,016% Si, 0,08% C | 20 | 679 (69,3) | 594 (60,5) | 60 | 28 |
| | 250 | 524 (53,5) | 469 (48,0) | 87 | 30 |
| | 1200 | 124 (12,65) | 65 (6,6) | 93 | 35 |
| | 1600 | 69,3 (7,1) | 30,4 (3,1) | 46 | 29 |

Key: (1). Alloy. (2). MN/m² (kg/mm²).

Page 327.

Investigation of deformation and decomposition under conditions of cyclic variation in the temperature.

In the process of the investigation of thermocyclic stress-rupture strength (conditions/mode a, Fig. 247) each of the selected alloys is experience/tested during different temperature cycles.

For each alloy maximum and minimum temperatures of different cycles were identical in all cases, variable was the holding time at the maximum temperature (see Table 40).

Alloy VM-1 is experience/tested according to programs AI, AII and AIII; the niobium alloy, containing to 10o/c Mo,-according to programs AIV and AV; alloy VN-2 - according to program AVI, while alloy Ta - 10o/o W - according to programs AVII and AVIII.

Figure 269 shows the temperature programs through which were conducted research of alloy Ta - 10o/o W. On this same figure shows to the dependence of elongation on the numbers of cycles of heating, presented in the form of curves, analogous by curve of creep under isothermal conditions. Similar curves were obtained also for the remaining investigated alloys.
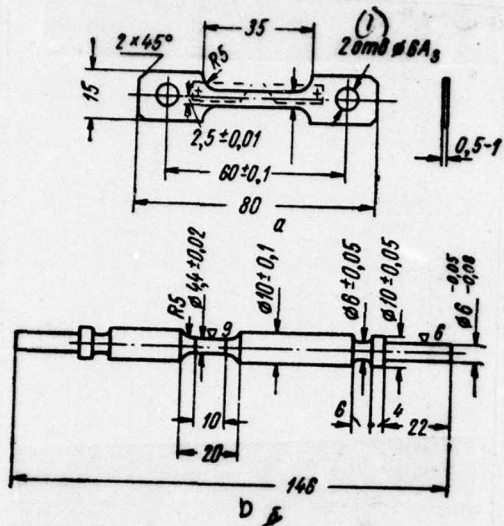
Fig. 268. Specimen/samples for the cyclic tests: a) for tests for thermocyclic stress-rupture strength; b) for tests for low-cycle fatigue.

Key: (1). OTV.

Page 328.

For determining the deformation of specimen/samples with the aid of microscope mg with accuracy/precision 0.002 mm, was measured the clearance between the fine/thin molybdenum plates, welded to the wide part of the specimen/sample (see Fig. 268). The deformation of

specimen/samples was measured after each cycle at constant temperature, equal to minimum temperature of cycle.

Curves, given Fig. 269, depicts in Fig. 270 in coordinates deformation - total time of holding at the maximum temperature of cycle,

The analysis of the results, shown on Fig. 269 and Fig. 270, makes it possible to assume that for alloy Ta - 10o/c W of the law governing process of creep under conditions of cyclic variations in the temperature in a small degree depend on a number of cycles of heating and are determined by stress level, by the maximum temperature and the total time of holding at this temperature.
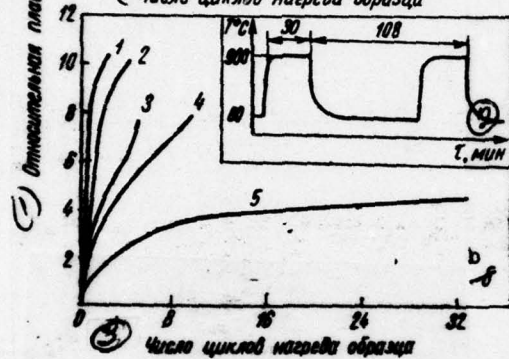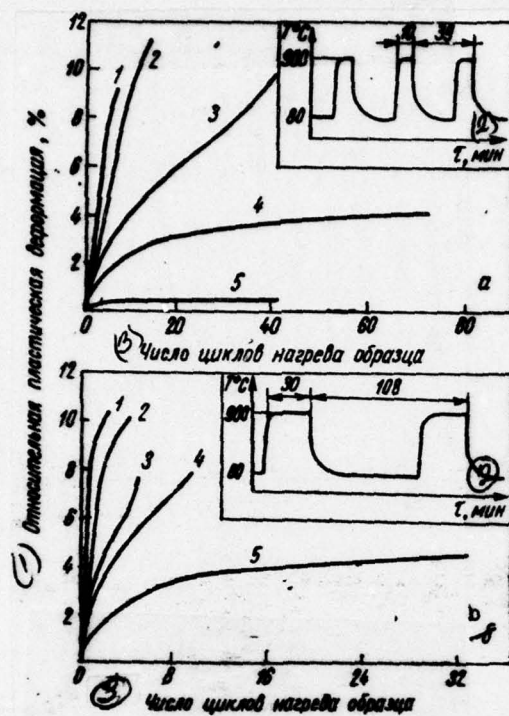
Fig. 269. Curves thermocyclic creep alloy Ia - 10o/o W: a) testing according to program AVII; 1 - σ=298 MN/m² (30.3 kg/mm²); 2 - σ=290 MN/m² (29.5 kg/mm²); 3 - σ=260 MN/m² (26.5 kg/mm²); 4 - δ=247 MN/m² (25.2 kg/mm²); 5 - σ=182 MN/m² (18.6 kg/mm²); b) testing according to program AVIII: 1 - σ=308 MN/m² (31.4 kg/mm²); 2 - σ=299 MN/m² (30.4 kg/mm²); 3 - σ=267 MN/m² (27.5 kg/mm²); 4 - σ=263 MN/m² (26.8 kg/mm²); 5 - σ=245 MN/m² (25 kg/mm²).

Key: (1). Relative plastic deformation, o/c. (2). min. (3). Number of cycles of heating specimen/sample.

Page 329.
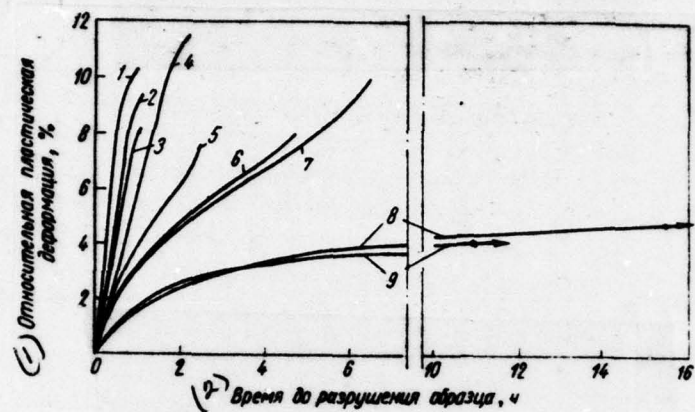


Fig. 270. Curves thermocyclic creep alloy Ta - 10o/o W:

$T_{max}=900°C; T_{min}=80°C:$ 1 - $\sigma=308$ MN/m² (31.4 kg/mm²); 2 - $\sigma=298$ MN/m² (30.3

kg/mm²); 3 - $\sigma=299$ MN/m² (30.4 kg/mm²); 4 - $\sigma=290$ MN/m² (29.5

kg/mm²); 5 - $\sigma=267$ MN/m² (27.2 kg/mm²); 6 - $\sigma=263$ MN/m² (26.8

kg/mm²); 7 - $\sigma=260$ MN/m² (26.5 kg/mm²); 8 - $\sigma=245$ MN/m² (25 kg/mm²);

9 - $\sigma=247$ MN/m² (25.2 kg/mm²).


Key: (1). Relative plastic deformation, o/c. (2). Time to failure of

specimen/sample, h.
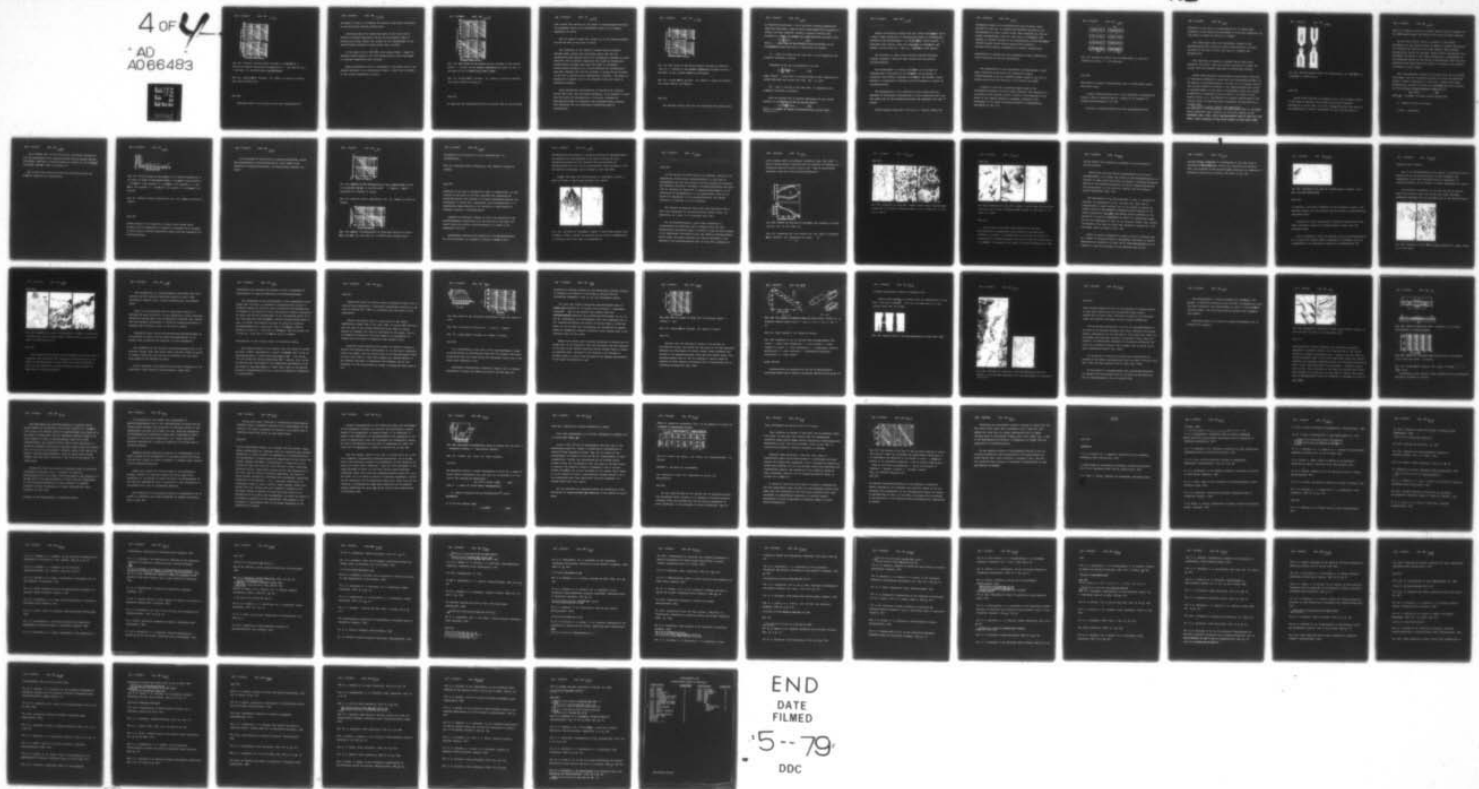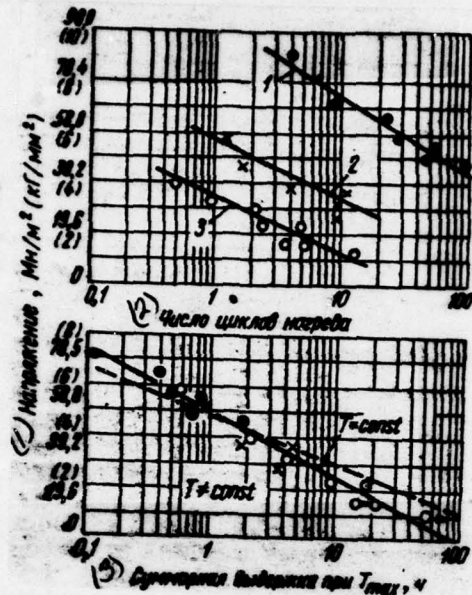
Fig. 271. Curves of stress-rupture strength of alloy VM-1: 1 - holding at maximum temperature of cycle 30 s; 2 - the same 30 min; 3 - the same, 4 h; T=1600°C=const; $T_{max}=1600°C; T_{min}=250°C$

Key: (1). Stress, MN/m² (kg/mm²). (2). Number of cycles of heating. (3). Total holding with.

Page 330.

Analogous results were obtained during the investigation of

processes of creep of molybdenum and niobium alloys under conditions
of the cyclically changing temperatures.

Conclusion about the determining value of the total time of
holding at maximum temperature during the thermocyclic tests of
high-melting alloys confirm the results of the investigation of the
stress-rupture strength of these alloys (Fig. 271-273).

In the upper of Fig. 271- 273, gives graphs stress - number of
heating-cooling cycles of up to the decomposition, which correspond
to different temperature test programs.

These experimental data are represented in the lower part of the
figures indicated in the coordinates: stress - total time of holding
at the maximum temperature of cycle.
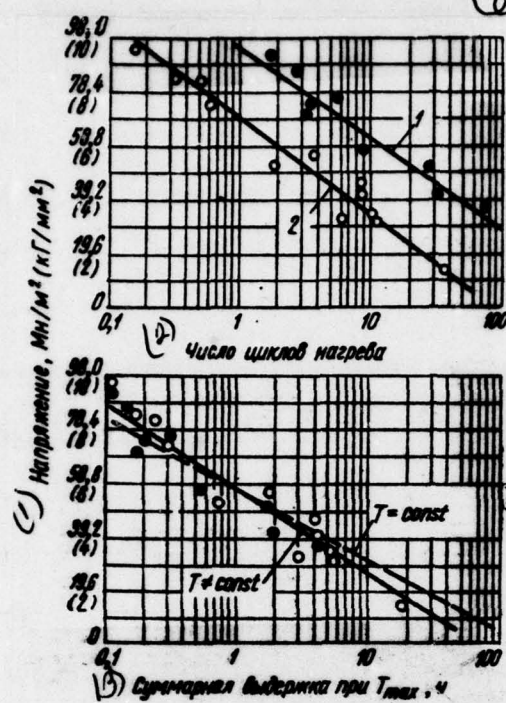
Fig. 272. The curves of the stress-rupture strength of the niobium alloy: 1 - holding at the maximum temperature of cycle 3.5 min; 2 - the same 30 min; T=1500°C—const; $T_{max}$=1500°C; $T_{min}$=250°C.

Key: (1). Stress, MN/m² (kg/mm²). (2). Number of cycles of heating. (3). Total holding with $T_{max}$, h.

Page 331.

In this case all experimental points are packed well to one straight

line. Dotted line carried out the curves of stress-rupture strength
for isothermal tests at the temperature, equal to the maximum
temperature of cycle.

Both of types of tests were carried out in the specimen/samples
one and the same of the batch of alloy.

The comparison of the graphs of stress-rupture strength,
obtained under various test conditions, shows that for all
investigated high-melting alloys with considerable stresses and short
retention time at maximum temperature the graphs of thermocyclic
stress-rupture strength pass above the lines of isothermal
stress-rupture strength, i.e., occurs thermocyclic strengthening;
then they intersect and with the decrease of stress and an increase
in the time to failure occurs thermocyclic softening - the graphs of
thermocyclic strength prove to be themselves below the lines of
isothermal strength.

Since thermocyclic strengthening is observed only initially
during small time, and then begins softening, it is possible to count
that the result of thermocycling is the larger softening of
high-melting alloys in comparison with isothermal tests. However,
this difference for the investigated conditions/modes is
insignificant.
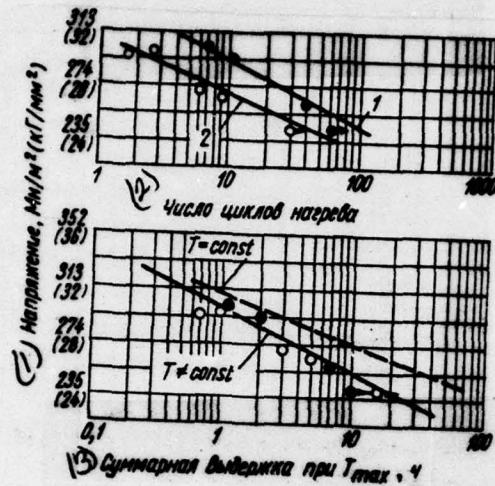
Fig. 273. The curves of the stress-rupture strength of alloy Ta - 10o/o W: 1 - holding at the maximum temperature of cycle 10 min; 2 - the same, 30 min; $T=900°C=const$; $T_{max}=900°C$; $T_{min}=80°C$.

Key: (1). Stress, MN/m² (kg/mm²). (2). Number of cycles of heating. (3). Total holding with $T_{max}$, h.

Page 332.

The obtained results show that for estimating the service life

of high-melting materials at the cyclically changing temperatures under the conditions, close to those investigated, it is possible to utilize the known summation formula of relative service life, proposed by a number of authors' for heat-resistant materials [209]:

$$A = \sum_{i=1}^{n} \frac{t_i}{\tau_i} = 1, \qquad (7.5)$$

where $t_i$ - total time of the holding of specimen/sample on the assigned/prescribed $i$-th level of temperature and stress;

$\tau_i$ - time to failure on the same level of the temperature and stress at isothermal loading.

Dependence (7.5) can be presented in the form

$$A = \sum_{i=1}^{n} \frac{(\tau_{T_{max}})_{n_i}}{\tau_p^{u_3}} = 1, \qquad (7.6)$$

where $(\tau_{T_{max}})_{n_i}$ - total time of holding at the maximum temperature of cycles with the $i$-th holding time when $T_{max}$ in cycle;

$\tau_p^{u_3}$ - time to failure on the same level of temperature and stress in isothermal conditions.

When the holding time at maximum temperature for all cycles equally, it is possible to put to use the formula

$$A = \frac{(\tau_{T_{max}})_n \cdot N}{\tau_p^{u_3}} = 1, \qquad (7.7)$$

where N - a number of cycles of heating-cooling cycles before decomposition.

decomposition.

Special investigation showed that for wrought alloys VN-2 and Ta - 10o/o W under conditions of thermocycling occurs an insignificant increase in the microhardness - to 195-245 MN/m² (20-25 kg/mm²) - in comparison with initial, which for alloy VN-2 is 2840 MN/m² (290 kg/mm²), and for alloy Ta - 10o/o W, - 2450 MN/m² (250 kg/mm²).

The structure of these alloys does not undergo noticeable changes, although is observed small grain-growth and partial recrystallization.

The microhardness of wrought alloy VN-1 in the process of thermocycling is decreased by 392-590 MN/m² (40-60 kg/mm²) in comparison with initial, component ~2650 MN/m² (270 kg/mm²), which, possibly, is explained by annealing and grain-growth as a result of recrystallization.

The decomposition of all enumerated alloys begins from the emergence of microcracks predominantly on grain boundaries which they are spread both on the boundary/interfaces and throughout the body of grains.

Unlike wrought alloys VN-1, VN-2 and Ta - 10o/o W, during the

679

thermocyclic tests of the recrystallized niobium alloy, which
contains to 10o/o Mo, is observed the essential increase of the
microhardness of alloy, several times, that exceeding the value of
initial microhardness, which for this alloy is 1765 MN/m² (180
kg/mm²). An intense increase in the microhardness to 3630-3920 MN/m²
(370-400 kg/mm²) occurs during several first cycles of
heating-cooling cycles, subsequently it becomes insignificant.

Investigation of deformation and decomposition under conditions of
cyclic variation of load and temperature.

The decomposition of the cylindrical specimen/samples, tested
under conditions of reheating and alternating loading
(conditions/modes b and c), preceded intense change in the form of
working section and the formation of the network of cracks.

A change in the form of specimen/samples made of the
investigated materials bore the double character: with formation in
the center of the working section of neck or with formation in the
center of the working section of convexity. Kinetics of the
development of two forms of shaping indicated is schematically
represented in Fig. 274.
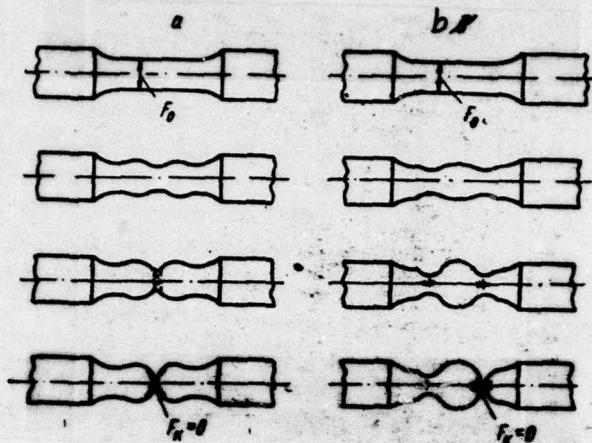
Fig. 274. Process of shaping the specimen/sample: a) with the formation of neck; b) - with buckling.

Page 334.

The process of shaping specimen/sample can be conditionally broken into three stage:

I stage occur/flow/lasts prior to the beginning of considerable shaping, which is characterized by a change in the diameter of working specimen/sample on 0.2 mm;

II stage is characterized by the slow accumulation of the

distortion of the form of specimen/sample and it passes under
conditions of the continuous development of necks and thickenings (in
this stage is formed the network of cracks);

III stage begins after the considerable shaping of the
specimen/sample when entire/all plastic deformation is virtually
localized in the zone of neck; this stage is finished with
decomposition.

This character of shaping is observed during tests under
conditions and "soft" (with the constant amplitude of stress) and
"rigid" (with the constant amplitude of deformation) loading.

During tests employing the procedure accepted under conditions
of alternating deformation, takes place the displacement/movement of
the material of specimen/sample of one part of it of working section
into another without an increase in the common/general/total length
of specimen/sample. In the zones of thickenings, occurs the gradual
accumulation of compressive strain, while in the zones of necks -
tensile strain, i.e., the material of different macrovolumes of the
working section of specimen/sample accumulates the deformations of
opposite sign.

The result of cyclic creep is the quasi-static
decomposition of specimen/sample. Specimen/samples made of alloy VN-2
failed themselves after formation in the center section of the
thickening (Fig. 275a), while specimen/samples made of alloy VN-1 and
TsSDN - after formation in the center section of neck (Fig. 275b).
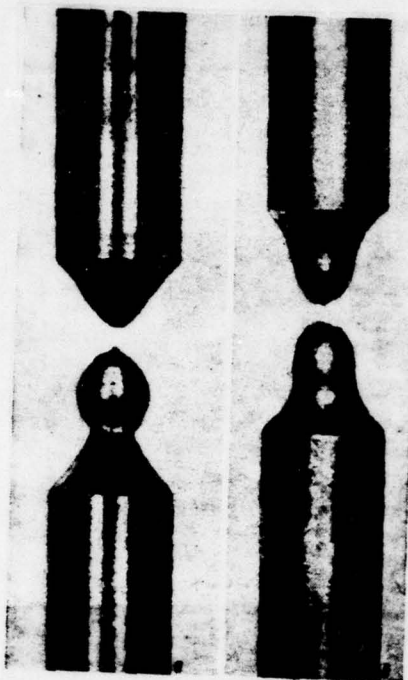
Fig. 275. Specimen/samples after the decomposition: a) alloy VN-2; b) alloy VM-1; T=1600°C=const.

Page 335.

During tests according to programs b and c as the characteristic of the state of material, was accepted the amount of plastic deformation as cycle [210, 211, 222]. Figures 276 gives the curves of the dependences of plastic deformation in cycle for the alloy of

TsSDM on a number of cycles of loading. These curves are typical for the investigated metals and alloys; they consist of three sections.

On the first section occurs an increase in the plastic deformation, on the second section the amount of plastic deformation is stabilized and finally on the third section, which precedes decomposition, occurs its increase. During further calculations were considered the values of the plastic deformation, corresponding to the stabilized section of the curves of deformation, since they most completely they characterize the ability of material to be resisted the effect of cyclic loads.

The investigations, carried out on alloys VN-2, VM-1 and TsSDM, they showed, that for high-melting alloys was valid the dependence between a plastic deformation in cycle and a number cycle before decomposition, proposed by Koffin for describing the laws governing the decomposition of heat-resistant alloys [2 ]:

$$\Delta \varepsilon_{n\pi} \cdot N^k = C, \qquad (7.8)$$

where $\Delta \varepsilon_{n\pi}$ - an amount of cyclic plastic deformation;

N - number of cycles of loading;

k and C - parameters.

As an example Fig. 277 and 278 in dual logarithmic coordinates give the experimental data, obtained during testing respectively of alloys VN-2, VN-1 and of TsSDM according to program B-I and B-II and of alloys VN-2 and VM-1 under conditions V-1.

It is known that crystal structure of refractory metals and alloys is stable at all temperatures.
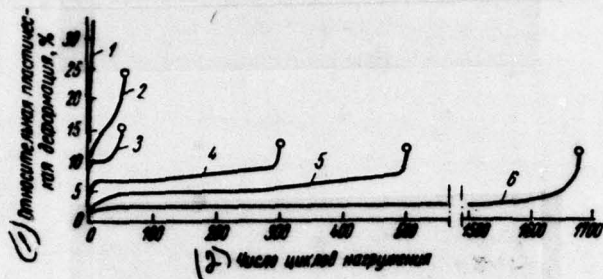
Fig. 276. Curved changes in the amount of the plastic deformation of the alloy of TsSDM (T=1600°C; const; $\sigma_a$ =const): 1 - $\sigma$=104 MN/m² (10.6 kg/mm²); 2 - $\sigma$=75 MN/m² (7.65 kg/mm²); 3 - $\sigma$=65 MN/m² (6.65 kg/mm²); 4 - $\sigma$=62 MN/m² (6.3 kg/mm²); 5 - $\sigma$=54 MN/m² (5.5 kg/mm²); 6 - $\sigma$=46 MN/m² (4.7 kgf/mm).

Key: (1). Relative plastic deformation, o/o. (2). Number of cycles of loading.

Page 336.

Certain change in the properties of these alloys during cyclic variation in the temperature in essence is determined by an increase in grain sizes at testing temperatures higher than the temperature of recrystallization.

686

In the process of grain-growth on boundary/interfaces, occurs the concentration of impurity/admixtures, which leads to the weakening of boundary/interfaces, and consequently, material as a whole,
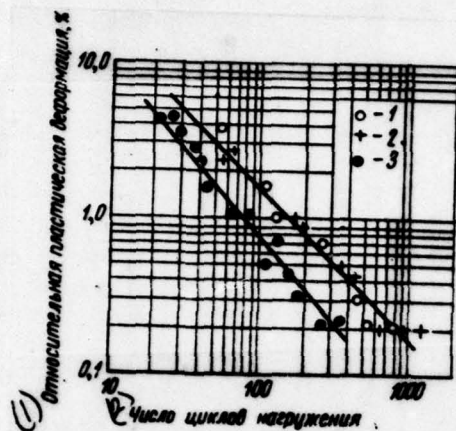
Fig. 277. Results of the investigation of the nonisothermal fatigue of alloys VM-1 and VN-2, $T_{max}=1000°C$; $T_{min}=250°C$:   1 - VN-2; 2 - VM-1; 3 - appearance of a network of cracks.

Key: (1). Relative plastic deformation, o/o. (2). Number of cycles of loading.
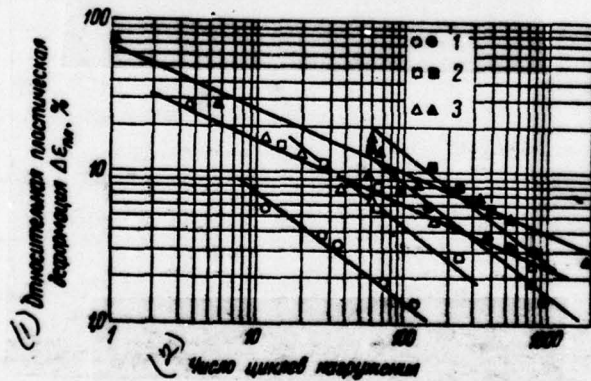


Fig. 278. Results of investigation of isothermal fatigue of alloys VN-2 (1), VM-1 (2) and IsSDE (3). T=1600°C=const (bright points

correspond to the formation of neck, black/ferrous - to
decomposition).

Key: (1). Relative plastic deformation. (2). Number of cycles of
loading.

Page 337.

Therefore in the case of thermocyclic tests at temperatures, on some
sections of the cycle of of these exceeding the temperature of
recrystallization, the character of origin/conception/initiation and
development of cracks and, consequently, also decompositions, to a
considerable degree depends on the intersity of grain-growth on
different sections of specimen/sample.

Research of structural changes in alloys was conducted in the
specimen/samples, manufactured from the material of one batch and
tested during the various conditions/modes of a change in the
temperature and load.

Longitudinal sections were prepared for the specimen/samples,
cut along axle/axis, for purpose of tracing a change of the

microstructure and hardness in different sections of specimen/sample.
Was measured the microhardness of the body of grains and their
boundary/interfaces and they observed the microstructure of
specimen/sample with the aid of metallographic (with increase in 200)
and electron microscopes (with increase in 1400 and 7500).

Figure 279 shows the microstructure of alloy VM-1, tested in
state of strain to short-time strength with 1600°C.
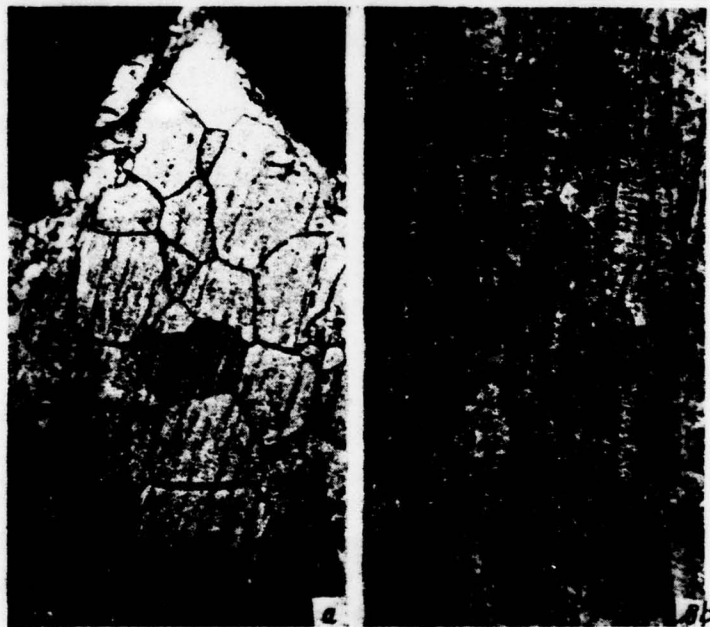


Fig. 279. Structure of alloy VM-1, tested to short-time strength with
T=1600°C, δ=54o/o, (x200): a) structure in the zone of decomposition;
b) structure out of the zone of decomposition.

Page 338.

As can be seen from this figure, the material, tested at the
temperature, which exceeds recrystallization, in the zone of
decomposition and the zone, distant from the position of fracture,
has different structure. Thickness of boundary/interfaces and grain
size is increased in proportion to approach/approximation to the
section/cut of decomposition. At the temperatures, which do not
exceed the temperature of the recrystallization, the changes
indicated in structure it is not observed.

The strength of material during the high-temperature tests,
which are accompanied by recrystallization, sharply falls, and
plasticity, as a rule, it is increased (Fig. 280).

For the specimen/samples, tested under conditions of
nonisothermal and isothermal cyclic loading, there are three
characteristic structural zones, an extents of each of which depends
on the temperature distribution along the length of specimen/sample
during tests. The zones indicated are clearly noticeable on the
sections of the specimen/samples made of alloy VM-1, subjected to

cyclic loading under norisothermal conditions (Fig. 281, 282): I - zone of coarse-grained structure near the position of fracture; II - transition zone with smaller grains; III - zone of fine-grained structure. Zones have sharp boundary/interfaces.
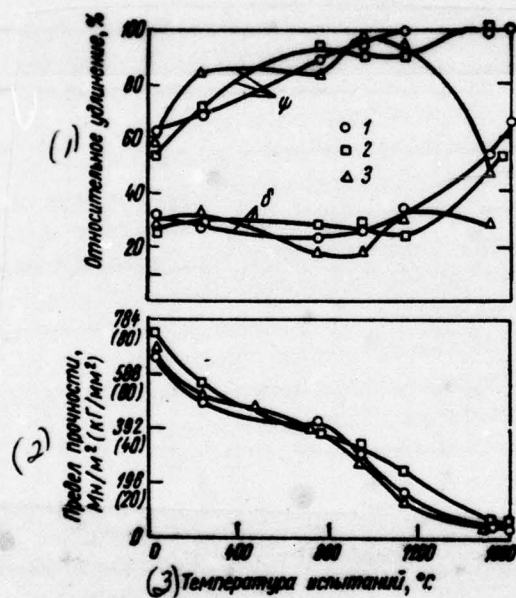


Fig. 280. Results of the test of the short-time strength of alloys VN-2(1), VM-1 (2) and TsSDM (3).

Key: (1). Elongation per unit length, o/o. (2). Limit of strength, MN/m² (kg/mm²). (3). Temperature of tests,   °C.

Page 239.
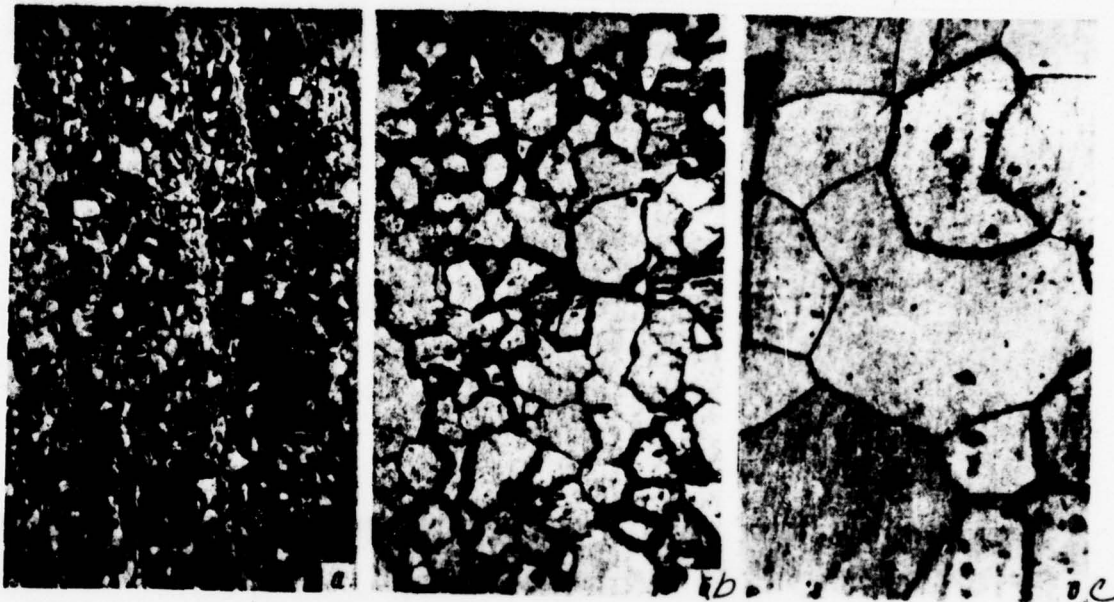


Fig. 281. Structure of alloy VM-1 (x200), tested under nonisothermal conditions of low-cycle fatigue $(T_{max} = 1000°C; T_{min} = 250°C)$: a) zone III; b) zone II; c) zone I.

DOC = 78133012     PAGE 693

Page 340.



Fig. 282. Structure of alloy VM-1 (x2400, tested under nonisothermal conditions of low-cycle fatigue $(T_{max}-1000°C, T_{min}-250°C)$: a) III zone; b) II zone; c) I zone.

Page 341.

Figures 281a, 282a shows characteristic for III zone microstructure; predominantly small grains are oriented along direction of rolling. The temperature of this zone was below the temperature of recrystallization, and stress level was insignificant [to 98 MN/m² (10 kg/mm²)]; the traces of plastic deformation in zone

III are absent, its structure is analogous to the structure of initial material.

Figures 281b and 282b depicts microstructure in II zone of specimen/sample. Are visible the results of the recrystallization: an increase in grain sizes and certain thickening of boundary/interfaces because of the liberation/isolation on them of impurity/admixtures with grain-growth. In this zone are observed also the traces of plastic deformation (Fig. 283).

The photographs of the microstructure of zone I - position of fracture, are represented in Fig. 281c and 282c. This zone is characterized by coarse grains, that it is possible to explain by intense growth in the process of recrystallization because of the higher temperature: $T_{max} = 1600°C$, and larger plastic deformation. The plasticity of metal at temperature of 1600°C is considerably higher than at the temperature of zone II, not exceeded 1400°C. This confirm the results of the tests of short-term strength of alloys VM-1, VM-2 and TsSDM, which are given to Fig. 280.

Traces of plastic deformation in zone I were not virtually kept as a result of recrystallization. Nevertheless the effect of plastic deformation on structure I of zone can be establish/installed, if is compared it with the structure of the analogous zone of the

specimen/sample, subjected to thermocycling in the same range of temperatures $(250° \rightleftharpoons 1600°C)$, but without the application of external load. The structure of the specimen/sample which was not subjected to mechanical loading during heating, was shown on Fig. 284.

Fig. 283. Structure of II zone of specimen/sample (x 12,000). Alloy
VH-1  $(T_{max}-$ 1600°C; $T_{min}-$ 200°C; $\sigma \neq const)$

Page 342.

Is observed a noticeable difference in the structure in zone I: the
unloaded material has more uniform and are smaller in size/dimensions
equi-axeds grain.

Location of three characteristic structural zones during tests
under isothermal conditions (T=1600°C=const) differs from that
described above.

Zone I completely covers the working section of specimen/sample;
in it occurs the intense plastic deformation of material, which is
accompanied by the considerable shaping of specimen/sample with

DOC = 78133012        PAGE  ᵇ 697

repeated static loading.

Zone II is arrange/located in the region of transition from the
working part of the specimer/sample to that thickened. The
temperature of this zone coincides with the temperature of
recrystallization, and the traces of plastic deformation are absent.

The structure of material in zcne III does not in practice
differ from initial. This zcne during tests under isothermal
conditions coincides with the thickened part cf the specimen/sample.



Fig. 284. Structure of allcy VД-1 $(T_{max}-1000°C; T_{min}-200°C; \sigma-0)$: a) I zone (x450);
b) II zone (x200).

Page 343.



Fig. 285. Structure in zcne of deccmpcsiticr, (x200): a) alloy VM-1, T=1600°C=const; $\Delta\varepsilon - 14\%$: b) allcy TsSDM; T=160C°C=ccnst; $\Delta\varepsilon = 78.6\%$: c) alloy TsSDM; T=1600°=const; $\Delta\varepsilon - 1.57\%$ .

Page 344.

Zcne indicated distributicn can be explained by the fact that at iscthermal test conditicns the temperature distribution alcng the length of specimen/sample is mcre everly than with ncnisothermal cnes, and the temperature cf entire wcrking section exceeds the temperature of recrystallizaticn.

The decomposition cf specimen/samples during tests both from constant and with variable temperature occurs in zone I. The mechanism of shaping, which precedes decomposition, was examined above.

During the nonisothermal mode of destructive testing, is developed by crack initiation cn grain boundaries. During isothermal destructive testing bears also intergranular character, but together with the preferred development of cracks on boundary/interfaces, is observed their formation, also, in the body cf grains.

Figures 285 gives typical microphotography/microphotographs of the structure of zone I for the tested specimen/samples of two alloys, which illustrate the character cf crack propagation.

The comparison of the structure of specimen/samples made of the identical alloys, which were failed after different number of cycles of loading, shows that not cnly fcrm cf fracture, but also grain sizes depend on the duration of tests.

With an increase in the duration of the stay of material at the temperature, which exceeds recrystallization, grain sizes

considerably are increased and because of this is increased the
concentration of impurity/admixtures in boundary/interfaces.

The measurement of the microhardness of the investigated alloys
showed that its value is decreased in comparison with initial to
different degree for different zones of structure and unessentially
it depends on the duration of tests and amount of plastic deformation
in cycle. The initial microhardness of all investigated alloys VN-2,
VM-1 and TsSDM was 2160-2260 MN/m$^2$ (220-230 kg/mm$^2$). Microhardness in
zone I of border and internal sections of grains for different
specimen/samples had a value from 1760 to 1910 MN/m$^2$ (180-195
kg/mm$^2$), in zone II, - from 1960 to 2060 MN/m$^2$ (200-210 kg/mm$^2$) and
in zone III - from 2010 to 2110 MN/m$^2$ (205-215 kg/mm$^2$).

Investigation of the fatigue failure of refractory metals.

The fatigue strength of the niobium alloy VN-2 feast the normal
and high (1100°C) temperatures in vacuum 1.33 MN/m$^2$ (10$^{-5}$ mm Hg) is
experience/tested in tubular specimen/samples ($d_{u}=$    11.6 mm; $d_{bu}$
=10.4 mm; $l$=300 mm) during installation UVV-1 (see pg. 321). As can
be seen from the curve/graph of the temperature distribution along
the length of specimen/sample at 1200°C (Fig. 286), on the working
section of specimen/sample 80 mm in long the gradient of temperature
is insignificant.

Page 345.


Figures 287 gives the fatigue curves, obtained for alloy VN-2 at
room and high temperature; a noticeably considerable reduction in the
limit of fatigue with 1100°C in comparison with its value at room
temperature.


Service life during tests in vacuum prove to bes itself
substantially higher than in air (Fig. 288). As can be seen from Fig.
288, the zone of the limited durability during tests in vacuum
sharply is expanded (S-N curve is misaligned to the right), that it
is possible to explain by the lower speed of the propagation of
fatigue crack in vacuum in comparison with testing in air.


Analogous conclusion/derivations about the effect of vacuum on
service life obtained other researchers. So, in the work of Wadsworth
[223] it is shown, that the service life of the specimen/samples made
of steel with 0.5o/o C, which were testing for reversed bending at
the constant amplitude of deformation and frequency 100 Hz, was
increased ~10 once during tests in vacuum in comparison with tests in
air.
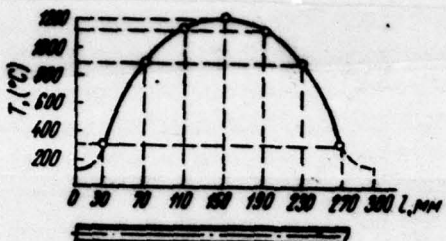
Fig. 286.
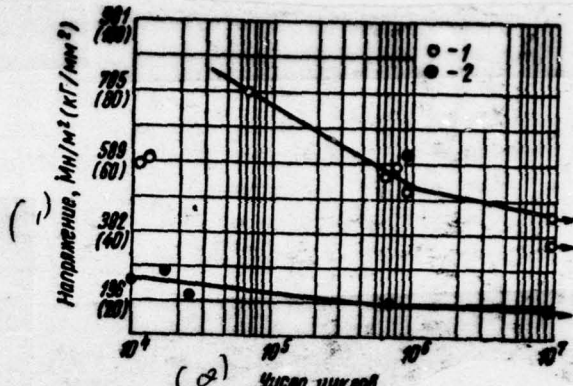


Fig. 287.

Fig. 286. Graph of the temperature distribution along the length of tube.

Fig. 287. S-N curves of alloy VN-2; 1 - 20°C; 2 - 1100°C.

Key: (1). Stress, MN/m² (kg/mm²). (2). Number of cycles.

Page 346.

It is interesting to note that in the specimen/samples, tested in vacuum during the deformations lower than the maximum, were small cracks which were not spread during the subsequent tests, even if the latter were conducted in air.

Interesting investigation conducted by Hempel [12]. It checked proposition of Schaub and Lidtke [221] about the fact that for

initiation of fatigue fracture at room temperature, besides sliding,
is necessary the reaction of the atoms of surface with the
surrounding atmosphere, first of all with atmospheric oxygen.

For this, were tested cylindrical specimen/samples made of
carbon steel (0.03o/o C) to fatigue with elongation - compression
($\sigma_m=0, f=35$     Hz) in the special test chamber where the
specimen/samples washed by the purified and dried gases: $O_2$, $N_2$, $H_2$
and Ar. Furthermore, the corresponding tests were conducted also in
air. Figures 289 depicts the results of fatigue tests in different
media. As can be seen from curve/graph, the composition of gaseous
medium at atmospheric pressure influences either service life or the
endurance limit of this steel.

Taking into account good corrosion resistance of niobium and its
alloys [47], it is possible to make the conclusion that the expansion
of the zone of the limited durability during fatigue tests in vacuum
is connected with a decrease in the velocity of an increase in
fatigue cracks, in view of the decrease of the wedging action/effect
of the layer of molecules of gas.
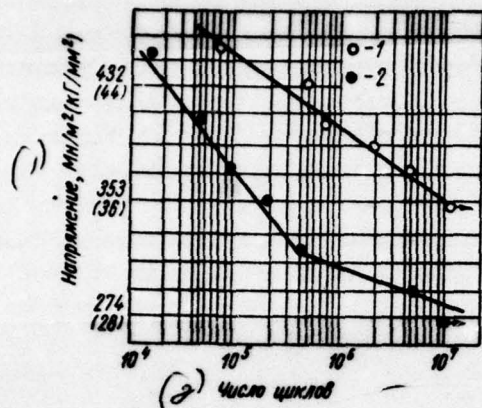
Fig. 288. The S-N curves cf alloy VN-2 in different media: 1 - vacuum; 2 - air.

Key: (1). Stress, MN/m² (kg/mm²). (2). Number of cycles.

Page 347.

Together with the plotting of curves of the fatigue of high-melting alloys, was carried out the study cf the laws governing emergence and development of fatigue cracks. These processes were studied in the specimen/samples, which were thin-walled tubes. From specimen/samples were cut out the sections sc that it would be possible to study changes in structure both in longitudinal and in transverse section/cuts (Fig. 290).
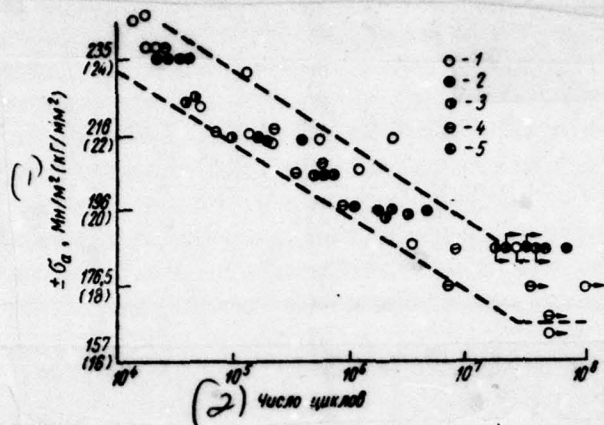
Fig. 289.                                    Fig. 290.

Fig. 289. The results of fatigue tests of carbon steel (0.09o/o C) in different gaseous media [221]: 1 - air; 2 - $O_2$; 3 - $H_2$; 4 - $N_2$; 5 - Ar.

Key: (1). $MN/m^2$ ($kg/mm^2$). (2). Number of cycles.
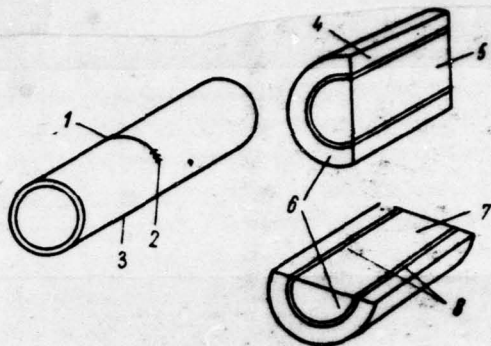
Fig. 290. Schematic of cut cf sections from specimen/sample with crack: 1 - began crack formations; 2 - end cf crack; 3 - side, opposite to crack; 4 - crack (beginning); 5 - longitudinal vertical section/cut; 6 - cross sections; 7 - longitudinal horizontal section/cut; 8 - crack (ends).

Pages 348-349.

Microstructure was studied with the aid of metallographic microscope MIM-8M and on electron microscope UEM-100 by the method of

collodion impressions, shaded by chromium [217].

Testing microhardness on grinding face was manufactured on tool PMT-3 with load 0.5 N (50 $\frac{g}{f}$). The time of loading was 10 s, and holding under load 12 s [120].



Fig. 291. Fatigue crack in the specimen/sample of alloy VN-2 (x5).

Fig. 292. Structure of alloy VN-2 after deccmpcsition with 20°C

(x800): a) the vertical section/cut of specimen/sample: b) horizontal
section/cut.

section/cut.

Page 350.

Crack occupies almost the half of the perimeter of specimen/sample.
On this same surface there are intermittent small cracks,
side-by-side to basic crack. From both of sides of the developing
crack, are observed fan-shaped zones of plastic deformation.

During vertical section/cut of one of the specimen/samples in
the zone of the greatest stresses (Fig. 292a) observed two parallel
cracks, intersecting all the section/cut. These main-line cracks are
rectilinear and they pass through it is sulfuric alloy, which are
proved to be substantially deformed. In horizontal section/cut the
crack has corrugated character and it passes both on grains and on
their boundary/interfaces (Fig. 292b).

By the method of electron microscopy were investigated the
surfaces of the tested specimen/sample from the side of fatigue crack
(Fig. 293a) and from opposite side of crack (Fig. 293b).

On the surface of specimen/sample near connection/inclusions,
are observed the microcracks; then it is greater on the destroyed
side of specimen/sample, than on opposite side.

The microhardness of initial specimens was 1450 MN/m² (152 kg/mm²). In vertical section/cut from the side of decomposition (near the crack initiation) the microhardness is equal to 1700-1730 MN/m² (173-176 kg/mm²), and from diametrically opposite side 1850 MN/m² (189 kg/mm²).

Refractory metals in a series of construction/designs work in compound with ceramics.
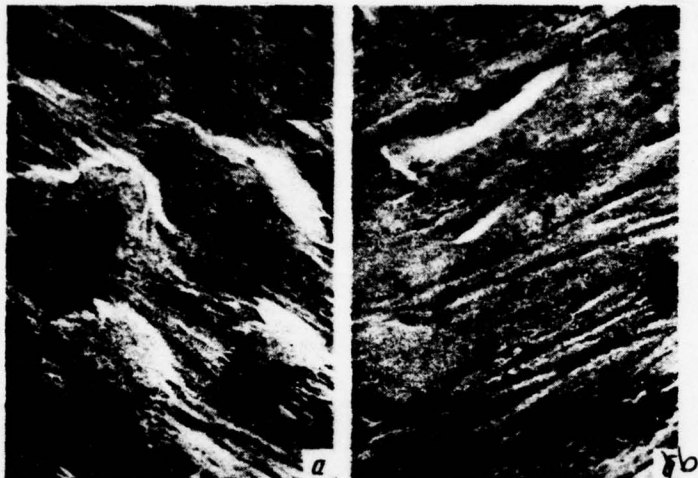
Fig. 293. Structure of alloy VN-2 (x1400) after testing. T=20°C; a) from the side of crack; b) from opposite side.

Page 351.

During operation similar assemblies are completely frequently subjected to vibration effects. The investigation of the fatigue strength of compound refractory metal - ceramics with the check of vacuum tightness, which is the basic requirement which must satisfy compound, was realize/accomplished during the modernized installation UVV-1. Joints refractory metal (niobium alloy) - ceramics ($Al_2O_3$), shown on Fig. 294a, elongated by the tubes from niobium alloy which were soldered to the ends of the metal tubes of joints. The general view of specimen/sample after the soldering of extenders is shown on

Fig. 294b).
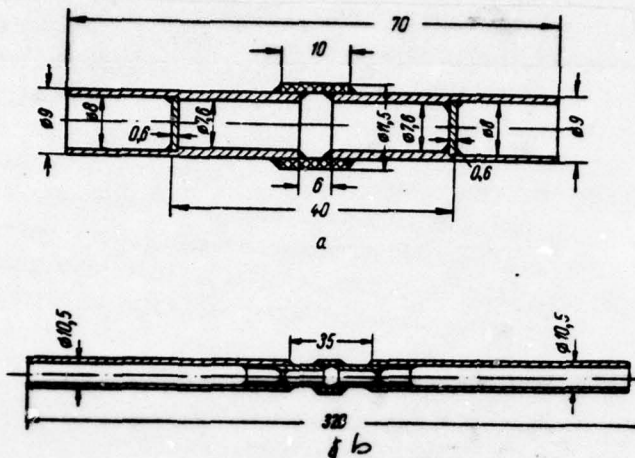
Fig. 294. Joint is refractory metal - ceramics: a) structural cell/element; b) specimen/sample.
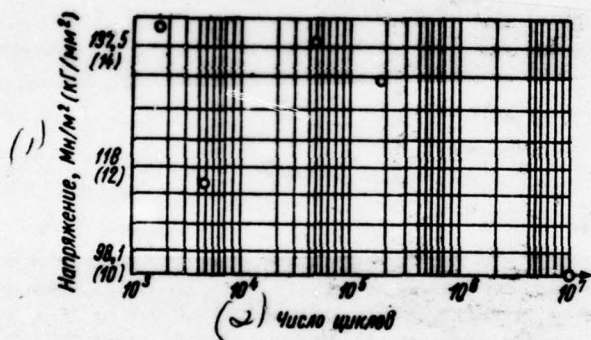


Fig. 295. Results of vibration tests of structural cell/element (joint refractory metal - ceramics).

Key: (1). Stress, MN/m² (kg/mm²). (2). Number of cycles.

Page 352.

Technology rations ensured vacuum tightness and the considerable mechanical strength of compound.

Specimen/sample was establish/installed in captures within vacuum chamber of installation, which they evacuated to 1.33 MN/m² ($10^{-5}$ mm Hg). The internal cavity cf specimen/sample was connected by the means cf vacuum hoses with the autonomous system of pumping out which created a vacuum in specimen/sample. After this inside specimen/sample, was supplied helium. During crack initiation as a result of transverse vibrations of specimen/sample which they excited with the aid of an electrodynamic vibration table of the type EV-1M, helium, contained specimen/sample, began to emerge inside vacuum chamber, that they noted according to the throw of the pointer of vacuum gauge.

Figures 295 gives some results of vibration tests of structural cell/element refractory metal - ceramics. To graph are plotted/applied only the points, which correspond to the breakage the ceramic part of the specimen/sample. In this case the torque/moment of the disturbance/breakdown cf vacuum tightness of compound coincided with the torque/moment of final fragmentation, which indicates its high rate.

Criteria of the decomposition of refractory metals.

Is accumulated at the present time considerable of
quantity-experimental data on the characteristics of short-time and
stress-rupture strength and plasticity of refractory metals at high
temperatures. Are much less studied the laws governing deformation
and decomposition of refractory metals under conditions of cyclic
variation in the load and temperature, i.e., under conditions,
maximally approximated to operating conditions of articles made of
refractory metals.

Therefore special importance acquires the establishment of the
basic criteria of the decomposition of refractory metals and alloys
with the aid of which it would be possible to estimate their strength
in real construction/designs.

Taking into account the limited volume of the experimental
results, obtained on refractory metals and alloys under these
conditions, it is possible to speak only about the establishment of
the tentative dependences which in proportion to the accumulation of
experimental data will be continuously improved.

The examination of the possible criteria of decomposition let us
conduct in connection with three schematics of loading and heating,
given to Fig. 247.

During tests under conditions A (thermocyclic stress-rupture strength) there is essential interest in the investigation of the effect of the cyclic recurrence of heating on the service life of refractory metals and alloys at high temperatures.

Page 353.

For all investigated alloys, as is evident from the results, given above, thermocycling was conducted under the conditions when maximum temperature a little exceeded the temperature of recrystallization and corresponded to optimum operating temperature for this alloy, but minimum composed 100-200°C. Investigations on alloys VM-1, VN-2, niobium of alloy with 10o/o Mo, alloy Ta+10o/o W under conditions, described earlier, sufficiently clearly showed that determining is the total time of holding at maximum temperature. The curves of stress-rupture strength for isothermal and thermocyclic conditions, constructed in coordinates $\sigma$ - lg $\tau$, virtually coincide in the investigated range of time to failure. These results, taking into account that that testing they were conducted according to the two-stage program of heating, at which the lower level of the temperature is very small, and consequently, was small the degree of the damage of material at this temperature, they testify to the conformity of experimental data to the linear hypothesis of the accumulation of damage.

Further investigations in this field must show, will correspond
to the hypothesis indicated the results, obtained during a program
change in the temperature on several levels, it is sufficient to
close to the temperature of recrystallization. The comparison of the
rates of steady-state creep with isothermal and thermocyclic loading
for one of the meltings of alloy VN-2 at temperature of 1200°C and
alloy VM-1 at temperature of 1600°C is carried out in Fig. 296.

From the results, given to Fig. 296, it follows that, as it was
to be expected, thermocycling misaligns dependences $V_n - \sigma$ to the
side of high stresses, moreover this difference is more essential for
alloy VN-2. Tests under conditions C (see Fig. 247) correspond to the
conditions/mode of tests for low-cycle fatigue under isothermal
conditions. Under this conditions experience/tested alloys VM-1, VN-2
and TsSDM. If is is based on results of numerous experiments, carried
out for structural and heat-resistant alloys [211, 222], then for the
criterion of decomposition under these conditions can be accepted
plastic deformation as cycle $\Delta\varepsilon_{en}$ by the stage of the stabilization
of hysteresis loop.
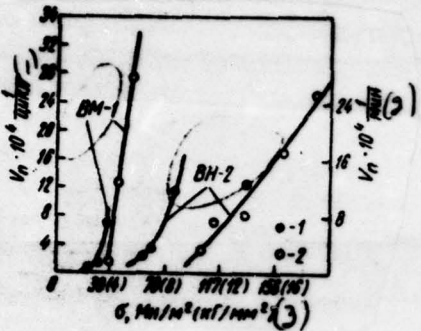
Fig. 296. The rates of steady-state creep for alloys VM-1 and VN-2: 1 - isothermal loading; 2 - thermocyclic loading.

Key: (1). 1/cycle. (2). 1/min. (3). MN/m² (kg/mm²).

Page 354.

The dependence between a plastic deformation in cycle and a number of cycles before decomposition for this case can be recorded or in the form of the equation of Coffin [211]

$$\Delta \varepsilon_{nn} \cdot N^k = C; \quad k = 0.5; \quad C = \frac{\varepsilon_p}{2}, \tag{7.9}$$

where N - a number of cycles before decomposition;

$\varepsilon_p$ - actual elongation during decomposition; C and k - parameters.

or in the more general view

$$\varepsilon_{nn} = \varepsilon_p (2N)^k. \tag{7.10}$$

where $\varepsilon_{nn}$ - amplitude of plastic deformation in cycle.

Both these dependences, as is known, correspond to straight line in coordinates $\lg \Delta\varepsilon_{nx} - \lg N$.

Given to Fig. 277 and 278 experimental data show that in the investigated range of a number of cycles before decomposition is observed linear dependence between $\Delta\varepsilon_{nn}$ and $\lg N$ both for the torque/moment of forming of neck and for the torque/moment of final fragmentation. Similar type dependences can be utilized within certain limits, for extrapolation into the range of the high values N. However, the numerical values of parameters k and C, as this follows from Table 42, do not correspond to the values, which figure as in the formula of Coffin. Experimentally obtained values k and C are considerably more than theoretical, moreover parameter k is changed within very wide limits.

All this excludes for refractory metals the possibility of the calculation of dependence $\lg \Delta\varepsilon - \lg N$ according to the results of static tests.

Table 42. Values of parameters k and C in the equation of Coffin for a series of high-melting alloys.

| Сплав (2) | Режим испыта- ния (3) | Значение k на стадии (1) | | | Значение C на стадии (1) | | |
|---|---|---|---|---|---|---|---|
| | | образова- ния шейки (4) | появле- ния трещин (5) | разруше- ния (6) | образова- ния шейки (4) | появле- ния трещин (5) | разруше- ния (6) |
| ВН-2 | IБ | 0,77 | 0,77 | 0,77 | 0,45 | 1,25 | 2,66 |
| ВМ-1 | IБ | 0,74 | 0,74 | 0,74 | 1,23 | 2,91 | 3,80 |
| ЦСДМ | IIБ | 0,43 | — | 0,43 | 0,42 | — | 0,71 |
| ВН-2 | IВ | — | 1,13 | 1,00 | — | 1,31 | 1,50 |
| ВМ-1 | IВ | — | 1,13 | 1,00 | — | 1,31 | 1,50 |

Key: (1). Value k for stage... (2). Alloy. (3). Conditions/mode [1] of testing.

FOOTNOTE [1]. See Table 40. ENDFOOTNOTE.

(4). formation of neck. (5). appearance of cracks. (6). decomposition.

Page 355.

For the rough estimate of the service life of refractory metals with isothermal cyclic loading, it is possible to utilize Peterson's criterion [220], who assumes that for all metals, independent of their properties, to the amplitude of cyclic deformation, equal to

2o/o, corresponds the service life of $10^3$ cycles.

This criterion is checked in work [219] for 48 different metals
and alloys. If one takes into account that for investigated
refractory metals $\Delta e_{nn} \approx \Delta \varepsilon$, since elastic comprising of high-temperature
deformation is low, then of the results, given to Fig. 278, it
follows that Peterson's criterion satisfies by findings.

Testings under conditions C (see Fig. 247), which is
conditionally named the conditions/mode of nonisothermal low-cycle
fatigue they showed that parameters k and C, entering the equation of
Coffin were different for ore and the same alloys with isothermal and
nonisothermal loading. The comparison of the numerical values of
these parameters, obtained for two conditions/modes of tests, is
carried out in Table 42.

It should be noted that this result is found in contradiction
with the experimental data, obtained for heat-resistant alloys [222],
which show that regardless of the fact, were conducted tests under
isothermal or nonisothermal conditions, to specific plastic
deformation in cycle corresponded an identical number of cycles
before decomposition.
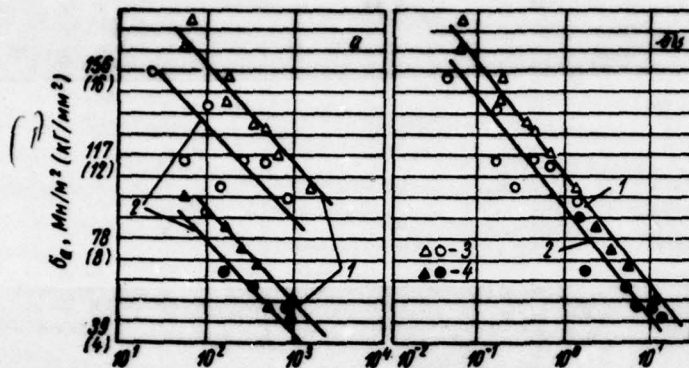
Fig. 297. The results of the test cf the lcw-cycle fatigue of alloys VN-2 and VM-1 under the isothermal and nonisothermal conditions: a) in coordinates the amplitude of the stress in cycle - a number of cycles; a) in coordinates amplitude - time cf loading when $\tau_{max} > \tau_{pexp}$ 1 - alloy on the basis of molybdenum; 2 - allcy on the basis of niobium; 3 - T≠const; σ≠const; 4 - T=const; σ=const.

Key: (1). MN/m² (kg/mm²).

Page 356.

The special feature/peculiarities cf the behavior of refractory metals, apparently, are connected with essential effect on the law governing the decomposition of the time/temporary factors the degree cf manifestation of which, as is known, grow/rises with an increase in the plasticity of the materials being investigated and temperature of testing.

Processing the experimental results, obtained on alloys VM-1 and VM-2 during their tests under conditions B and C (see Fig. 247), showed that these data are packed sufficiently well to single straight lines in coordinates $\sigma - \lg \tau_{r_{max}}$ (Fig. 297), where $\tau_{r_{max}}$ - time of the determination of material at temperature is higher than the temperature of recrystallization.

On the essential effect of time/temporary factors on the law governing deformation and decomposition of refractory metals and alloys during their tests according to programs B and C (see Fig. 247) testifies also analysis of structural transformations in them and kinetics of shaping.

Page 357.

REFERENCES

1. M. A. Filyand, Ye. I. Semenova. Properties of rare elements. Publishing house "metallurgy", 1964.

2. Encyclopedia of contemporary technology. Structural materials. Vol. I-III. Publishing house "Soviet encyclopedia", 1963.

3. K. Agte, L. Vatsek. Tungsten and molybdenum. Publishing house

"energy", 1964.

4. Coll. "Molybdenum", Foreign Languages Publishing House, 1959.

5. N. A. Shaposhnikov. Mechanical tests of metals. Mashgiz [State Scientific and Technical Publishing House of Literature on Machinery Manufacture], 1954.

6. G. S. Pisarenko et al. Strength of materials at high temperatures. Publishing house of "Scientific Thought", 1966.

7. P. K. P'yu. In the collection "problem of contemporary metallurgy". Metallurgizdat, 1959, No 5, p. 90.

8. S. D. Gertsriken, I. Ya. Dekhtyar. Diffusion in metals and alloys in solid phase. Fizmatgiz, 1960.

9. A. G. Bloch. Bases of heat exchange by emission/radiation. State Technical Press, 1962.

10. O. K. Nazarenko. Electron-beam welding. Publishing house of "Scientific Thought", 1965.

11. E. Melan, G. Parkus. Thermoelastic stresses, caused by stationary fields. Fizmatgiz, 1958.

DOC = 78133012    PAGE ~~38~~ 724

12. Coll. "atomic mechanism of decomposition". Metallurgizdat, 1963.

13. N. J. Grant. Investigations at high temperatures. IL, 1962.

14. Harper D. L., Feilbach W. H., Libsch J. F. Proc. ASTM, 1963
v. 63, p. 684.
15. Doering H., Shahinian P. Mater. Res. and Stand., 1966, v. 6,
№ 3, p. 134.

16. V. I. Likhtman, Ye. D. Shchukin, P. A. Rebinder. Physicochemical
mechanics of metals. Ed.s of the AS USSR, 1962.

17. I. Cramer, L. Demer. Effect of medium on the mechanical
properties of metals. Publishing house "metallurgy", 1964.

18. A. M. Borzdyk. Methods of the hot mechanical tests of metals.
Metallurgizdat, 1962.

19. Ya. B. Fridman. Mechanical properties of metals. Oborongiz, 1951.

20. A. N. Kobylkin, V. R. Grigorovich, V. E. Kishenevskiy. Plant
laboratory, 1962, No 12, p. 1513.

Page 358.

21. G. V. Zakharov et al. Niobium and its alloy. Metallurgizdat,
1961.

22. Coll. "refractory metals and alloys". Publishing house "metallurgy", 1965.

23. Mordaike B. J. Inst. Metals, 1960, v. 88, № 6, p. 272.

24. Coll. "niobium and tantalum". IL, 1960.

25. Coll. "questions of high-temperature strength in machine-building". Ed.s of AS UkSSR, 1963.

26. E. M. Marmer. Powder metallurgy, 1962, No 2, p. 60.

27. Niobium and tantalum. Publishing house "metallurgy", 1966.

28. Braun H., Sedlatcheck K. Less — Common metals, 1960, № 2—4, p. 277.

29. G. V. Samsonov, A. P. Epik. Coatings from refractory compounds. Publishing house "metallurgy", 1964.

30. Coll. "thermal stability of materials and structural cell/elements. Publishing house of "Scientific Thought", 1965.

31. V. A. Lanis, L. Ye. Levina. Vacuum tests technique. Gosenergoizdat, 1963.

32. M. M. Aleksyuk, V. N. Rudenko. In the collection "Technology and organization of production". Izd. UkrNITI, 1969, No 2, p. 20.

33. M. M. Aleksyuk, V. N. Rudenko. In the collection "Machine-building". Izd. UkrNITI, 1966, No 4, p. 96.

34. S. F. Malikov, N. I. Tyurin. Introduction to metrology. Ed.s of the committee of standards, 1966.

35. G. P. Katys. Methods and tools for measuring The parameters of unsteady thermal processes. Mashgiz, 1959.

36. B. A. Glagovskiy, I. D. Piven. Electrotensometers of resistance. Publishing house "energy", 1964.

37. A. N. Gordov. Bases of pyrometry. Publishing house "metallurgy", 1964.

38. O. A. Gerashchenko, V. G. Fedorov. Thermal and temperature measurements. Publishing house of "Scientific Thought", 1965.

39. A. A. Poskachey, S. P. Rusin. Measurement of the temperature in

DOC = 78133012      PAGE ~~41~~ 727

electrometric installations. Publishing house "energy", 1967.

40. S. V. Yeliseyev. The determination technique of the mechanical properties of materials. Publishing house "machine-building", 19~~65~~ 56.

41. B. A. Avdeyev. A technique of determining the mechanical properties of materials. Mashinostroyeniye Publishing House, 1965.

42. S. I. Ivin. Statistical methods of check and analysis of the quality of the light sources. Ed.s of the committee of standards, 1968.

43. A. K. Mitropol'skiy. Statistical computations technique. Fizmatgiz, 1961.

44. Yu. V. Linnik. Method of least squares and basis of the theory of perfecting observations. Fizmatgiz, 1962.

45. E. M. Savitskiy et al. Izv. of the AS USSR, OTN (metallurgy and fuel/propellant), 1963, No 6, p. 40.

46. D. McLean. Mechanical properties of metals. Publishing house "metallurgy", 1965.

47. Ye. M. Savitskiy, G. S. Burkhanov. Physical metallurgy of refractory metals and alloys. Publishing house "metallurgy", 1967.

Page 359.

48. Mackenzie I. K. Proc. Phys. Soc., 1950, v. 63, № 1, p. 2.

49. M. Yu. Bal'shin. Powder physical metallurgy. Metallurgizdat, 1948.

50. V. V. Skorokhod. Powder metallurgy, 1961, No 1 p. 50.

51. Gatto F. Alluminio, 1950, № 1, p. 19.

52. Чехова О. А. Магнітом"які металокерамічні матеріали. Вид-во АН УРСР, 1959.

53. Coble R. L. and Kingery W. D. „J. Amer. Ceram Soc.". 1956, v. 39, № 11, p. 337.

54. Sh. N. Plyat, Yu. M. Rapoport, Ye. T. Chofnus. Physical engineering journal, 1958, No 1, p. 96.

55. Mc. Adam D. J. Iron a. Steel Inst., 1951, v. 68, p. 346.

56. A. Ya. Artamonov, V. A. Danilerkc, Yu. A. Kashtalyan. Powder metallurgy, 1964, No 1, p. 42.

57. K. V. Zener. In the coll. "elasticity and inelasticity". IL, 1965, p. 1.

58. Coll. "questions of high-temperature strength in machine-building". Ed.s UkrNITI, 1961.

DOC = 78133012       PAGE <s>#3</s> 729

59. Yu. A. Kashtalyan. Powder metallurgy, 1962, No 1, p. 61.

60. V. A. Kuz'menko. Sonic and ultrasonic oscillations during the dynamic tests of materials. Ed.s of AS UkSSR, 1963.

61. Köster W. Z. Metallk. 1948, Bd. 39, H. 1, S. 149.

62. M. G. Lozinskiy. Structure and the property of metals and alloys at high temperatures. Metallurgizdat, 1963.

63. G. S. Pisarenko, V. A. Borisenko, Yu. A. Kashtalyan. Powder metallurgy, 1962, No 5, p. 79.

64. A. B. Lyashchenko, P. I. Mel'nichuk, I. N. Frantsevich. Powder metallurgy, 1961, No 5, p. 64.

65. V. A. Dreshpak — Dopovidi AN UkSR, 1967, A. Seriya, No 10, p. 917.

66. Physicochemical properties of cell/elements. Publishing house of "Scientific Thought", 1965.

67. K. D. Smitels. Tungsten. Metallurgizdat, 1958.

68. B. Chalmers. Physical physical metallurgy. Metallurgizdat, 1963.

69. Broun H. L., Armstrong P. E. Rev. Sci. Instrum. 1963, № 6, p. 61.

70. Bernstein B. T. J. Appl. Phys., 1962, v. 33, № 6, p. 2140.

71. Lowrie R., Gonas A. M. J. Appl Phys., 1965, v. 36, № 7, p. 2189

72. E. N. Marmer, O. S. Gurvich, L. F. Mal'tseva. High-temperature materials. Publishing house "metallurgy", 1967.

73. Coll. "molybdenum". II, 1962.

74. K. C. Aleksandrov, T. V. Ryzhova. Crystallography, 1961, No 6, p. 56.

75. B. A. Kalugin, I. G. Mikhaylov. Acoustic journal, 1966, Vol. 12, issue 1, p. 144.

76. Niobium, tantalum and their alloys. Publishing house "metallurgy", 1966.

77. Gebhardt E., Preisedau H. Z. Metallk, 1955, Bd. 46, H. 8, S. 560.

78. D. A. Prokoshkin, Yye. V. Vasil'yeva. Niobium fusions. Publishing house "science", 1964.

Page 360.

79. Reynolds M. Trans. ASM., 1953, v. 45., p. 839.
80. Tottle C. R. J. Inst. Metals, 1956—1957, v. 85, p. 375.
81. Hazelton P. SAE Journal, 1958, 5, p. 66.
82. Livesey D. J. J. Inst. Metals, 1959, v. 27, p. 114.

83. A. I. Dashkovskiy, Ye. A. Savitskiy. In the collection "metallurgy and physical metallurgy of pure metals". Atomizdat, 1960, issue 11, p. 224.

84. Osterman F. Metall, 1962, Bd. 16, S. 656.

85. I. M. Nedyukha, V. G. Chernyy. Dopovidi AN URSR, 1965, No 3, p. 339.

86. N. D. Tarasov, R. A. Ul'yanov, Ya. C. Mikhaylov. In the collection "high-temperature inorganic compounds". Publishing house of "Scientific Thought", 1965, p. 55.

87. Armstrong P. E., Broun H. L. Trans. ASM, 1965, v. 58, p. 30.
88. Köster W. Appl. Sci. Rec., 1954, v. A4, p. 329.

89. G. V. Samsonov, V. I. Ccnstantinov. Tantalum and niobium. Metallurgizdat, 1959.

90. Seybolt A. J. Inst. Metals, 1954, v. 6. p. 774.

91. M. V. Mal'tsev, A. I. Baykov, S. Ya. Sclovyev. Technology of the production of niobium and his alloys. Publishing house "metallurgy", 1966.

92. Köster W., Rausher W. Z. Metallk, 1948, Bd. 39, S. 111.

93. Coll. "transactions of scientific and technical conference on study of dissipation of energy during oscillations of elastic bodies", publishing house of AS UkSSR, 1958.

94. V. A. Zhuravlev. Plant laboratory, 1948, No 5, p. 614.

95. E. I. Bolkhovitinova. Effect of shot peening on the properties of steel parts. Mashgiz, 1953.

96. Yu. V. Piguzov et al. In the collection "internal friction in metals and alloys". Publishing house "science", 1966, p. 18.

97. Coll. "relaxation phenomena in metals and alloys". Metallurgizdat, 1963.

98. Coll. "refractory metals and their alloys". (Materials of international conference on refractory metals and alloys. Sheffield, 1960). IL, 1962.

99. N. N. Davidenkov. Some problems of the mechanics of materials. Lenizdat, 1943.

100. Petty E. R. Metallurgia, 1957, v. 56, p. 231.
101. Fitzgerald L. M. Brit. J. Appl. Phys, 1960, v. 11, № 12, p. 551.
102. Fitzgerald L. M. J. Less—Common Metals, 1963, v. 5, № 4, p. 356.

103. A. A. Kul'bakh, V. M. Shchevelin, N. A. Evstyukhin. In the

collection "Cermet and high-melting materials". Ed.s MIFI, 1967, p. 29.

104. N. A. Evstyukhin, V. M. Shchavelin. In the collection "Metallurgy and physical metallurgy of pure metals". Atomizdat, 1967, p. 101.

105. Damagala R. F., Johnson W. Metal. Progr. 1951, v. 60, p. 73.

106. V. D. Kuznetsovs. Ed.s of the AS USSR. Sections of mathematical and natural sciences, ser. phys., 1937, No 6, p. 751.

107. M. G. Lozinskiy. High-temperature metallography. Mashgiz, 1956.

108. S. I. Gubkin, R. I. Tamilin. Izv. AN ESSR, ser. phys-tech. sciences, 1958, No 2, p. 5-9.

109. Gemmell G. D., Trans. Metallurg. Soc. AIME, 1959, v. 215, p. 898.

Page 361.

110. Semchyshen M., Torgerson C. S. Trans. Amer. Soc. Metals, 1958, v. 50, p. 830.

111. O. S. Ivanov et al. Physical metallurgy and heat metal working, 1962, No 7, p. 4-7.

112. M. M. Khrushchov. Plant laboratory, 1947, No 9, p. 1121.

DOC = 78133012　　　PAGE ~~48~~ 734

113. Atkins A. G., Tabor D. Brit. J. Appl. Phys., 1965, v. 16, № 7, p. 1015.

114. Engl J., Fölmer J. Z. Phys., 1936, Bd. 98, H. 11/12, S. 702.

115. A. I. Betaneli. Hardness of steels and hard alloys at elevated temperatures. Mashgiz, 1958.

116. F. Garofalo, P. R. Meylnok, G. V. Smith. In the collection "Problem of contemporary metallurgy", IL, 1954, No 2 (14), p. 10.

117. B. V. Motte. Indentation tests. Metallurgizdat, 1960.

118. V. K. Grigorovich. Transactions of the institute of metallurgy im. A. A. Baykov. Ed.s of AS UkSSR, issue 5, 1960, p. 244.

119. In the collection "thermal stability of materials and structural/design elements", issue 4. Publishing house of "Scientific Thought", 1967.

120. V. M. Glazov, V. N. Vigdorovich. Microhardness of metals. Metallurgizdat, 1962.

121. V. V. Dzhemelinskiy et al. In the collection "Carbides". Publishing house of "Scientific Thought", 1965, p. 41.

122. M. S. Koval'chenko, V. V. Dzhemelinskiy, V. A. Borisenko. Problems of strength, Vol. 1, No 5, 1969, & p. 20.

123. R. Kiffer, F. V. Benezovskiy. In the collection "Problem of contemporary metallurgy", 1959, No 2 (44), p. 21.

124. G. O'Neyl'. Hardness of metals and its measurement. Metallurgizdat, 1940.

125. Westbrook J. H. Proc. ASTM, 1957, v. 57, p. 873.
126. Westbrook J. H. ASTM Bull., 1960, № 246, p. 53.
127. Mallock A. Nature, v. 117, № 2934, 1926, p. 117; v. 119, № 2990, p. 276; № 3001, p. 669, 1927.

128. R. Hill. Mathematical theory of plasticity. State Technical Press, 1956.

129. V. N. Skuratovskiy, V. A. Borisenko. In the collection "Thermal stability of materials and structural cell/elements", issue 5, Kiev, "Scientific Thought", 1969, p. 435-439.

130. V. A. Borisenko, G. S. Pisarenko. Powder metallurgy, 1961, No 5, p. 95.

131. Haddow J. B., Johnson W. International Journal of Mechanical Sciences, 1962, v. 4, № 1—2, p. 66.

132. V. A. Borisenko. Powder metallurgy, 1962, No 3, p. 55.

133. G. S. Pisarenko, V. A. Borisenko. DAN of UkrSSR, 1962, No 8, p.

1053.

134. I. N. Frantsevich, I. Ye. Shiyanovskaya, V. A. Lavrenko. Physics of metals and physical metallurgy, 1960, Vol. 9, issue 4, p. 593.

135. Sims C. T. J. Metals, 1958, № 5, p. 340.

Page 362.
136. G.V. Zakharova. et al. Nonferrous metals, 1959, No1, p.73.

137. Mincher A. L., Sheely W. F. Trans. Metallurg Soc. AIME, 1961, v. 221, p. 19.
138. V. D. Kuznetsov. Investigations in heat-resistant alloys. Vol. 5. Publishing house of AS USSR, 1959, p. 397.

139. A. A. Bochvar. Izv. of the AS USSR, OTN, 1947, No 10, p. 1369.

140. I. L. Mirkin, D. Ye. Lifshitz. Plant laboratory, 1949, No 9, p. 1011.

141. V. P. Shishokin. ZhTF, 1938, 7, iss. 18, pg. 201.

142. Plant laboratory, 1949, No 7, p. 842.

143. A. P. Gulyayev, Ye. F. Trusova, R. I. Eitel'berg. Plant laboratory, 1949, No 4, p. 447.

144. K. P. Yakovlev. Mathematical processing of the results of measurements. State Technical Press, 1953.

145. V. P. Shishokin, L. N. Bazilevskiy. FMM, 1961, Vol. 11, issue 6, p. 942.

146. I. I. Kornilov, N. T. Domotenko. Investigations in heat-resistant alloys, Vol. 3. Ed.s of the AS USSR, 1958.

147. V. A. Borisenko. Powder metallurgy, 1964, No 5, p. 47.

148. V. P. Shishokin. Nonferrous metals, 1930, No 4, p. 31.

149. V. P. Shishokin, V. A. Ageyeva, N. A. Vikhoreva. ZhTF, 1940, Vol. 10, p. 491.

150. Coll. "problems of contemporary metallurgy". IL, 1960, No 5.

151. V. A. Borisenko. Powder metallurgy, 1964, No 6, p. 79.

152. G. S. Pisarenko et al. In the collection "Transactions VII All-Union scientific-technical conf on powder metallurgy". Ed.s of State Committee SM ARM of SSR on press/printing, 1964, p. 50.

153. Parker R. J. Metallurgia, 1963, v. 67, № 403, p. 219.

154. K. A. Osipov. Questions of the theory of the heat resistance of metals and alloys. Ed.s of the AS USSR, 1960.

155. Ye. V. Vasil'yeva, D. A. Prokoshkin, L. M. Belova. Physical metallurgy and heat metal working, 1966, No 12, p. 21.

156. V. S. Ivanov, I. M. Kop'yev, Yu. G. Liberov. In the collection "Structure and the properties of heat-resistant metallic materials". Publishing house "science", 1967, p. 14.

157. Ya. S. Gintsburg, A. G. Bobrov. Stands for testing engineering materials at high temperatures. Publishing house "Mashinostroyeniye', 1964.

158. Fisher D. H., Carlson R. L., Holden F. C. Mater. Res. Stand., 1962, v. 2, N 1, p. 26.

159. G. S. Pisarenko. Plant laboratory, 1963, No 3, p. 364.

160. M. D. Sadovskiy et al. Investigations in high-strength alloys and filamentary crystals. Ed.s of the AS USSR, 1963, p. 41.

161. Coll. "heat-resistant alloys under conditions of supersonic flights". Metallurgizdat, 1962.

162. Coll. "high-melting metallic materials for space technology". Publishing house "peace/world", 1966.

Page 363.

163. Coll. of "investigation at high temperatures". IL, 1962.

164. Hant A. J. Less—Common Metals, 1960, v. 2, № 2—4, p. 95.

165. Coll. of "property and working refractory metals and alloys". IL, 1961.

166. Ye. M. Savitskiy, M. A. Tylkina, K. B. Povarova. Rhenium fusions. Publishing house "science", 1965.

167. M. I. Gavrilyuk et al. Physics of metals and physical metallurgy, 1962, Vol. 13, issue 5, p. 693.

168. Harmon V. J. Metals, 1960, v. 12, № 9, p. 140.

169. M. S. Kaufman et al. Production of helices, grids and input/introductions of electro-vacuum tools. Gosenergoizdat, 1962.

170. Coll. "some questions of large plastic metal deformations at

high pressures". Ed.s of the AS USSR, 1960.

171. M. V. Bronfin, V. A. Marichev. In the collection "Processes of
diffusion, structure and the property of metals". Publishing house
"machine-building", using 1964, p. 15.

172. Ye. M. Savitskiy et al. Alloys of rare-earth metals. Ed.s of the
AS USSR, 1962.

173. Coll. "electronic melting of metals". Publishing house
"peace/world", 1964.

174. V. P. Shishokin. Journal of Applied Chemistry, 1929, Vol. 2, No
6, p. 657.

175. M. I. Bratskiy, I. N. Frantsevich. "steel", 1932, No 7-8, p. 74.

176. S. I. Gubkin. Theory of the flow of metallic substance.
Moscow-Leningrad, ONTI, 1935.

177. S. A. Pogodin, V. Ya. Anosov. Basic of the beginning of the
physicochemical analysis. Publishing house of the AS USSR, 1947.

178. Ye. M. Savitskiy. Temperature effect on the mechanical

properties of metals and alloys. Ed.s of the AS USSR, 1957.

179. Westbrook J. H. Trans. ASM, 1953, v. 45, p. 221.
180. Ito K. Science Rep. Tohoku Emp. Univ., 12, 137, 1923; Z. Metall-kunde, 92, 1925.
181. Petty E. R. J. Inst. Metals, 1960, v. 89, № 4, p. 123.

182. B. A. Klypin, A. P. Gulyayev, N. N. Morguncva. Physical

metallurgy and heat metal working, 1966, Nc 12, p. 15.

183. Conrad H. J. Metals, 1964, v. 16, № 7, p. 582.

184. Ccll. "investigaticn in heat-resistant allcys". Vol. 7.

Publishing house of AS USSR, 1961.

185. V. A. Borisenko. Powder metallurgy, 1965, No 2, p. 57.

186. M. A. Zaykov. ZhTF, 1948, Vol. 18, issue 6, p. 405.

187. V. A. Pavlov. Physical bases of the plastic metal deformation.

Ed.s of the AS USSR, 1962.

188. L. N. Aleksandrov, V. S. Mordyuk. In the ccllection

"Investigation of steels and alloys". Publishing house "science",

1964, p. 125.

189. V. P. Yelyutin et al. Physics of metals and physical metallurgy,

1963, Vol. 15, issue 5, p. 748.

Page 364.

190. E. S. Yakovlev. Physics of metals and physical metallurgy, 1957, Vol. 4, issue 1-2, p. 150.

191. M. A. Zaykov. Conditions of deformation and effort/force during the hot rolling. Metallurgizdat, 1960.

192. Coll. "mechanical properties of metallic compounds". Metallurgizdat, 1962.

193. L. N. Aleksandrov, V. s. Mordyuk. The internal friction of refractory metals. Saransk. The ed.s of Mordvinian university, 1966.

194. Coll. "new machines and testers of metals". Metallurgizdat, 1963.

195. A. P. Sotnichenko. Plant laboratory, 1960, Vol. 6, p. 760.

196. M. G. Lozinskiy. Izv. of the AS USSR, OTN, 1957, No 11, p. 14.

197. Coll. of "machine and testers of materials". Publishing house "metallurgy", 1968.

198. N. I. Mikheev et al. Plant laboratory, 1963, No 8, p. 371.

199. A. P. Tereshchenko, G. S. Pisarenko. Plant laboratory, 1961, No 1, p. 81.

200. V. I. Kov ak. Plant laboratory, 1961, No 5, p. 585.

201. Larson F. R., Miller J. Trans. ASME, 1952, v. 74, № 5, p. 765.
202. Graham A., Walles K. F. A. J. Iron Steel Inst., 1955, v. 28., № 6, p. 255.

203. N. D. Sazonova. Heat-resistant material testing for creep and stress-rupture strength. Publishing house "machine-building", using 1965.

204. Ya. S. Gintsburg. Plant laboratory, 1960, No 7, p. 863.

205. S. Menson, G. Sakkop. In the collection "heat-resistant metallic materials". IL, 1958, p. 63.

206. I. I. Trunin. Plant laboratory, 1963, No 3, p. 344.

207. V. N. Nikitin. Plant laboratory, 1959, Nc 12, p. 1492.

208. A. Krish, V. Vepner. In the collection "investigation of heat-resistant steels and alloys". Metallurgizdat, 1960, p. 50.

209. S. N. Zhurkov, E. Ye. Tomashevskiy. In the collection "some problems of the strength solid". Ed.s of the AS USSR, 1959, p. 68.

210. A. D. Kennedi. Creep and fatigue in metals. Publishing house "metallurgy", 1965.

211. L. F. Koffin. In the collection "heat-resistant alloys at the changing temperatures and with stresses". Gosenergoizdat, 1960, p. 188.

212. G. K. Leonenko, V. T. Troshenko. In the collection "oscillation of elastic systems taking into account the dissipation of energy". Ed.s of "Scientific Thought", 1968, p. 183.

213. S. V. Sorensen, A. D. Garf, L. A. Kozlcv. Endurance testing machines, Mashgiz, 1957.

214. S. V. Sorensen, A. D. Garf, V. A. Kuz'menkc. Dynamics of endurance testing machines. Mashgiz, 1967.

215. V. A. Strizhalo. Plant laboratory, 1967, Nc 3, p. 367.

216. V. A. Strizhalo. Plant laboratory, 1967, Nc 5, p. 620.

217. G. Thomas. Electron microscopy of metals, IL, 1968.

218. Halford G. R. J. Mater, 1966, v. 1. № 1, p. 3.
ge 365.

**Page 365.**

219. Morrow J. D., Johnson T. A. Mater. Res. Stands, 1965, v. 5, № 1, p. 30.
220. Peterson R. E. Mater. Res Stands, 1963, v. 3, № 2, p. 122.
221. Schaub C., Liedtke W. Colloquium on Fatigue, Springer, 1956, S. 244.
222. Taira S. High Temperature structure and Material, Pergamon Press, 1964, p. 187.
223. Wadsworth N. I. Phil. Mag., 1961, v. 6, p. 397.

224. M. T. Gudtsov, M. G. Lozinskiy. In the collection "microhardness". Ed.s of the AS USSR, 1951, p. 25.

225. G. V. Bokuchav. Izv. of VUZ [~~ssep4~~ - Institute of Higher Education]. Machine-building, ~~using~~ 1959, No 5, p. 184.

226. V. A. Shapochkin. Thermophysics of high temperatures, 1964, Vol. 2, No 6, p. 922.

227. A. A. Kul'bakh, V. M. Shchavelin, E. A. Makarychev. Plant laboratory, 1965, No 3, p. 374.

228. Yu. G. Godin et al. In the collection "metallurgy and physical metallurgy of pure metals", of issue 5. Atomizdat, 1966, p. 189-198.

229. M. G. Mozinskiy, V. S. Mirotvorskiy. Izv. of the AS USSR, OTN, metallurgy and fuel/propellant, 1959, No 3, p. 62.

230. Koester R. D., Moak D. P. J. Amer. Ceram. Soc., 1967, v. 50, № 6, p. 290.

## DISTRIBUTION LIST

### DISTRIBUTION DIRECT TO RECIPIENT

| ORGANIZATION | MICROFICHE | ORGANIZATION | MICROFICHE |
|---|---|---|---|
| A205 DMATC | 1 | E053 AF/INAKA | 1 |
| A210 DMAAC | 2 | E017 AF/RDXTR-W | 1 |
| B344 DIA/RDS-3C | 9 | E403 AFSC/INA | 1 |
| C043 USAMIIA | 1 | E404 AEDC | 1 |
| C509 BALLISTIC RES LABS | 1 | E408 AFWL | 1 |
| C510 AIR MOBILITY R&D LAB/FIO | 1 | E410 ADTC | 1 |
| | | E413 ESD | 2 |
| C513 PICATINNY ARSENAL | 1 | FTD | |
| C535 AVIATION SYS COMD | 1 | CCN | 1 |
| C591 FSTC | 5 | ASD/FTD/NIIS | 3 |
| C619 MIA REDSTONE | 1 | NIA/PHS | 1 |
| D008 NISC | 1 | NIIS | 2 |
| H300 USAICE (USAREUR) | 1 | | |
| P005 DOE | 1 | | |
| P050 CIA/CRS/ADD/SD | 1 | | |
| NAVORDSTA (50L) | 1 | | |
| NASA/KSI | 1 | | |
| AFIT/LD | 1 | | |
| LLL/Code L-389 | 1 | | |

FTD-ID(RS)T-1330-78